Nuclear physics* outputs of CEνNS measurements

*and electroweak parameters.

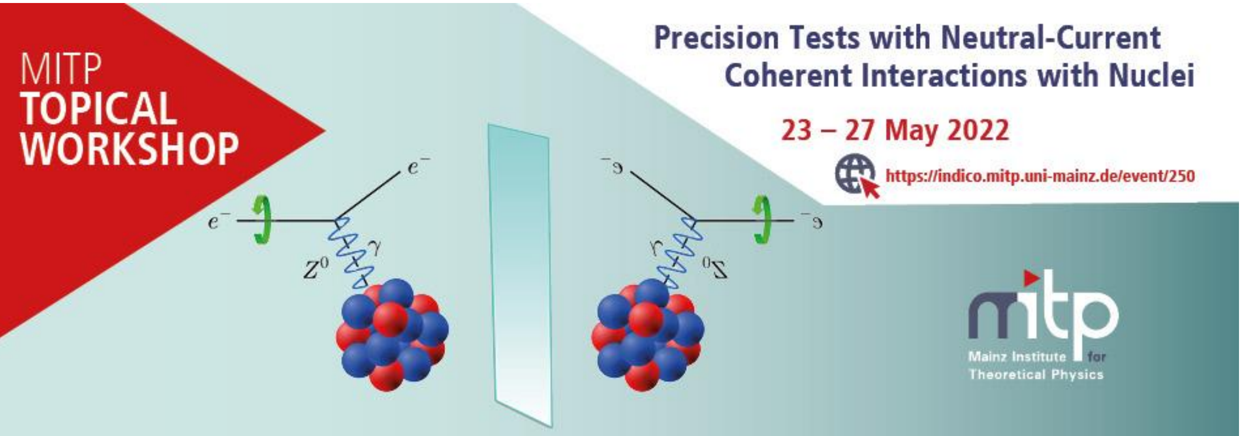

Matteo Cadeddu
matteo.cadeddu@ca.infn.it

INFN CAGLIARI

In collaboration with

M. Atzori Corona
N. Cargioli
F. Dordei
C. Giunti
G. Masia
Y. F. Li
C. A. Ternes
Y. Y. Zhang

Coherent elastic neutrino nucleus scattering (aka CEνNS)

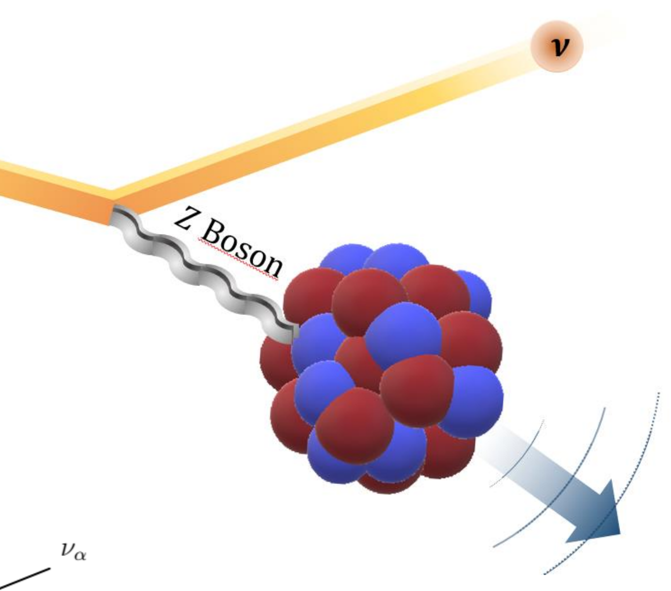

+A pure weak neutral current process

$$\boxed{\frac{d\sigma_{\nu_\ell\text{-}\mathcal{N}}}{dT_{\mathrm{nr}}}(E, T_{\mathrm{nr}}) = \frac{G_{\mathrm{F}}^2 M}{\pi}\left(1 - \frac{M T_{\mathrm{nr}}}{2E^2}\right)\left(Q^V_{\ell,\mathrm{SM}}\right)^2}$$

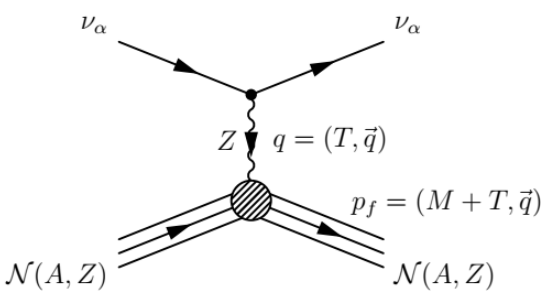

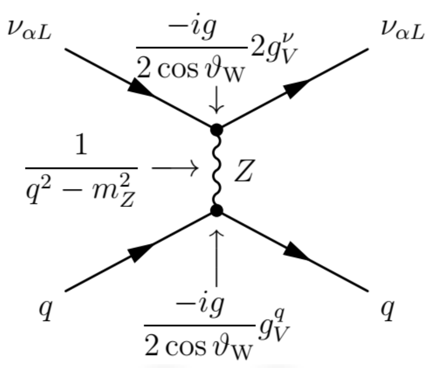

+Weak charge of the nucleus

$$Q^V_{\ell,\mathrm{SM}} = \Big[\underbrace{g_V^p\,(\nu_\ell)\, Z F_Z\left(|\vec{q}|^2\right)}_{\text{protons}} + \underbrace{g_V^n N F_N\left(|\vec{q}|^2\right)}_{\text{neutrons}}\Big]$$

$$g_V^{p,\mathrm{tree}} = \frac{1}{2} - 2\sin^2(\vartheta_W) \cong \mathbf{0.0229}$$

$$g_V^{n,\mathrm{tree}} = -\frac{1}{2}$$

In general in a weak neutral current process which involves nuclei, one deals with **nuclear form factors** that are different for protons and neutrons and cannot be disentangled from the neutrino-nucleon couplings!

The coupling to proton depends on the weak mixing angle!

Interplay between nuclear and electroweak physics

+ This feature is always present when dealing with electroweak processes.

- Atomic Parity Violation (APV): atomic electrons interacting with nuclei. Cs and Pb available.
- Parity Violation Electron Scattering (PVES): polarized electron scattering on nuclei. PREX(Pb), CREX(Ca), Qweak(Al), Qweak(p).
- Coherent elastic neutrino-nucleus scattering (CEνNS). Cesium-iodide (CsI), argon (Ar) and germanium (Ge) available.

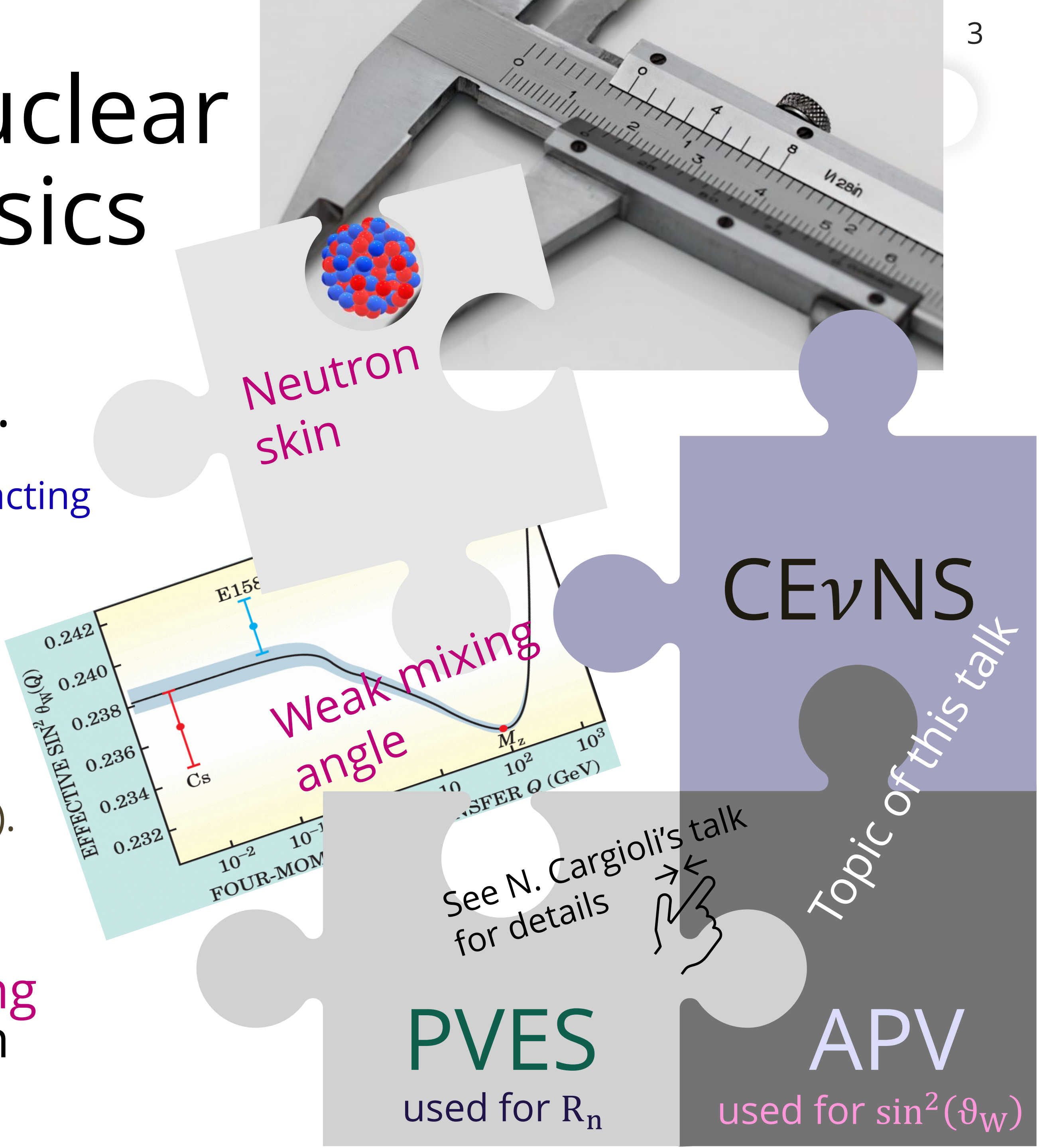

+ Can we gain information combining different EW processes together in order to break this degeneracy?

CEνNS players so far

See K. Scholberg's talk for details

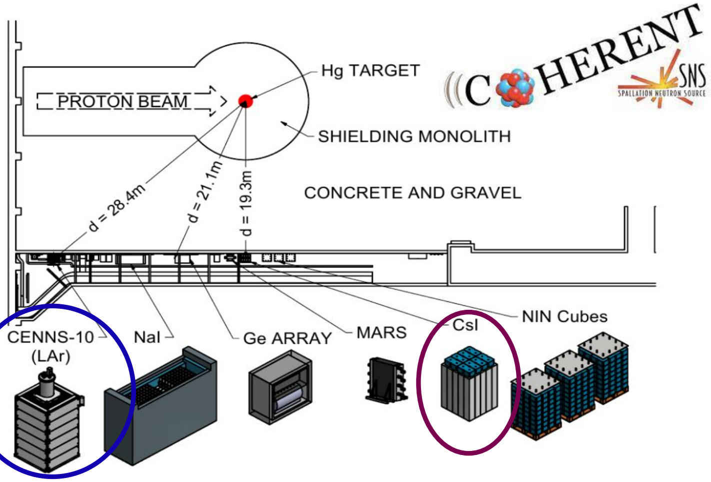

COHERENT CsI

D. Akimov et al. **Science** 357.6356 (2017)

+ Updated in arXiv:2110.07730v1

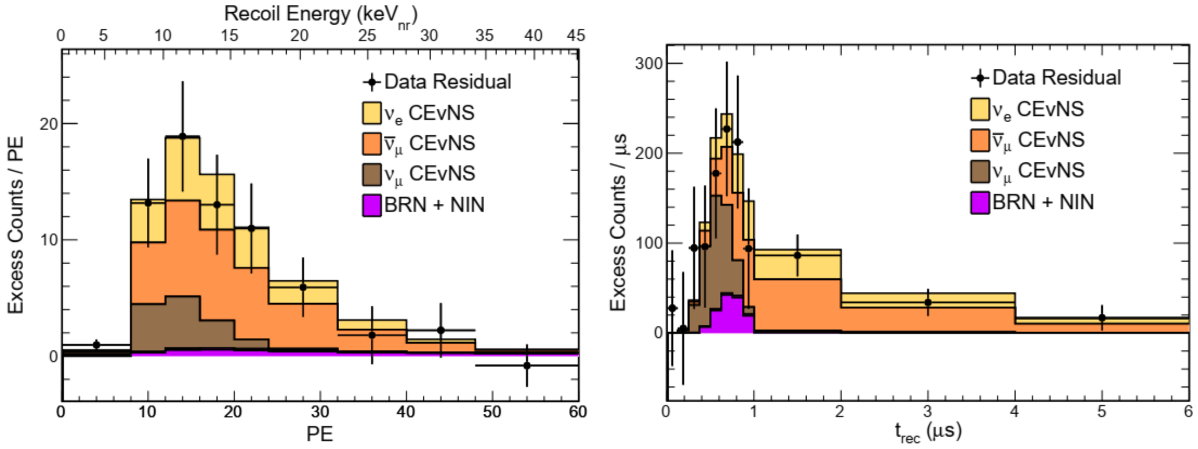

	Prior Prediction	Best-Fit Total
Steady-state background	1286 ± 27	1273 ± 24
BRN	18.4 ± 4.6	17.3 ± 4.5
NIN	5.6 ± 2.0	5.5 ± 2.0
CEvNS	–	306 ± 20

Table I. A summary of prior prediction and best-fit event rates and statistical uncertainties for CEvNS and each background type. The standard-model expectation for CEvNS is $341 \pm 11 \pm 42$.

COHERENT Ar

Akimov et al., COHERENT Coll. PRL 126, 01002 (2021)

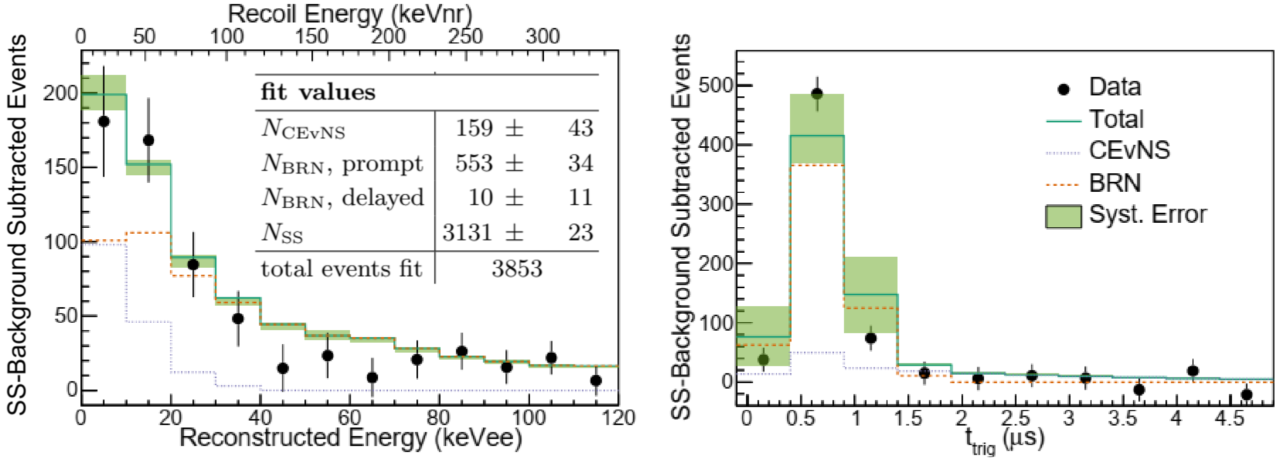

2022 New player: Dresden-II

+ 3 kg ultra-low noise germanium detector.

A strong preference for the presence of CEνNS is found.

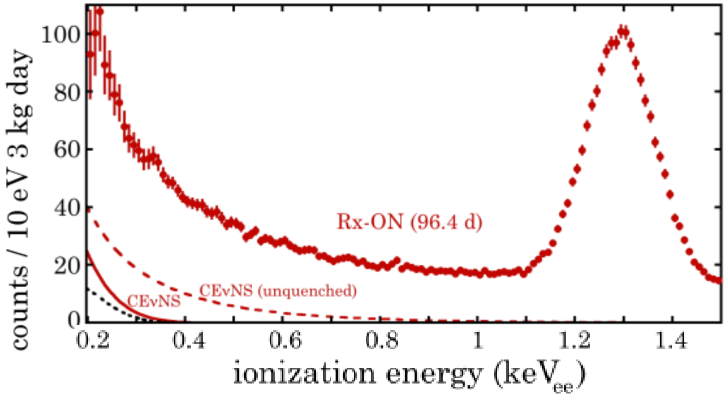

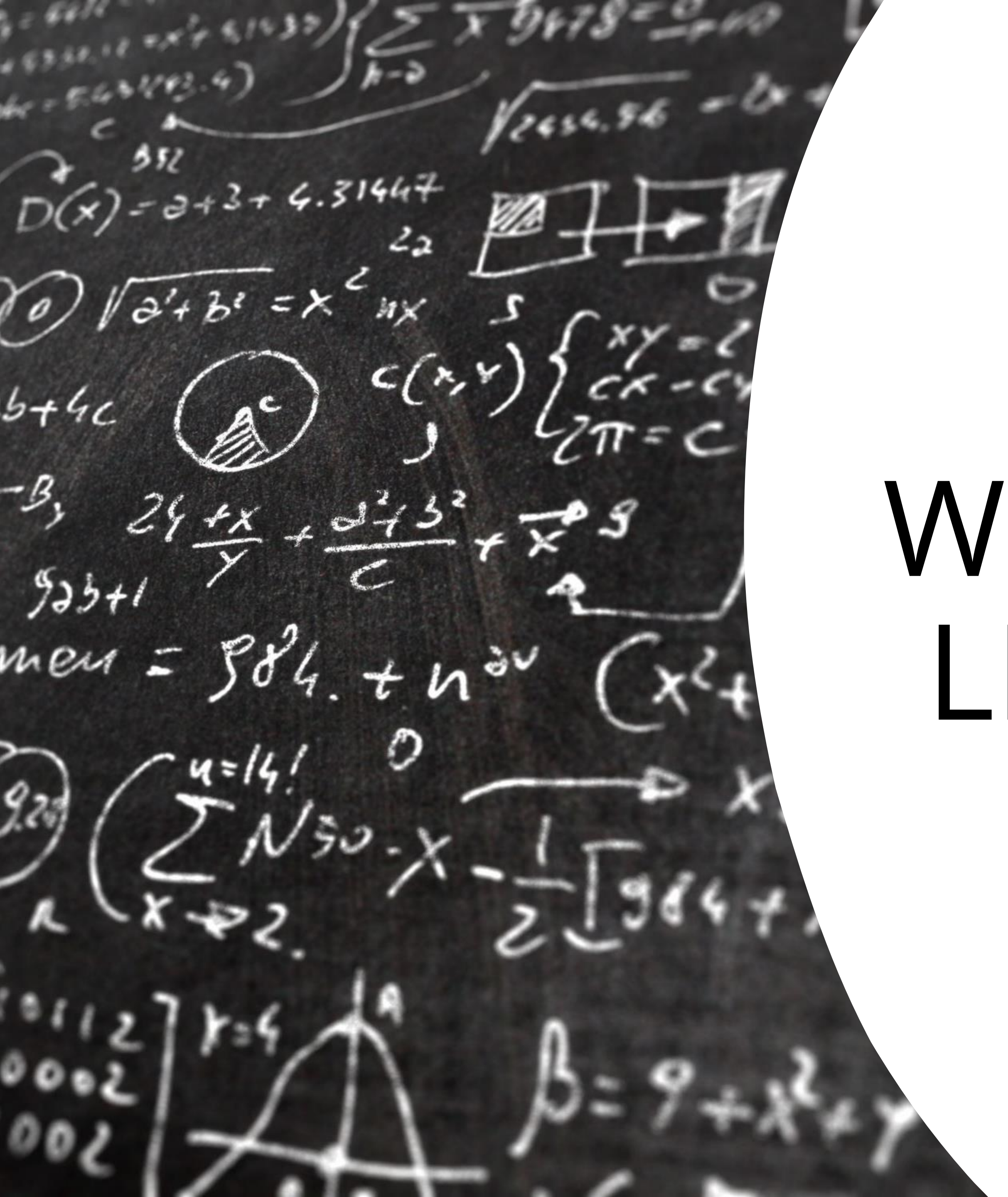

WHAT CAN WE LEARN FROM CEνNS?

What can we learn from CEνNS?

Mass of the nucleus

Neutrino energy

Fermi constant

SM vector proton coupling

SM vector neutron coupling

$$\frac{d\sigma(E_\nu, E_r)}{dE_r} \cong \frac{G_F^2 M}{\pi}\left(1-\frac{M E_r}{2E_\nu^2}\right)\left[\boldsymbol{g_V^p}\left(\sin^2(\vartheta_W)\right) Z\, \boldsymbol{F_Z}\left(|\vec{q}|^2\right) + \boldsymbol{g_V^n}\, N\, \boldsymbol{F_N}\left(|\vec{q}|^2\right)\right]^2$$

Nuclear recoil energy

Weak mixing angle

Proton Form Factor

Neutron Form Factor

Nuclear physics, but since $g_V^n \approx -0.51 \gg g_V^p(\nu_\ell) \approx 0.03$ neutrons contribute the most

- Neutrino-nucleon tree-level couplings

$$g_V^p = \frac{1}{2} - 2\sin^2(\vartheta_W) \cong \mathbf{0.0229}$$

$$g_V^n = -\frac{1}{2} = -0.5$$

J. Erler and S. Su. *Prog. Part. Nucl. Phys.* 71 (2013). arXiv:1303.5522 & PDG2021

- Radiative corrections are expressed in terms of WW, ZZ boxes and the neutrino charge radius diagram.

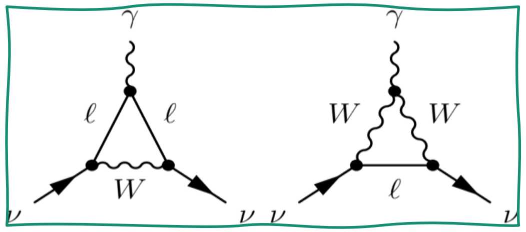

$$\underbrace{g_V^p(\nu_e) = 0.0382,\ g_V^p(\nu_\mu) = 0.0300}_{\text{Flavour dependence}} \text{ and } g_V^n = -0.5117$$

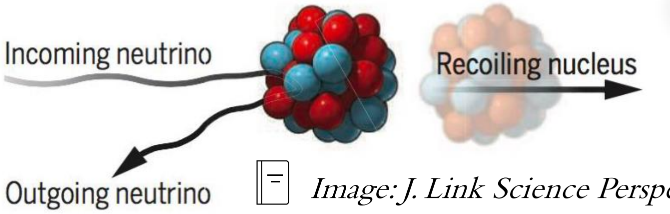

Image: J. Link Science Perspectives

$$\boxed{\frac{d\sigma}{dE_r} \propto N^2}$$

What can we learn from CEνNS?

See also E. Peinado's talk

M. Cadeddu et al., JHEP 01 (2021) 116, arXiv:2008.05022

O. G. Miranda et al., JHEP 05 (2020) 130, arXiv:2003.12050

M. Atzori Corona et al., JHEP 05 109 (2022), arXiv:2202.11002

C. Giunti, *PRD* 101 (2020) 3, 035039, arXiv:1909.00466

D. K. Papoulias and T. S. Kosmas, PRD 97, 033003 arxiv:1711.09773

D. A. Sierra et al., PRD 98, 075018 (2018) arXiv:1806.07424

L. J. Flores et al., JHEP 06 (2020) 045, 2002.12342

New ν interaction

M. Cadeddu et al., PRD 102, 015030 (2020), arXiv:2005.01645

O. G. Miranda et al., JHEP 05 (2020) 130, arXiv:2003.12050

A. N. Khan et al., PRD 100 (2019) 11, 113003, arXiv:2003.12050

O. G. Miranda et al., JHEP 07 (2019) 103, arXiv: 1905.03750

New ν properties

SM vector proton coupling

Proton Form Factor: very well-known

$$\frac{d\sigma(E_\nu,E_r)}{dE_r} \cong \frac{G_F^2 M}{\pi}\left(1-\frac{ME_r}{2E_\nu^2}\right)\left[g_V^p\left(\sin^2(\vartheta_W)\right) Z\, F_Z(|\vec{q}|^2) + g_V^n\, N\, F_N(|\vec{q}|^2)\right]^2 + \mathrm{add.\,terms}$$

Weak mixing angle

Neutron Form Factor

J. Erler and R. F. Hernandez JHEP03(2018)196 arXiv:1712.09146

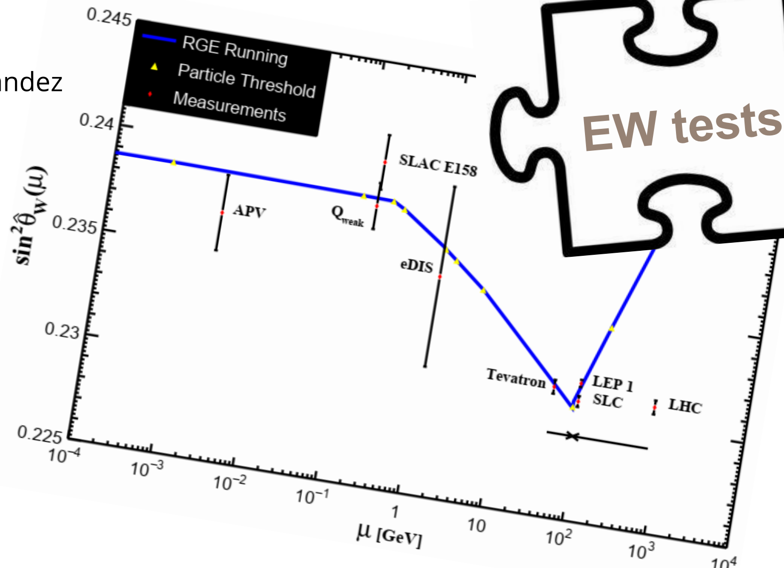

EW tests

See R. F. Hernandez's talk

This talk!

Nuclear physics

Nuclear physics with COHERENT(CsI) data… a chronological summary

Other works related to this topic I will not touch during this presentation

- X. R. Huang and L. W. Chen, PRD 100 (2019) 7, 071301, arXiv:1902.07625
- D. Papoulias et al., PLB 800 (2020) 135133, arXiv:1903.03722
- Coloma et al., JHEP 08 (2020) 08, 030, arXiv:2006.08624
- D. A. Sierra et al., JHEP 1906:141 (2019) arXiv: 1902.07398
- B. Canas et al., PRD 101, 035012 (2020), arXiv:1911.09831
- K. Patton, J. Engel, G. C. McLaughlin, and N. Schunck, Phys. Rev. C 86, 024612 (2012).

First average CsI neutron radius measurements (2018)

+ Using the first CsI dataset from D. Akimov et al. **Science** 357.6356 (2017)

M. Cadeddu, C. Giunti, Y.F. Li, Y.Y. Zhang, PRL 120 072501, (**2018**), arXiv:1710.02730

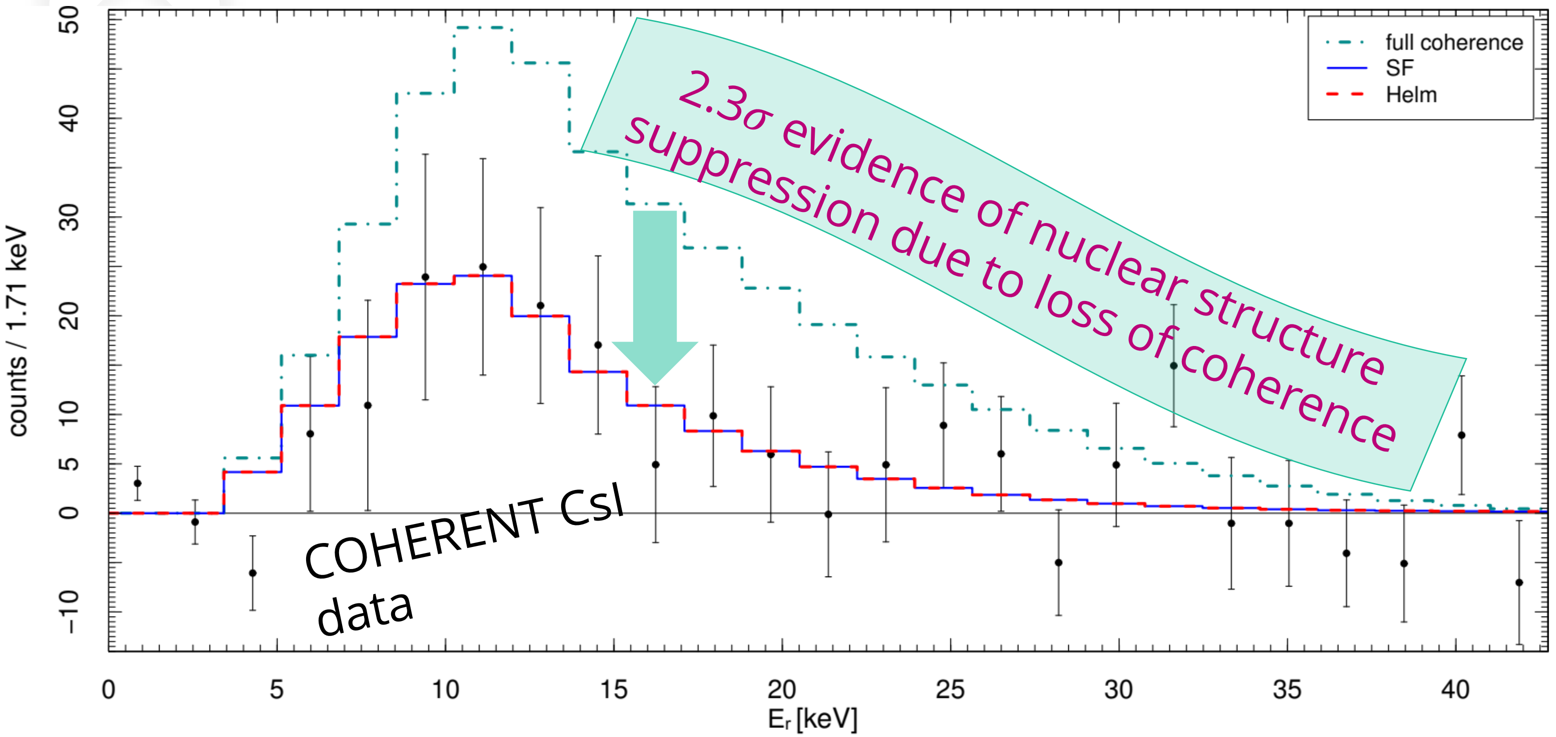

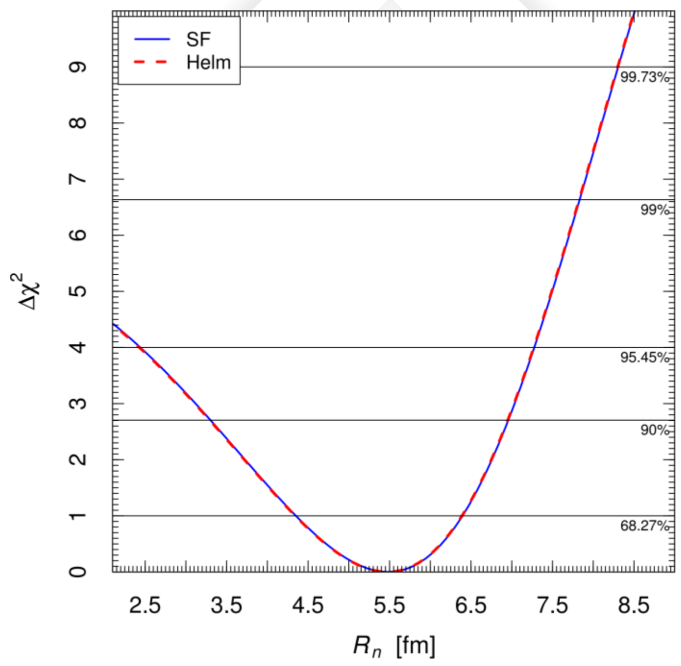

$$R_n^{CsI} = 5.5^{+0.9}_{-1.1}\ \text{fm}$$

✓ Only energy information used
x No energy resolution
x No time information
x Small dataset and big syst. uncer.

- We first compared the data with the predictions in the case of full coherence, i.e. all nuclear form factors equal to unity: the corresponding histogram does not fit the data.
- We fitted the COHERENT data in order to get information on the value of the neutron rms radius R_n, which is determined by the minimization of the χ^2 using the symmetrized Fermi (t=2.3 fm) and Helm form factors (s=0.9 fm).

The CsI neutron skin (in 2018)

$$R_n^{CsI} = 5.5^{+0.9}_{-1.1}\ \text{fm}$$

Proton rms radius for Cs and I

$R_p^{Cs} = 4.821(5)$ fm and
$R_p^{I} = 4.766(8)$ fm
are around 4.78 fm, with a difference of about 0.05 fm

G. Fricke et al., At. Data Nucl. Data Tables **60**, 177 (1995).

The neutron skin

$$\Delta R_{np}^{CsI} \equiv R_n - R_p \cong 0.7^{+0.9}_{-1.1}\ \text{fm}$$

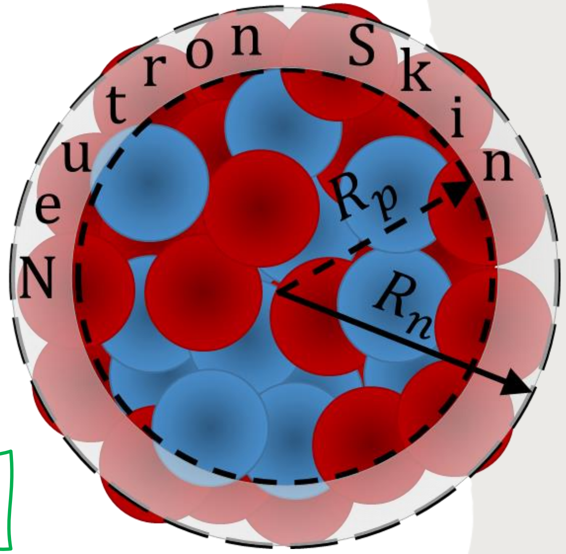

Theoretical values of the proton and neutron rms radii of Cs and I obtained with nuclear mean field models. The value was compatible with all the models…

Model	^{127}I R_p^{point}	R_p	R_n^{point}	R_n	$\Delta R_{np}^{\text{point}}$	ΔR_{np}	^{133}Cs R_p^{point}	R_p	R_n^{point}	R_n	$\Delta R_{np}^{\text{point}}$	ΔR_{np}
SHF SkI3 [81]	4.68	4.75	4.85	4.92	0.17	0.17	4.74	4.81	4.91	4.98	0.18	0.18
SHF SkI4 [81]	4.67	4.74	4.81	4.88	0.14	0.14	4.73	4.80	4.88	4.95	0.15	0.14
SHF Sly4 [82]	4.71	4.78	4.84	4.91	0.13	0.13	4.78	4.85	4.90	4.98	0.13	0.13
SHF Sly5 [82]	4.70	4.77	4.83	4.90	0.13	0.13	4.77	4.84	4.90	4.97	0.13	0.13
SHF Sly6 [82]	4.70	4.77	4.83	4.90	0.13	0.13	4.77	4.84	4.89	4.97	0.13	0.13
SHF Sly4d [83]	4.71	4.79	4.84	4.91	0.13	0.12	4.78	4.85	4.90	4.97	0.12	0.12
SHF SV-bas [84]	4.68	4.76	4.80	4.88	0.12	0.12	4.74	4.82	4.87	4.94	0.13	0.12
SHF UNEDF0 [85]	4.69	4.76	4.83	4.91	0.14	0.14	4.76	4.83	4.92	4.99	0.16	0.15
SHF UNEDF1 [86]	4.68	4.76	4.83	4.91	0.15	0.15	4.76	4.83	4.90	4.98	0.15	0.15
SHF SkM* [87]	4.71	4.78	4.84	4.91	0.13	0.13	4.76	4.84	4.90	4.97	0.13	0.13
SHF SkP [88]	4.72	4.80	4.84	4.91	0.12	0.12	4.79	4.86	4.91	4.98	0.12	0.12
RMF DD-ME2 [89]	4.67	4.75	4.82	4.89	0.15	0.15	4.74	4.81	4.89	4.96	0.15	0.15
RMF DD-PC1 [90]	4.68	4.75	4.83	4.90	0.15	0.15	4.74	4.82	4.90	4.97	0.16	0.15
RMF NL1 [91]	4.70	4.78	4.94	5.01	0.23	0.23	4.76	4.84	5.01	5.08	0.25	0.24
RMF NL3 [92]	4.69	4.77	4.89	4.96	0.20	0.19	4.75	4.82	4.95	5.03	0.21	0.20
RMF NL-Z2 [93]	4.73	4.80	4.94	5.01	0.21	0.21	4.79	4.86	5.01	5.08	0.22	0.22
RMF NL-SH [94]	4.68	4.75	4.86	4.94	0.19	0.18	4.74	4.81	4.93	5.00	0.19	0.19

Theoretically

$$0.12 < \Delta R_{np}^{CsI} < 0.24\ \text{fm}$$

But this is not the end of the story…
In 2020 the COHERENT Collaboration released a new CsI dataset

Improvements with the latest CsI dataset

+ New quenching factor

$$E_{ee} = f(E_{nr}) = aE_{nr} + bE_{nr}^2 + cE_{nr}^3 + dE_{nr}^4.$$

a=0.05546, b=4.307, c= -111.7, d=840.4

Akimov et al. (COHERENT Coll), arXiv:2111.02477

+ 2D fit, arrival time information included

$$N_{ij}^{\text{CE}\nu\text{NS}} = (N_i^{\text{CE}\nu\text{NS}})_{\nu_\mu} P_j^{(\nu_\mu)} + (N_i^{\text{CE}\nu\text{NS}})_{\nu_e,\bar{\nu}_\mu} P_j^{(\nu_e,\bar{\nu}_\mu)}$$

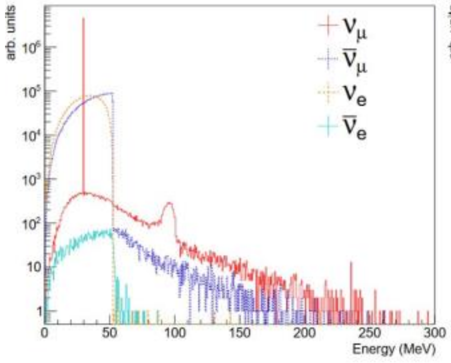

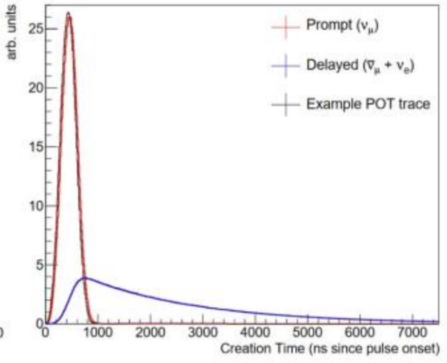

+ Doubled the statistics and reduced syst. uncertainties

$$\sigma_{\text{CE}\nu\text{NS}} = 13\%, \sigma_{\text{BRN}} = 0.9\%,$$
$$\text{and } \sigma_{\text{SS}} = 3\%$$

➢ Theoretical number of CEvNS events

$$N_i^{\text{CE}\nu\text{NS}} = N(\text{CsI}) \int_{T_{\text{nr}}^i}^{T_{\text{nr}}^{i+1}} dT_{\text{nr}}\, A(T_{\text{nr}}) \int_0^{T'^{\text{max}}_{\text{nr}}} dT'_{\text{nr}}\, R(T_{\text{nr}}, T'_{\text{nr}}) \int_{E_{\text{min}}(T'_{\text{nr}})}^{E_{\text{max}}} dE \times \sum_{\nu=\nu_e,\nu_\mu,\bar{\nu}_\mu} \frac{dN_\nu}{dE}(E) \frac{d\sigma_{\nu\text{-CsI}}}{dT'_{\text{nr}}}(E, T'_{\text{nr}}),$$

➢ With the inclusion of energy resolution

$$R(N_{\text{PE}}, N'_{\text{PE}}) = \frac{[a_R(1+b_R)]^{1+b_R}}{\Gamma(1+b_R)} N_{\text{PE}}^{b_R} e^{-a_R(1+b_R)N_{\text{PE}}}$$

✓ Analysis with a Gaussian least-square function

$$\chi^2_{\text{C}} = \sum_{i=2}^{9} \sum_{j=1}^{11} \left(\frac{N_{ij}^{\text{exp}} - \sum_{z=1}^{3} (1+\eta_z) N_{ij}^z}{\sigma_{ij}} \right)^2 + \sum_{z=1}^{3} \left(\frac{\eta_z}{\sigma_z} \right)^2,$$

Cadeddu et al., PRC 104, 065502, arXiv:2102.06153

Analysis updated in this talk using a Poissonian least-square function after the COHERENT data release!

The CsI neutron skin (updated in 2022)

$R_n^{CsI} = 5.4 \pm 0.4$ fm

~7% precision

Average proton rms radius for CsI

$R_p^{CsI} \approx 4.78$ fm

$\Delta R_{np}^{CsI} = 0.6 \pm 0.4$ fm

Cadeddu et al., PRC 104, 065502 arXiv:2102.06153
Updated in this talk!

Cadeddu et al., PRD 101, 033004 (2020), arXiv:1908.06045

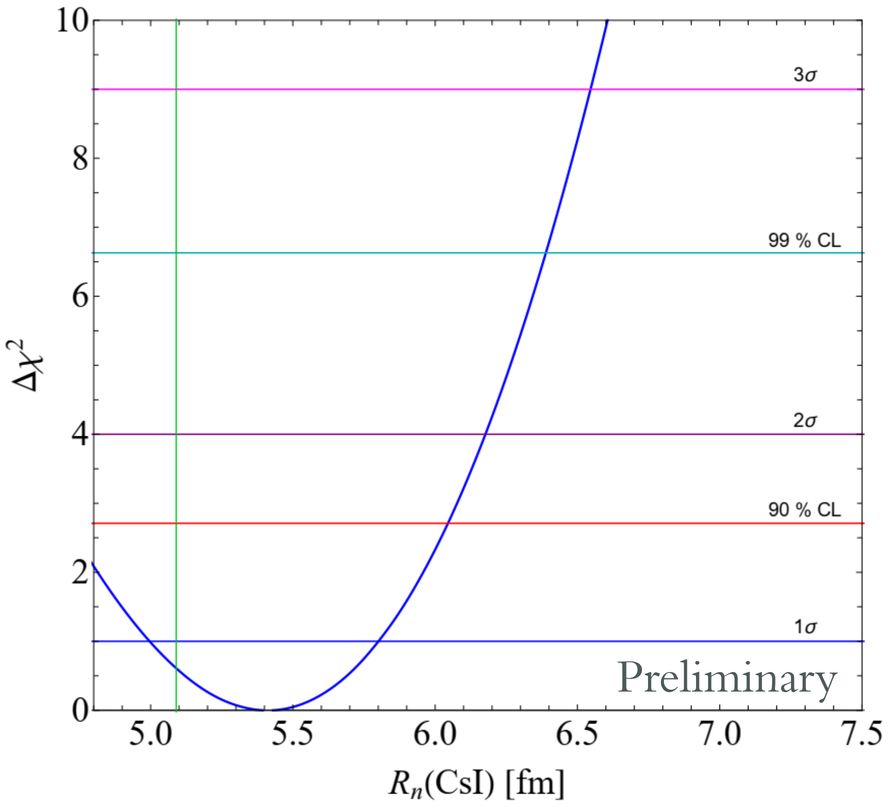

Only an averaged information is obtained, could we do more?

Use another electroweak process that measures the weak charge of Cs

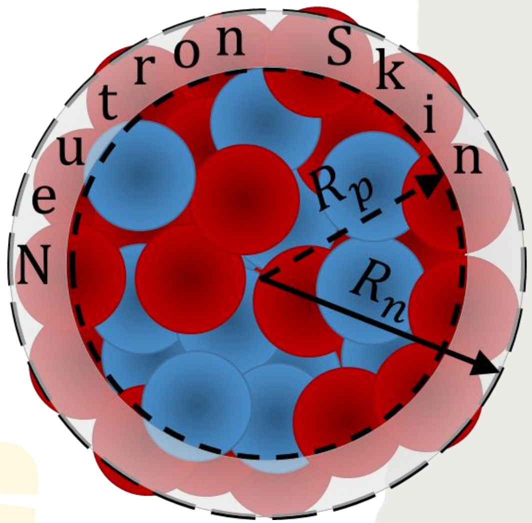

Atomic Parity Violation in cesium APV(Cs)

M. Cadeddu and F. Dordei, PRD 99, 033010 (2019), arXiv:1808.10202

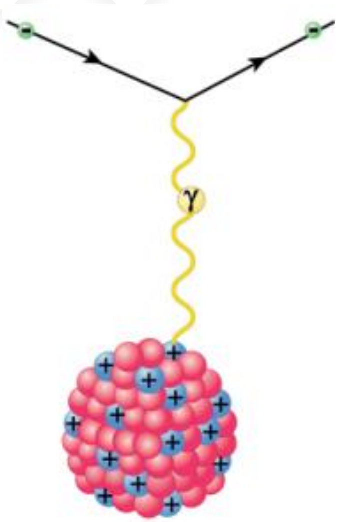

Interaction mediated by the photon and so mostly sensitive to the charge (proton) distribution

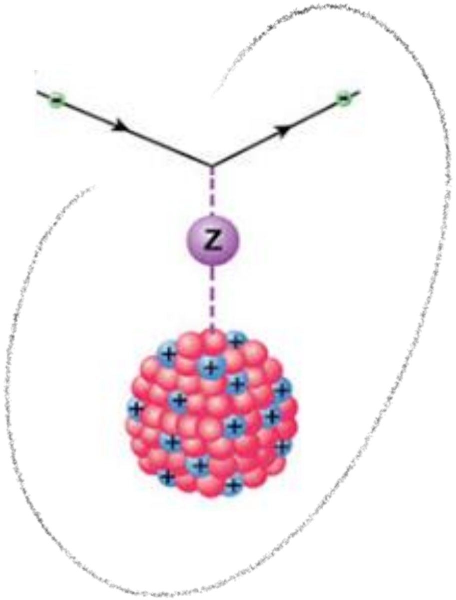

Interaction mediated by the Z boson and so mostly sensitive to the weak (neutron) distribution.

- Parity violation in an atomic system can be observed as an **electric dipole transition amplitude between two atomic states with the same parity**, such as the $6S$ and $7S$ states in cesium.
  - ➢ Indeed, a transition between two atomic states with same parity is forbidden by the parity selection rule and cannot happen with the exchange of a photon.
  - ✓ However, an electric dipole transition amplitude can be induced by a Z boson exchange between atomic electrons and nucleons → Atomic Parity Violation (APV) or Parity Non Conserving (PNC).

- The quantity that is measured is the usual **weak charge**

$$Q_W^{SM} \approx Z(1 - 4\sin^2\theta_W^{SM}) - N$$

Extracting the weak charge from APV

See talks of M. Safronova and B. K. Sahoo

$$Q_W = N \left(\frac{\mathrm{Im}\, E_{\mathrm{PNC}}}{\beta}\right)_{\mathrm{exp.}} \left(\frac{Q_W}{N\, \mathrm{Im}\, E_{\mathrm{PNC}}}\right)_{\mathrm{th.}} \beta_{\mathrm{exp.+th.}}$$

+ Experimental value of electric dipole transition amplitude between 6S and 7S states in Cs

C. S. Wood et al., Science **275**, 1759 (1997)

J. Guena, et al., PRA **71**, 042108 (2005)

PDG2020 average

$$\mathrm{Im}\left(\frac{E_{\mathrm{PNC}}}{\beta}\right) = -1.5924(55)\ \mathrm{mV/cm}$$

✓ Theoretical amplitude of the electric dipole transition

$$E_{\mathrm{PNC}} = \sum_n \left[\frac{\langle 6s|H_{\mathrm{PNC}}|np_{1/2}\rangle\langle np_{1/2}|\boldsymbol{d}|7s\rangle}{E_{6s} - E_{np_{1/2}}} + \frac{\langle 6s|\boldsymbol{d}|np_{1/2}\rangle\langle np_{1/2}|H_{\mathrm{PNC}}|7s\rangle}{E_{7s} - E_{np_{1/2}}}\right],$$

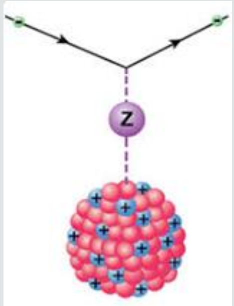

- where ***d*** is the electric dipole operator, and

$$H_{\mathrm{PNC}} = -\frac{G_F}{2\sqrt{2}} Q_W \gamma_5 \rho(\boldsymbol{r})$$

S. G. Porsev et al. PRD 82, 036008 (2010)

B. K. Sahoo et al. PRD 103, L111303 (2021)

$$\mathrm{Im}\, E_{\mathrm{PNC}} = (0.8977 \pm 0.0040) \times 10^{-11} |e|\, a_B\, Q_W/N$$

Used by PDG2020 (V. Dzuba *et al.*, PRL 109, 203003 (2012)) but see also

nuclear Hamiltonian describing the **electron-nucleus weak interaction**

$\rho(\boldsymbol{r}) = \rho_p(\boldsymbol{r}) = \rho_n(\boldsymbol{r}) \rightarrow$ **neutron skin correction** needed

β: tensor transition polarizability

It characterizes the size of the Stark mixing induced electric dipole amplitude (external electric field)

Bennet & Wieman, PRL 82, 2484 (1999)

Dzuba & Flambaum, PRA 62 052101 (2000)

PDG2020 average

$\beta = 27.064\ (33)\ a_B^3$

Atomic Parity Violation for weak mixing angle measurements

✓ Weak charge in the SM including radiative corrections

Using SM prediction at low energy
$\sin^2\hat{\theta}_W(0) = 0.23857(5)$

$$Q_W^{SM+\text{r.c.}} \equiv -2\left[Z\left(g_{AV}^{ep} + 0.00005\right) + N\left(g_{AV}^{en} + 0.00006\right)\right]\left(1 - \frac{\alpha}{2\pi}\right) \approx Z\left(1 - 4\sin^2\theta_W^{SM}\right) - N$$

Theoretically

$$Q_W^{SM\ \text{th}}\left({}^{133}_{55}Cs\right) = -73.23(1)$$

1σ difference

Experimentally

$$Q_W^{\text{exp.}}\left({}^{133}_{55}Cs\right) = -72.82(42)$$

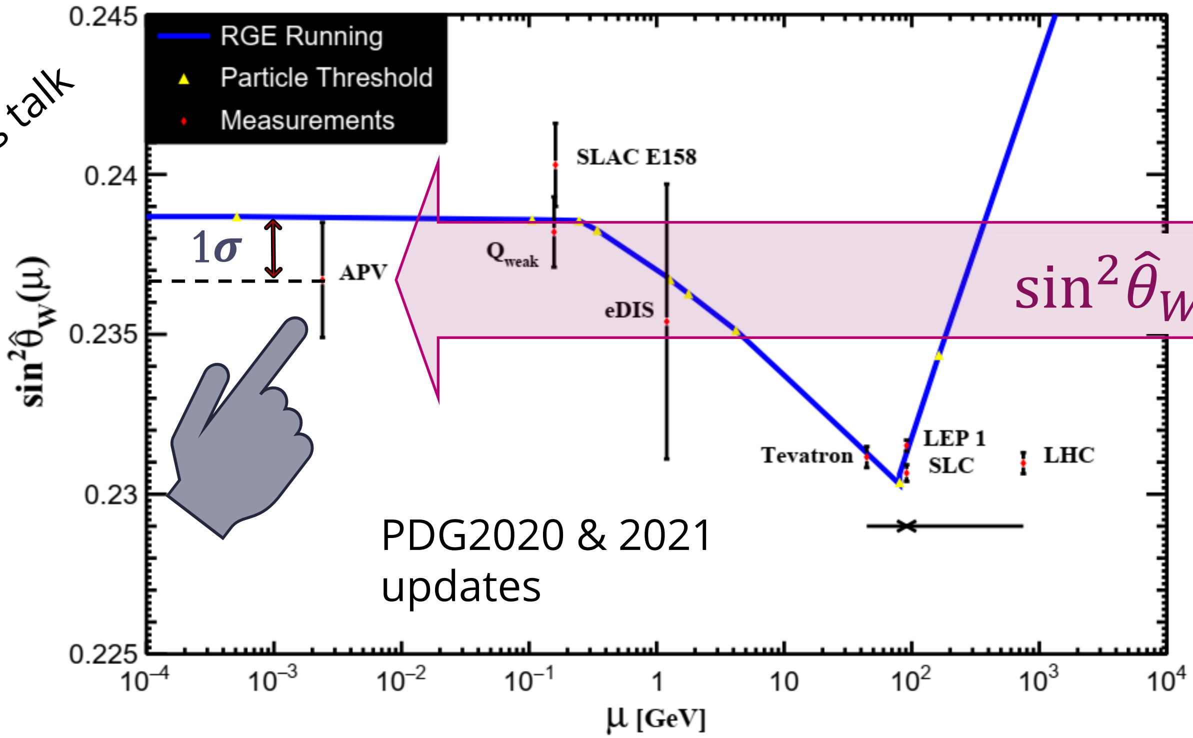

$\sin^2\hat{\theta}_W(2.4\ \text{MeV}) = 0.2367 \pm 0.0018$

See R. F. Hernandez's talk

P.A. Zyla et al. (PDG), Prog. Theor. Exp. Phys. 2020, 083C01 (2020) and 2021 update.

But which Cs neutron skin correction is used?

Extrapolated value of ΔR_{np}^{Cs}

- Neutron-skin of a variety of nuclei as extracted from **antiprotonic data** as a function of the asymmetry parameter, I.

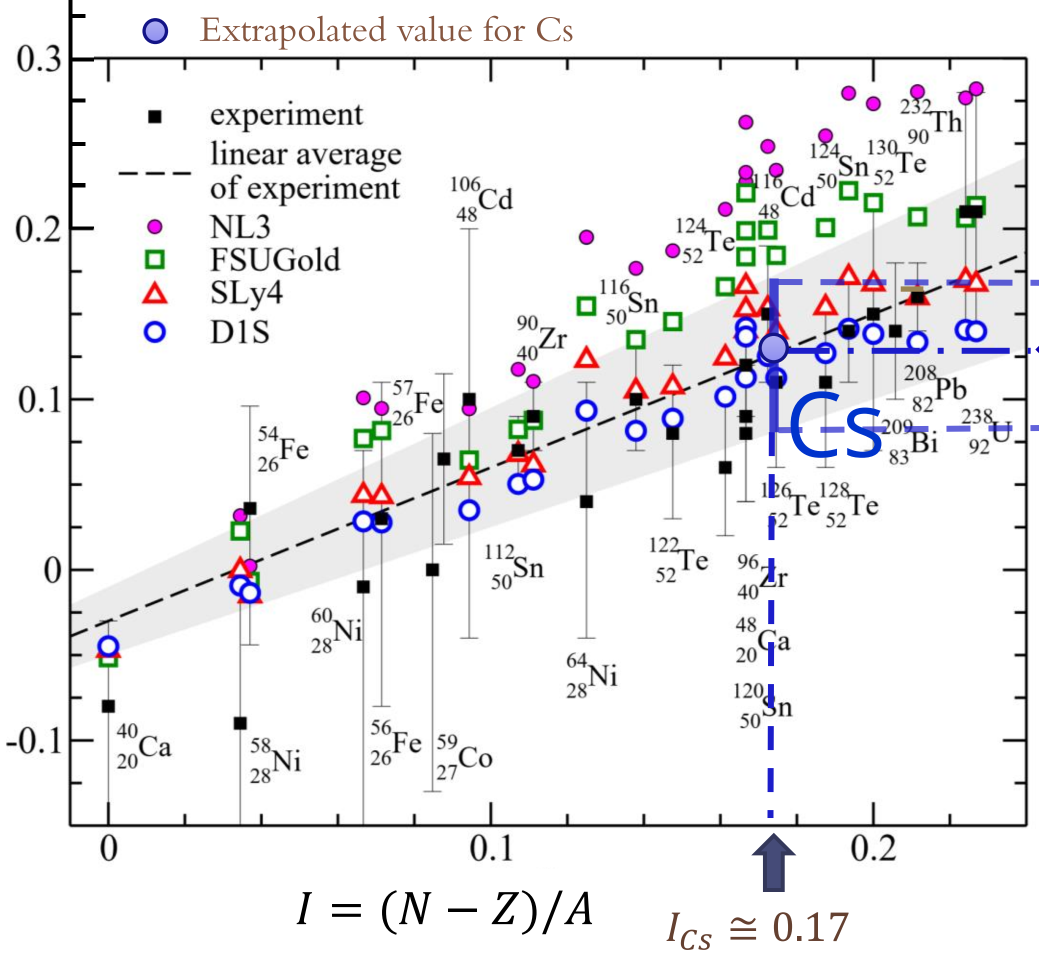

A. Trzcinska et al. s, PRL. 87, 082501 (2001)

- ✓ From this **linear fit** one obtains the relation for the neutron skin for every nuclei

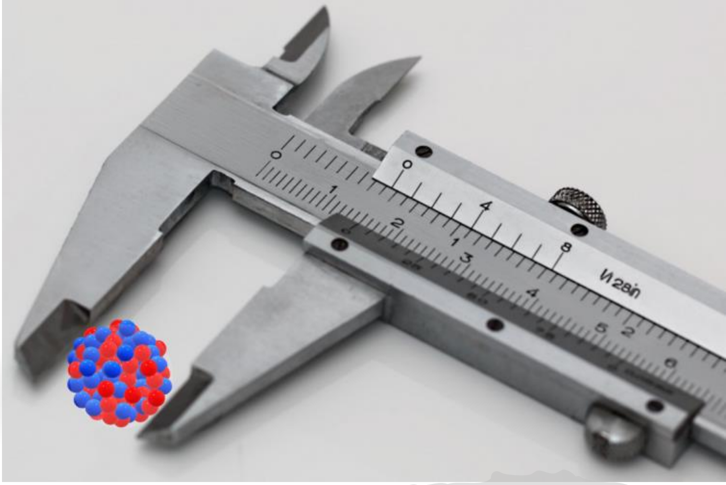

$$\Delta R_{np}[\text{fm}] = -(0.04 \pm 0.03) + (1.01 \pm 0.15)\frac{N-Z}{A}$$

For cesium it gives

$$\Delta R_{np}^{Cs}(\text{extrap}) \cong 0.13 \pm 0.04 \text{ fm}$$

Extrapolated (not measured) value for cesium!

Antiprotonic data: radiochemical and the other based on x-ray data constraining the neutron distribution at the nuclear periphery

M. Thiel et al., Journal of Physics G, 46, 9 (2019), arXiv:1904.12269v1

Extrapolated value of ΔR_{np}^{Cs}

See also G. Hagen's talk

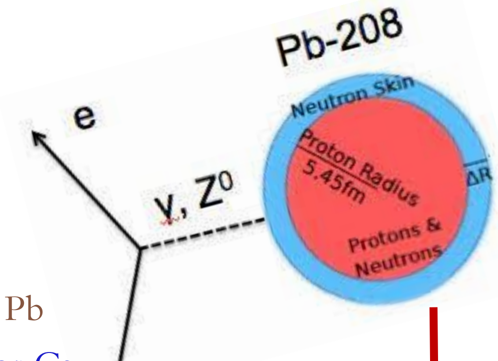

PREX-I & PREX-II

$\Delta R_{np}^{Pb} = 0.283 \pm 0.071$ fm

D. Adhikari *et al.* PRL 126, 172502 (2021)

See talks of K. Kumar and N. Cargioli

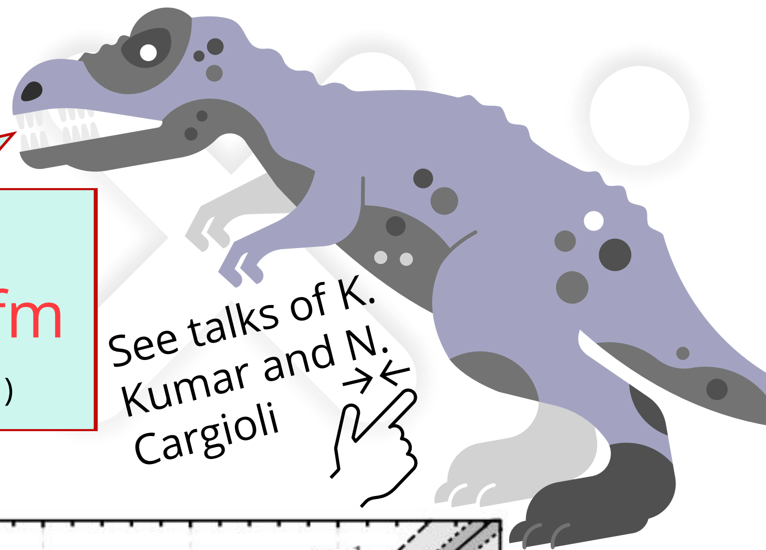

Meausered value for Pb

Extrapolated value for Cs

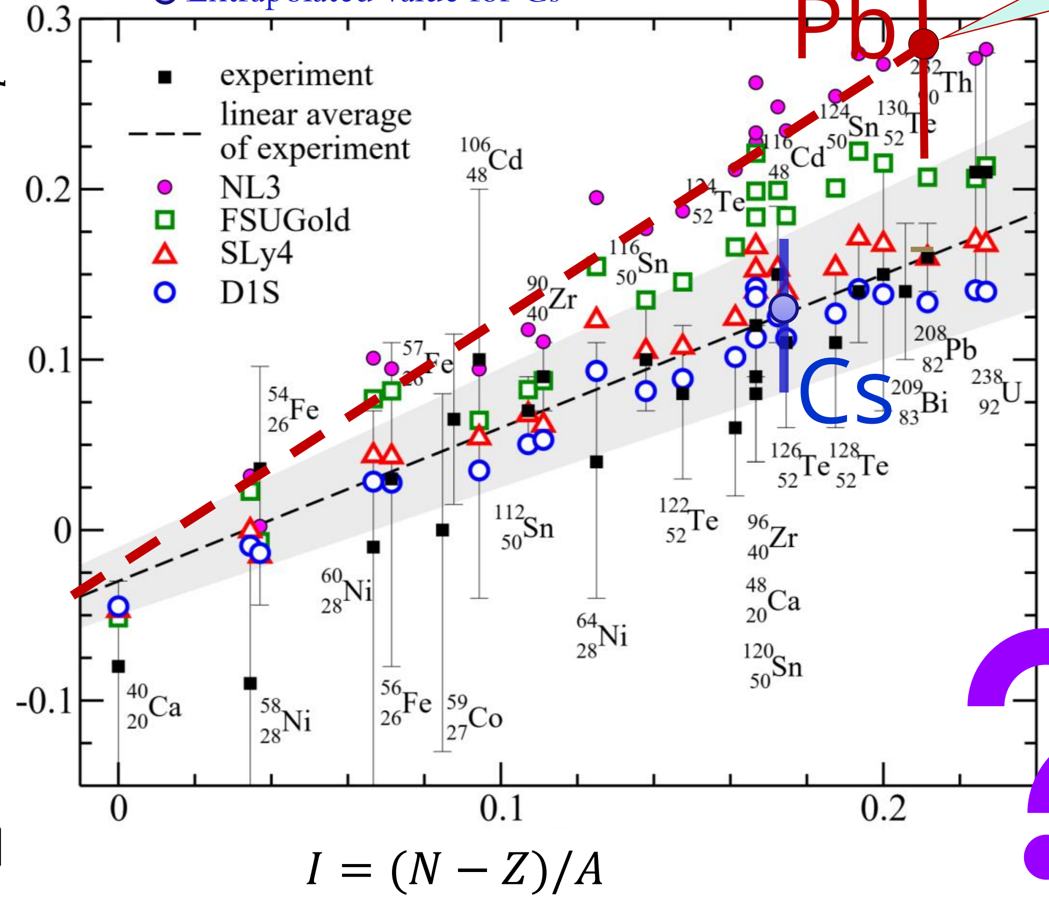

A. Trzcinska et al. s, PRL. 87, 082501 (2001

?

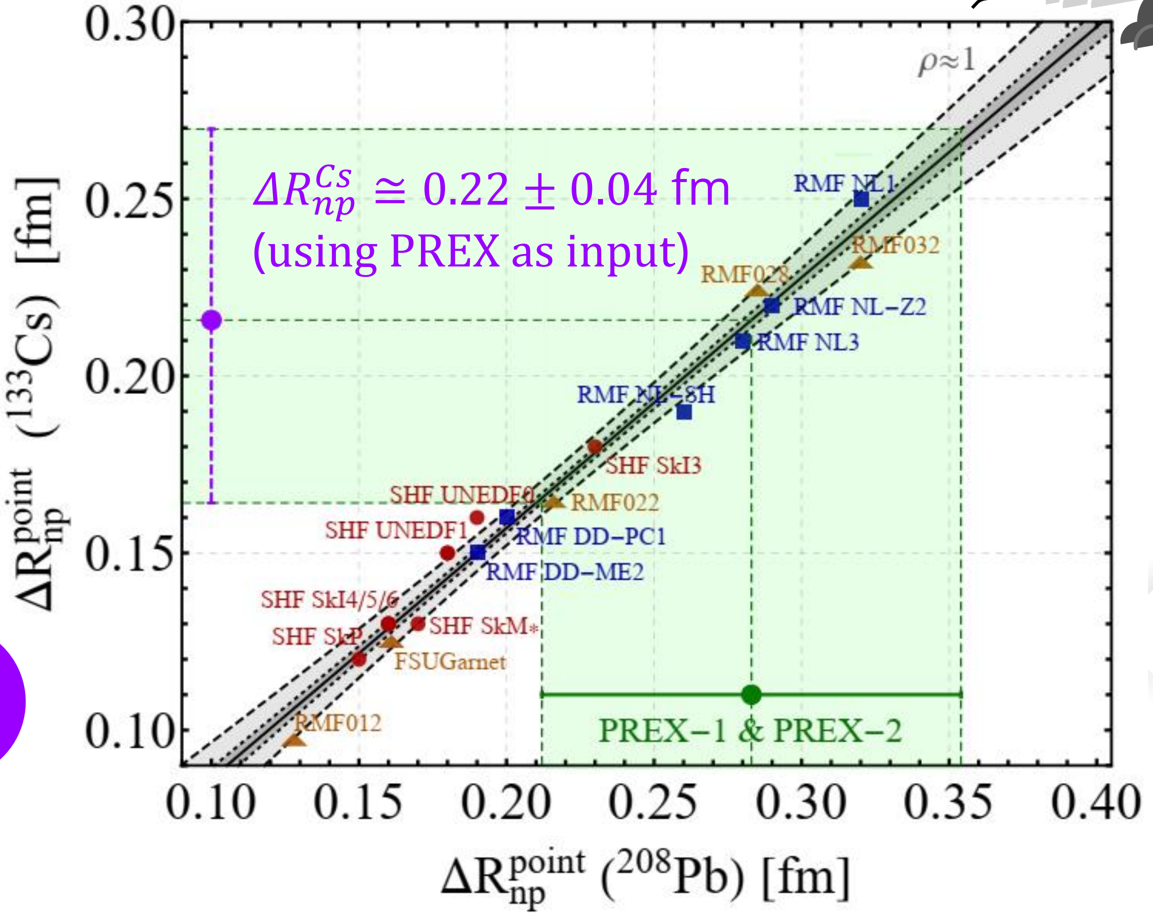

M. Cadeddu et al. PRD 104, L011701 (2021), arXiv:2104.03280

The dilemma

APV (Cs)

+ Sensitive to the weak mixing angle
+ Less sensitive to the neutron skin

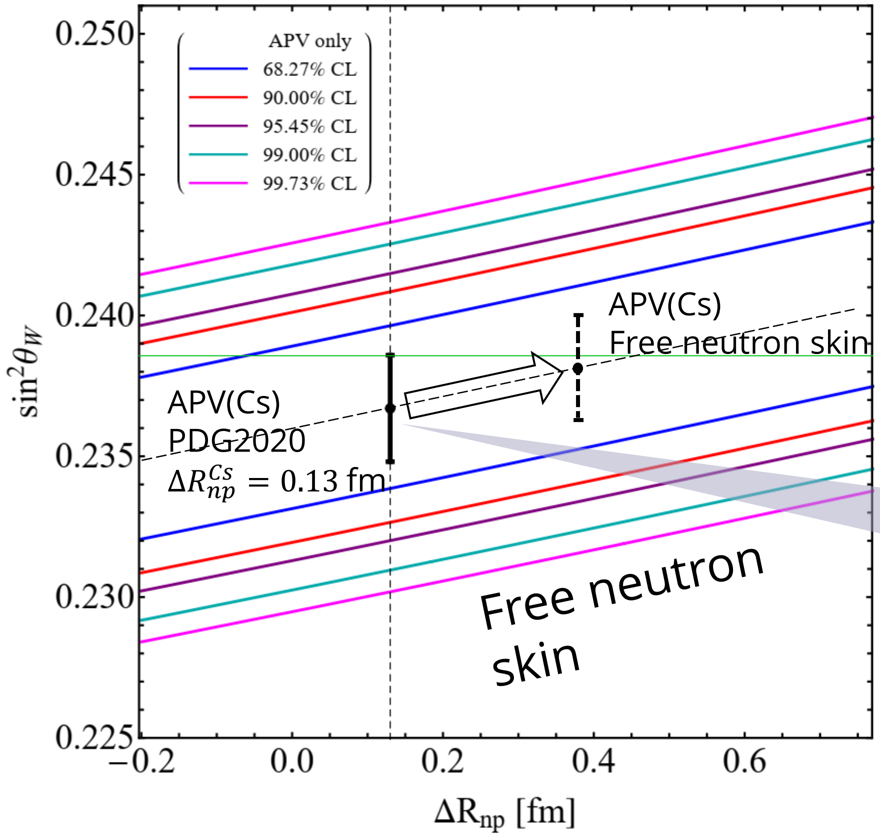

APV(Cs) PDG2020 corresponds to $\Delta R_{np}^{Cs}(\text{Extr.}) = 0.13$ fm

Extrapolated from antiprotonic atoms…

COHERENT (CsI)

+ CEνNS is sensitive to the neutron skin
+ But less sensitive to the weak mixing angle

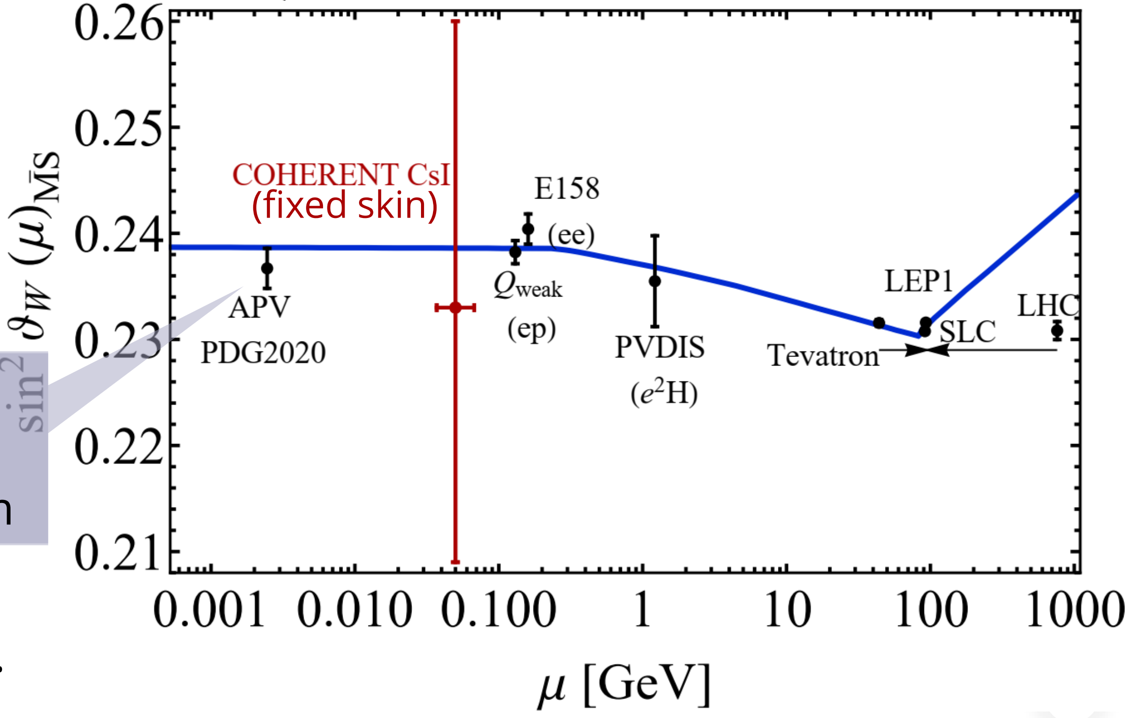

The solution

to make a combined COHERENT (CsI) & APV(Cs) fit in order to exploit properly the ΔR_{np}^{Cs} - $\sin^2 \hat{\theta}_W$ correlation using experimental data and minimizing external assumptions

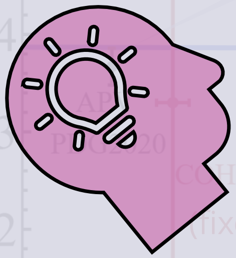

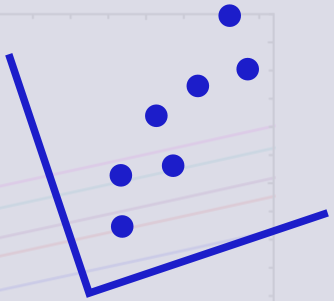

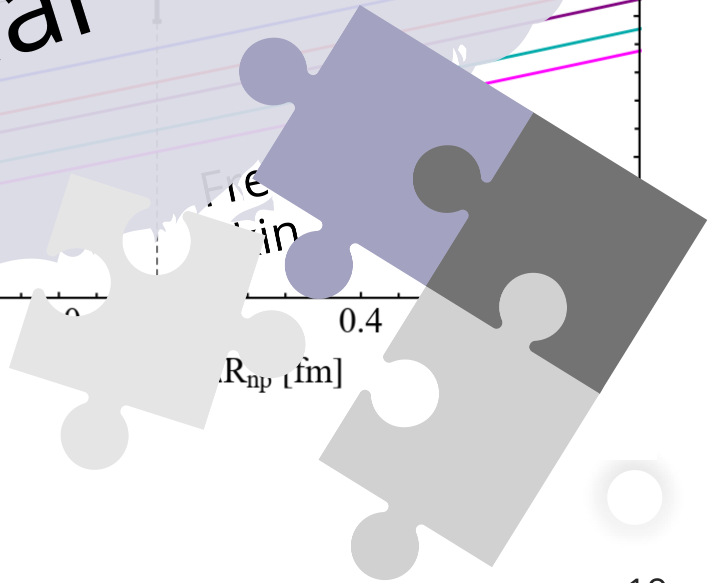

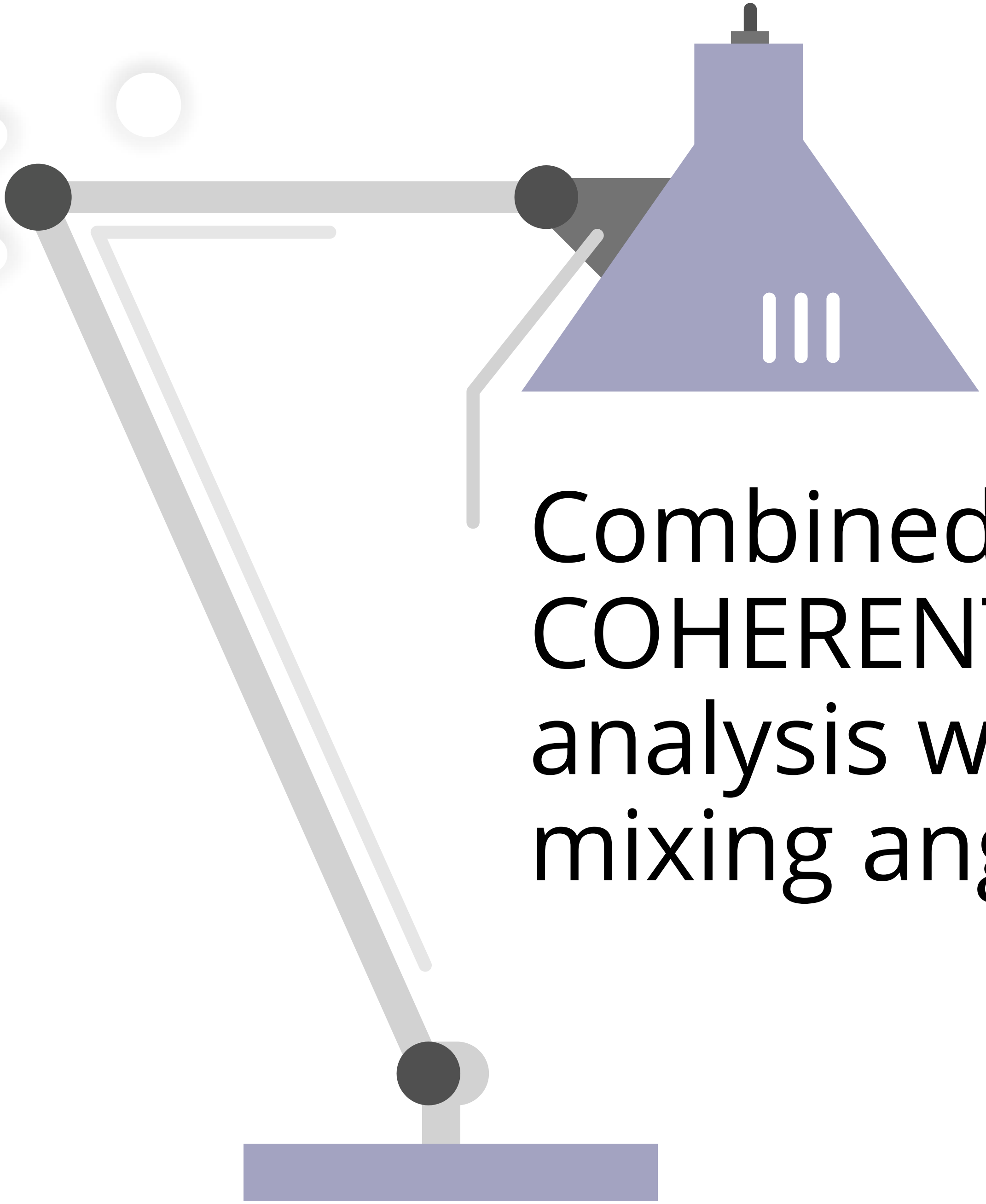

Combined COHERENT(CsI)+ APV(Cs) analysis with fixed weak mixing angle

First advantage of the combination

✓ Assuming to know the value of the weak mixing angle at low energy $\sin^2\hat{\theta}_W(0) = 0.23857(5)$

COHERENT χ^2 APV χ^2

$$\chi^2 = \chi^2_{\mathrm{C}} + \left(\frac{Q_W^{\mathrm{Cs\,ns}}(R_n) - Q_W^{\mathrm{th}}(\sin^2\vartheta_W)}{\sigma_{\mathrm{APV}}(R_n, \sin^2\vartheta_W)} \right)^2$$

$\Delta R_{np}(^{127}\mathrm{I}) = R_n - R_p = 0.8^{+0.9}_{-0.8}$ fm

$\Delta R_{np}(^{133}\mathrm{Cs}) = R_n - R_p = 0.45^{+0.33}_{-0.33}$ fm

Contribution of Cs and I disentangled!!

$R_n(\mathrm{Cs}) = 5.27^{+0.33}_{-0.33}$ fm $R_n(\mathrm{I}) = 5.6^{+0.9}_{-0.8}$ fm $\chi^2_{\mathrm{min}} = 85.3$

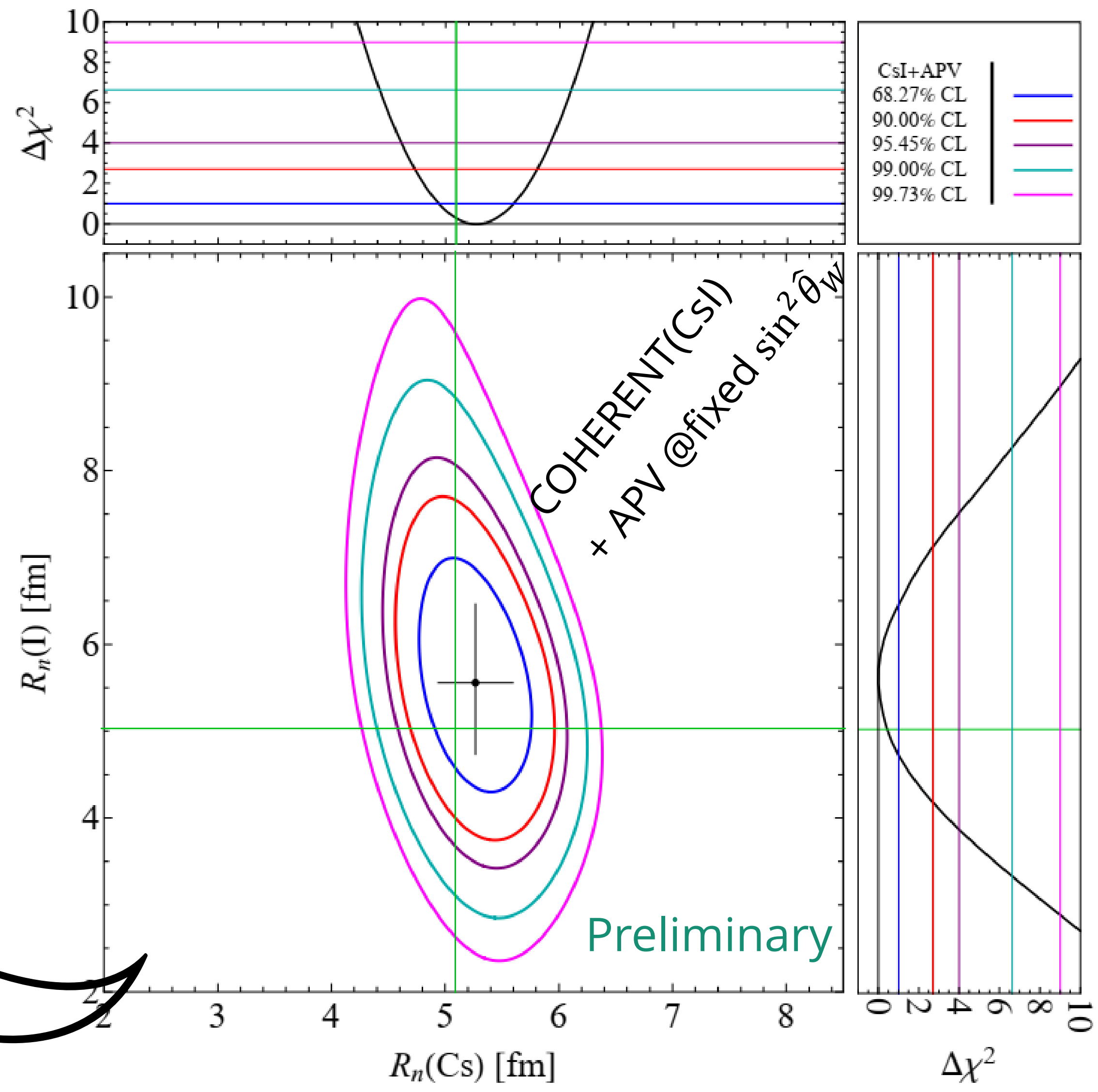

Cadeddu et al., PRC 104, 065502
arXiv:2102.06153 Updated in this talk!

Leaving free to vary both the weak mixing angle and the neutron radius*

*average CsI neutron radius

Second advantage: extract both R_n(CsI) and $\sin^2\hat{\theta}_W$ from data

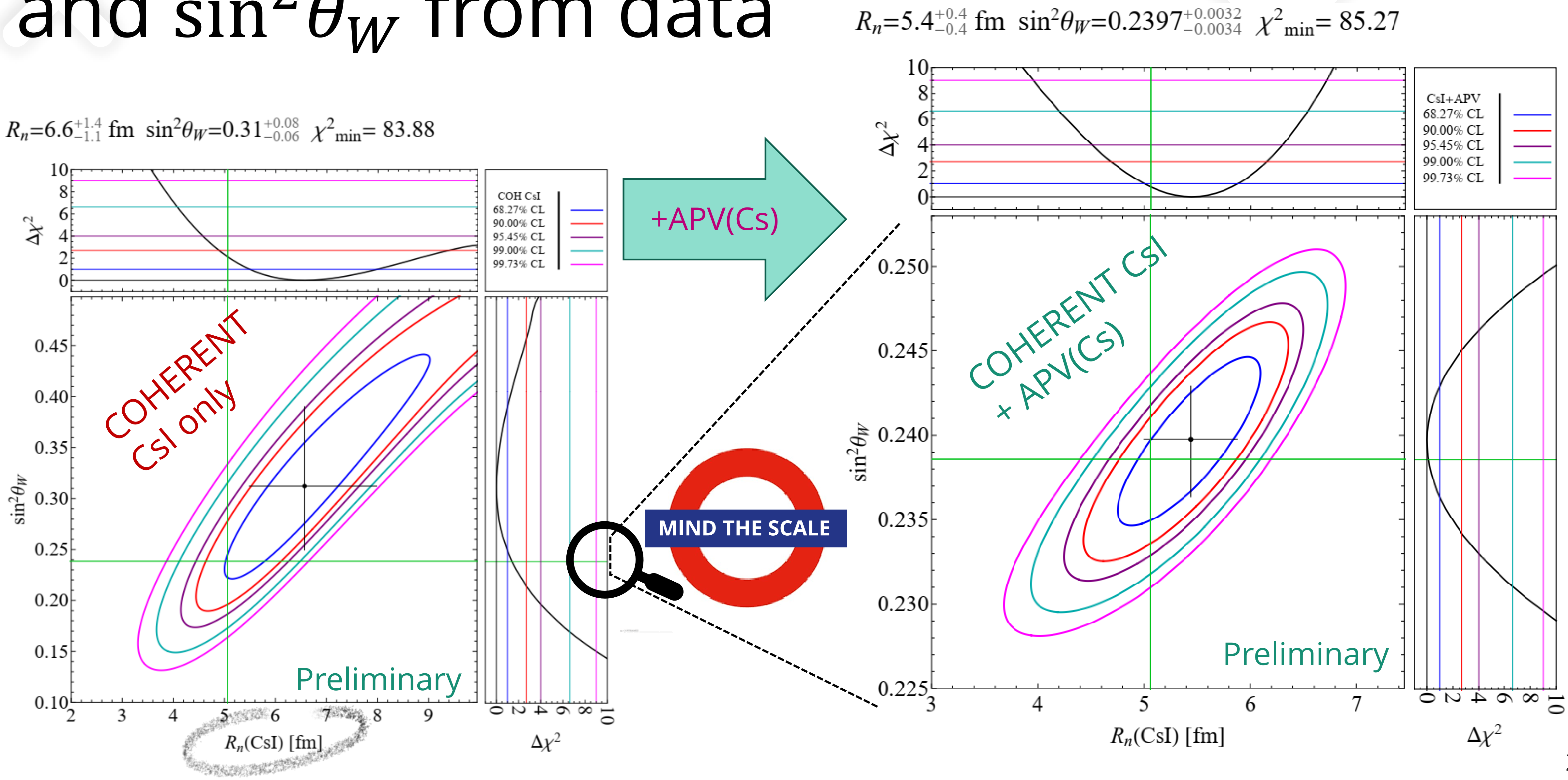

Second advantage: extract both R_n(CsI) and $\sin^2\hat{\theta}_W$ from data

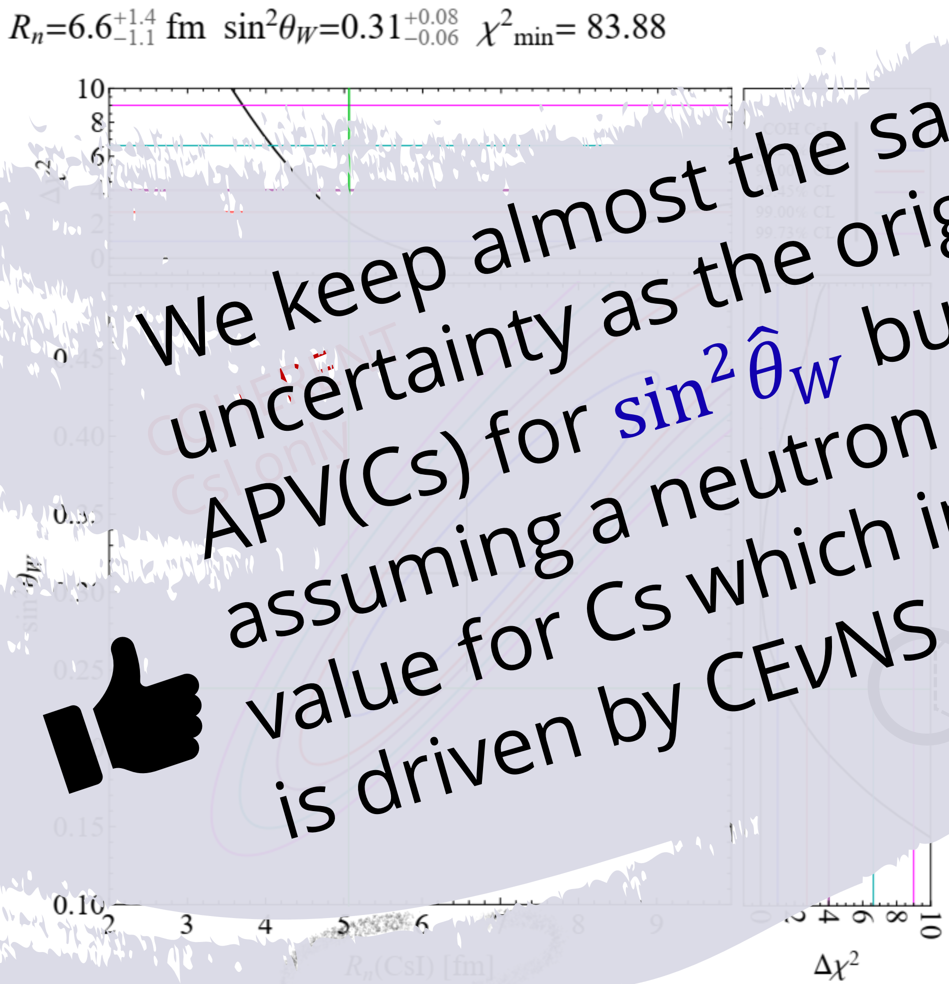

We keep almost the same uncertainty as the original APV(Cs) for $\sin^2\hat{\theta}_W$ but not assuming a neutron skin value for Cs which instead is driven by CEνNS

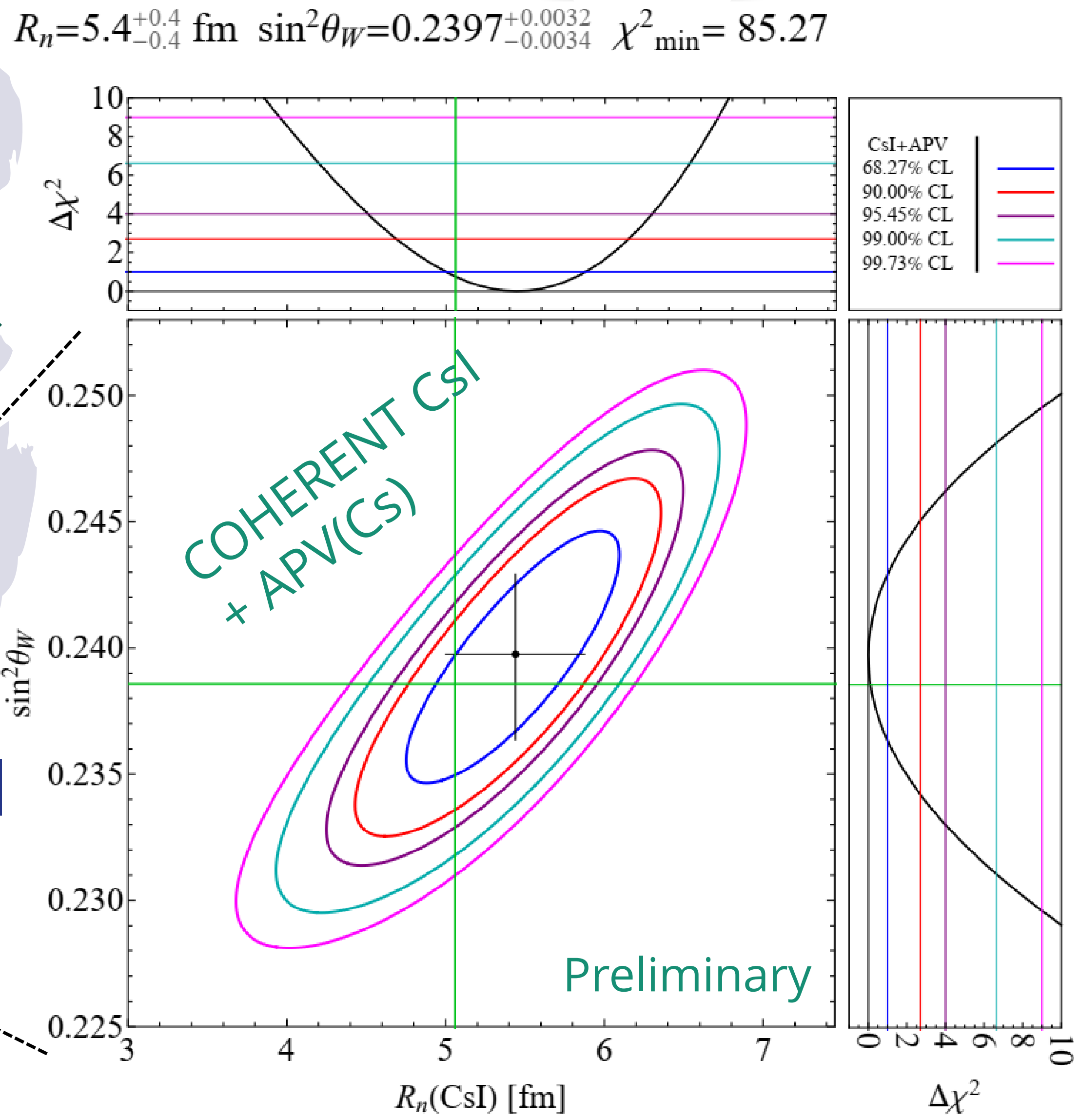

Second advantage: extract both R_n and $\sin^2\hat{\theta}_W$ from data

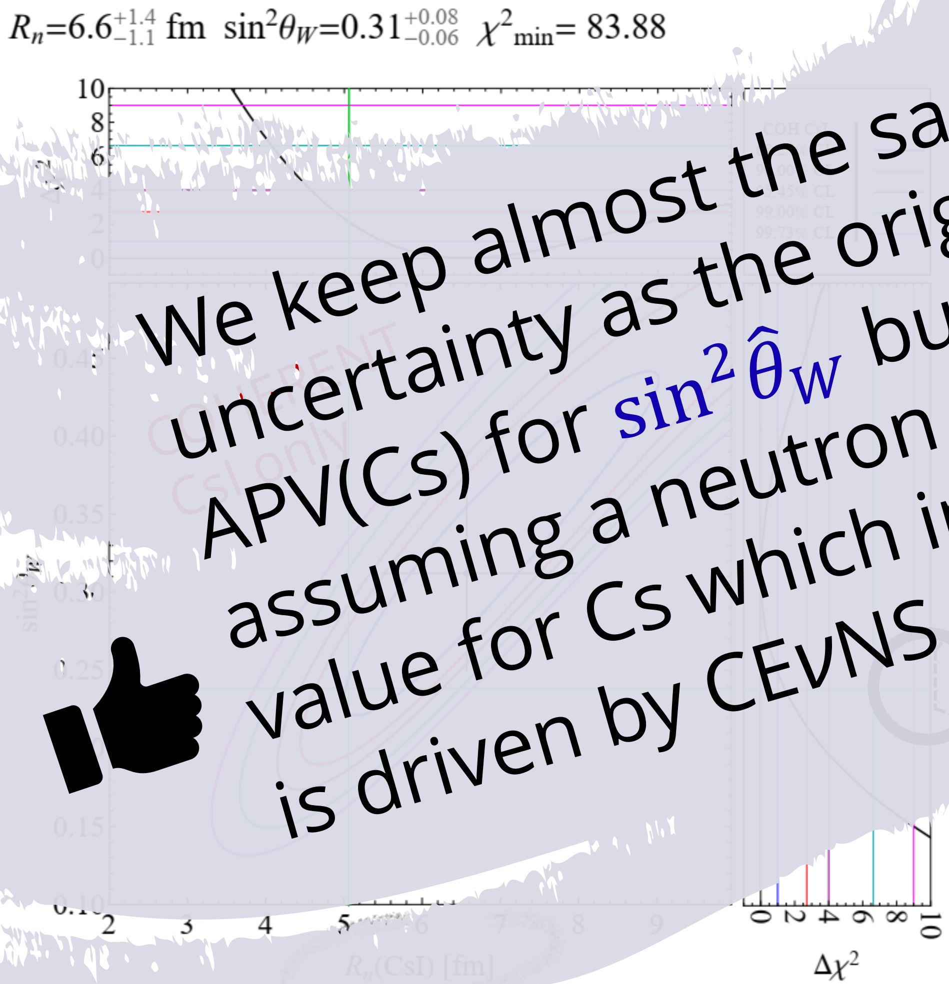

We keep almost the same uncertainty as the original APV(Cs) for $\sin^2\hat{\theta}_W$ but not assuming a neutron skin value for Cs which instead is driven by CEνNS

No assumptions on ΔR_{np}^{Cs} are made. The skin is taken directly from CEνNS experimental data

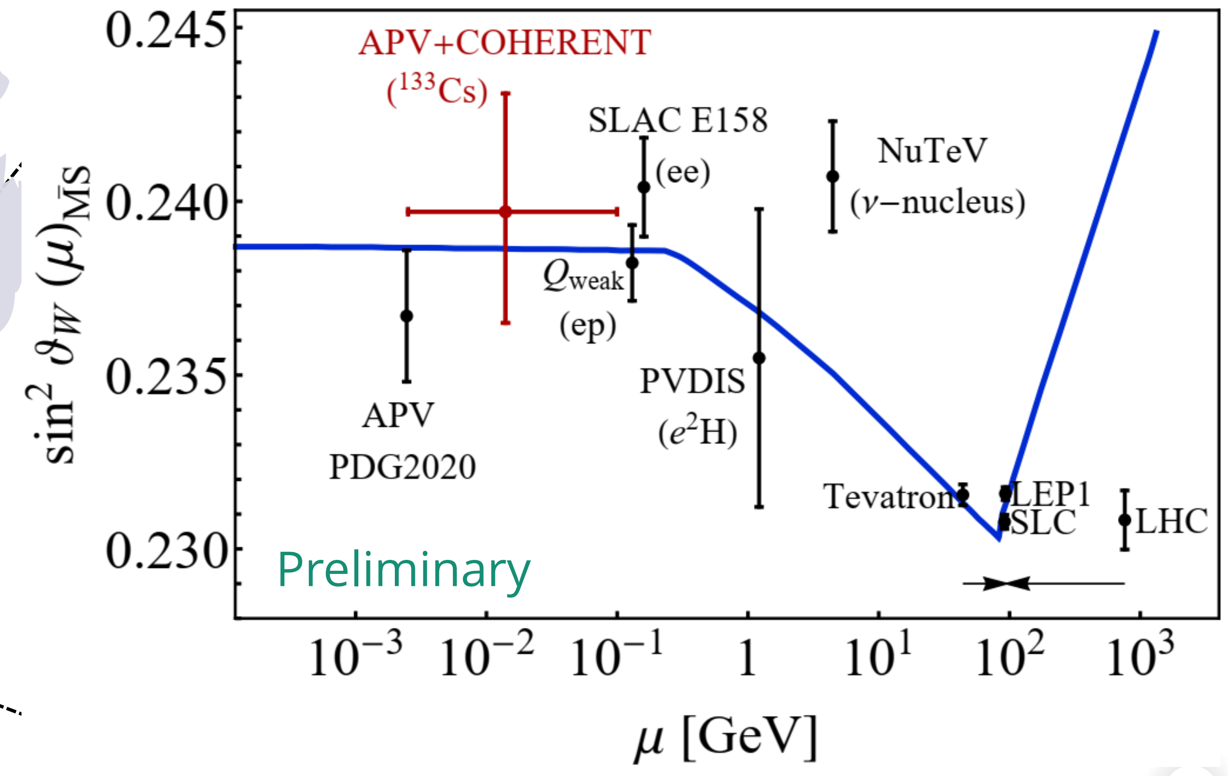

A new player in the game: CEνNS from Dresden-II reactor neutrinos

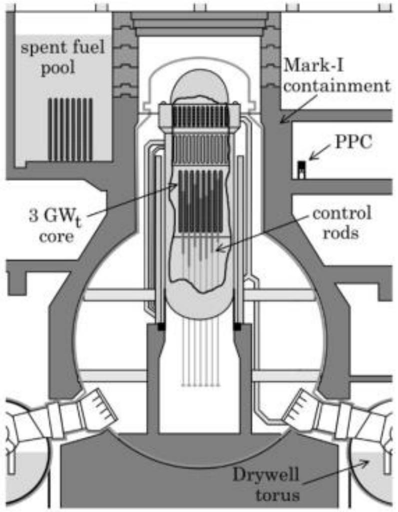

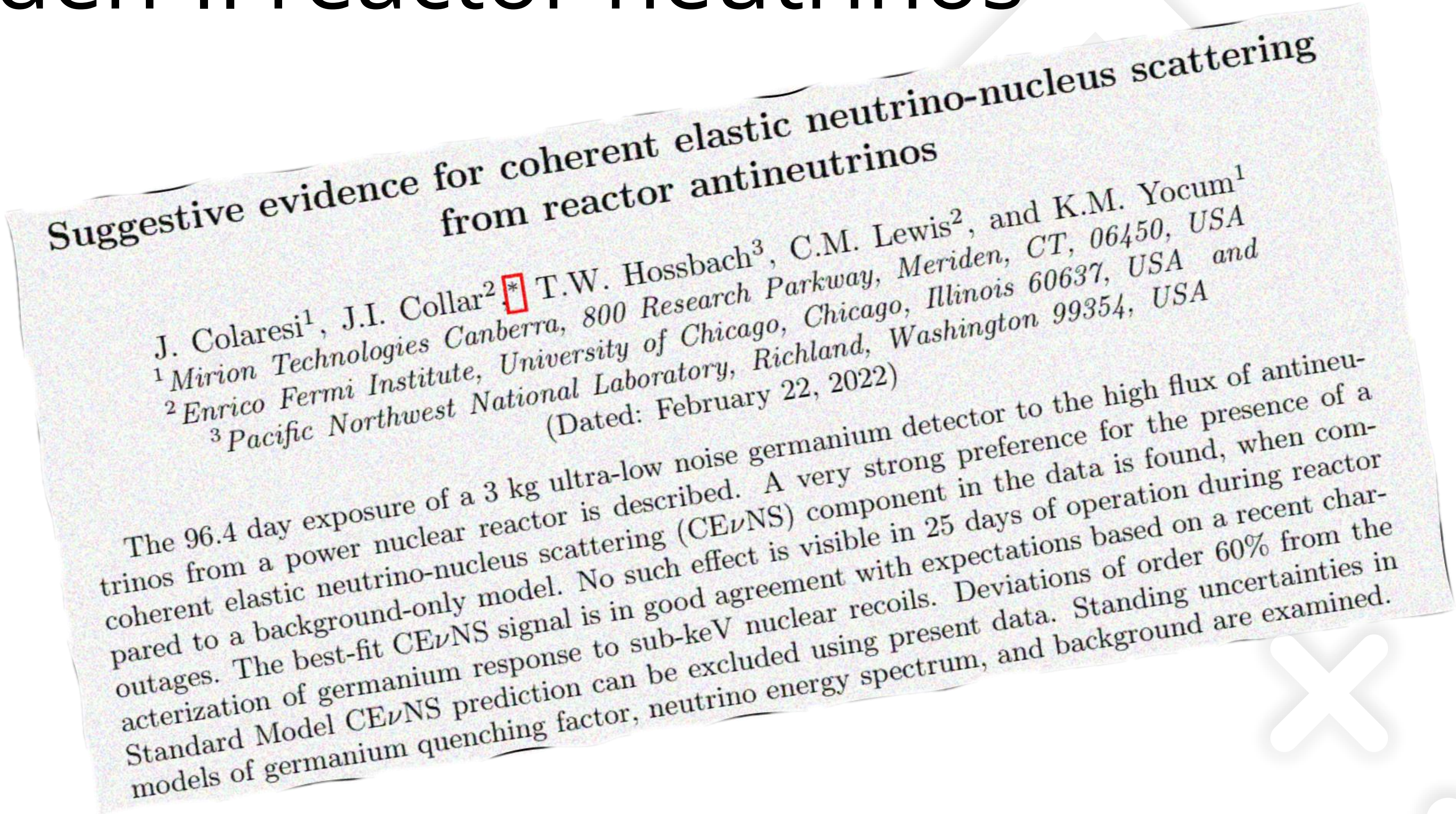

Suggestive evidence for coherent elastic neutrino-nucleus scattering from reactor antineutrinos

J. Colaresi[1], J.I. Collar[2,*], T.W. Hossbach[3], C.M. Lewis[2], and K.M. Yocum[1]
[1] *Mirion Technologies Canberra, 800 Research Parkway, Meriden, CT, 06450, USA*
[2] *Enrico Fermi Institute, University of Chicago, Chicago, Illinois 60637, USA* and
[3] *Pacific Northwest National Laboratory, Richland, Washington 99354, USA*
(Dated: February 22, 2022)

The 96.4 day exposure of a 3 kg ultra-low noise germanium detector to the high flux of antineutrinos from a power nuclear reactor is described. A very strong preference for the presence of a coherent elastic neutrino-nucleus scattering (CEνNS) component in the data is found, when compared to a background-only model. No such effect is visible in 25 days of operation during reactor outages. The best-fit CEνNS signal is in good agreement with expectations based on a recent characterization of germanium response to sub-keV nuclear recoils. Deviations of order 60% from the Standard Model CEνNS prediction can be excluded using present data. Standing uncertainties in models of germanium quenching factor, neutrino energy spectrum, and background are examined.

Colaresi et al. arXiv:2202.09672v1, 19 Feb 2022

Dresden-II result

- 3 kg ultra-low noise germanium detector 10.39 m away from a rector (P=2.96 Gw_{th}) with an estimated antineutrino flux of $4.8 \times 10^{13}\ cm^{-2}s^{-1}$
- the background comes from the elastic scattering of epithermal neutrons and the electron capture in ^{71}Ge.

$$\frac{dN^{\mathrm{bkg}}}{dT_{\mathrm{e}}} = \underbrace{N_{\mathrm{epith}} + A_{\mathrm{epith}} e^{-T_{\mathrm{e}}/T_{\mathrm{epith}}}} + \underbrace{\sum_{i=L_1,L_2,M} \frac{A_i}{\sqrt{2\pi}\sigma_i} e^{-\frac{(T_{\mathrm{e}}-T_i)^2}{2\sigma_i^2}}}$$

- 96.4 days reactor ON (Rx-ON) and 25 days reactor OFF (Rx-OFF)
- Ultra-low energy threshold $\boxed{0.2 < T_e < 1.5\ \mathrm{keV_{ee}}}$

➢ This feature makes reactor neutrinos very sensitive to possible ν electromagnetic properties (millicharged, magnetic moment) since the related cross section goes like 1/T

$$\frac{d\sigma^{\mathrm{MM}}_{\nu_\ell\text{-}\mathcal{N}}}{dT_{\mathrm{nr}}}(E, T_{\mathrm{nr}}) = \frac{\pi\alpha^2}{m_e^2}\left(\frac{1}{T_{\mathrm{nr}}} - \frac{1}{E}\right) Z^2 F_Z^2(|\vec{q}|^2) \left|\frac{\mu_{\nu_\ell}}{\mu_{\mathrm{B}}}\right|^2$$

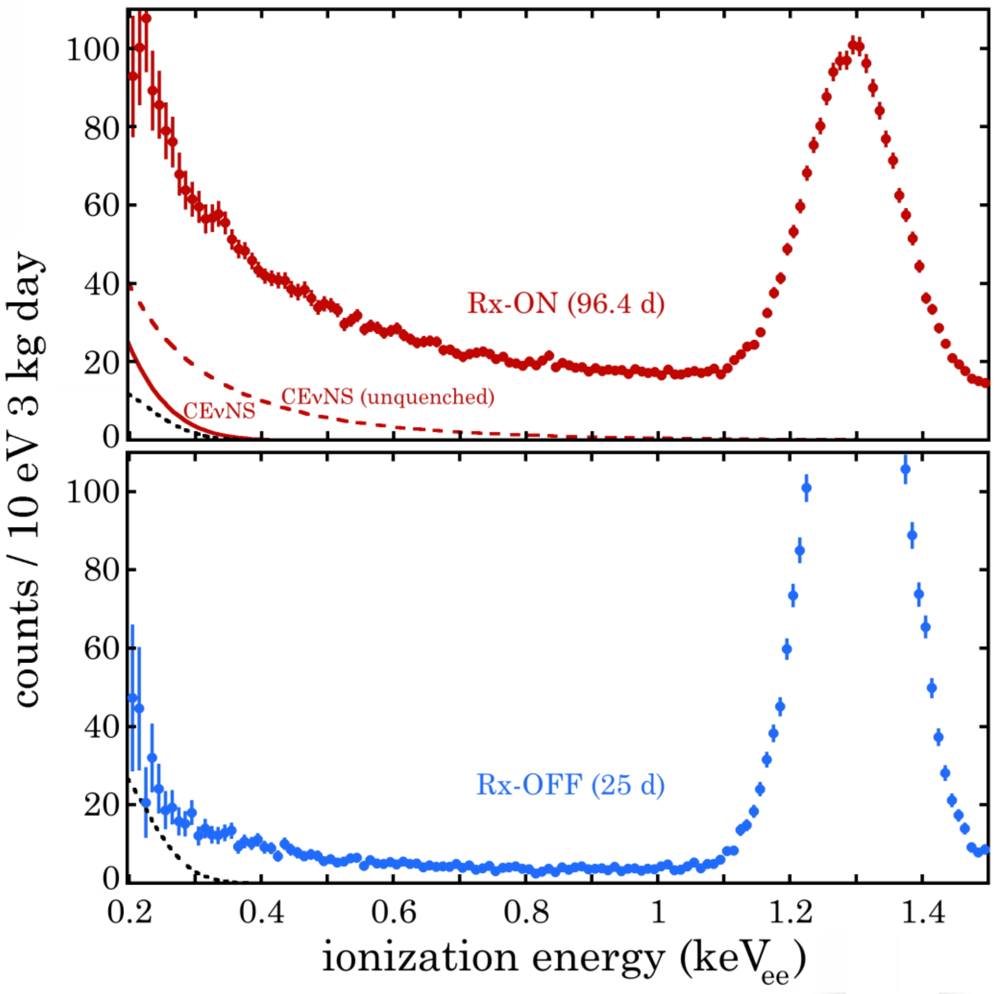

✓ A strong preference for the presence of CEνNS is found

DRESDEN-II our own analysis

Impact of the Dresden-II and COHERENT neutrino scattering data on neutrino electromagnetic properties and electroweak physics

M. Atzori Corona,[1,2,*] M. Cadeddu,[2,†] N. Cargioli,[1,2,‡] F. Dordei,[2,§] C. Giunti,[3,¶] Y.F. Li,[4,5,**] C. A. Ternes,[3,††] and Y.Y. Zhang[4,5,‡‡]

arXiv: 2205.09484

CHECK IT OUT!

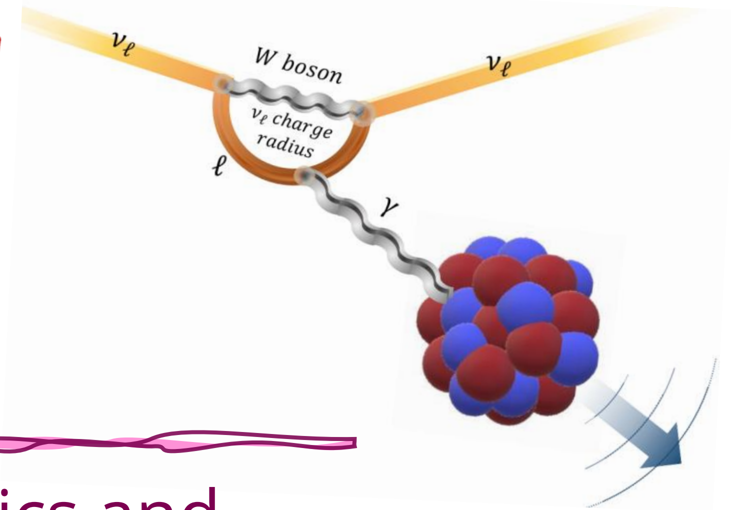

+ We fitted the Dresden-II data looking for neutrino EM properties and we combine with COHERENT CsI and Ar data, funding very interesting results.
+ **Most stringent upper limit** on the electron neutrino charge radius

$$-7.1 \times 10^{-32}\,\mathrm{cm}^2 < \langle r^2_{\nu_{ee}} \rangle < 5 \times 10^{-32}\,\mathrm{cm}^2$$

But what is the impact of Dresden-II for nuclear physics and electroweak parameters?

$$Q^V_{\ell,\mathrm{SM}} = \left[g_V^p(\nu_\ell)\, Z F_Z\left(|\vec{q}|^2\right) + g_V^n N F_N\left(|\vec{q}|^2\right)\right]$$

$$F_Z(|q|^2) = F_N(|q|^2) \approx 1$$

Both form factors are practically equal to unity making CEνNS from reactor insensitive to neutron radius $R_n(\mathrm{Ge})$ measurements but also makes the data insensitive to nuclear uncertainties.

So, what is the advantage here?

A weak mixing angle measurement at low energies independent from $R_n(\mathrm{Ge})$

Dresden-II weak mixing angle results

- Insensitive to $R_n(\mathrm{Ge})$
- Insensitive to the antineutrino flux parametrization

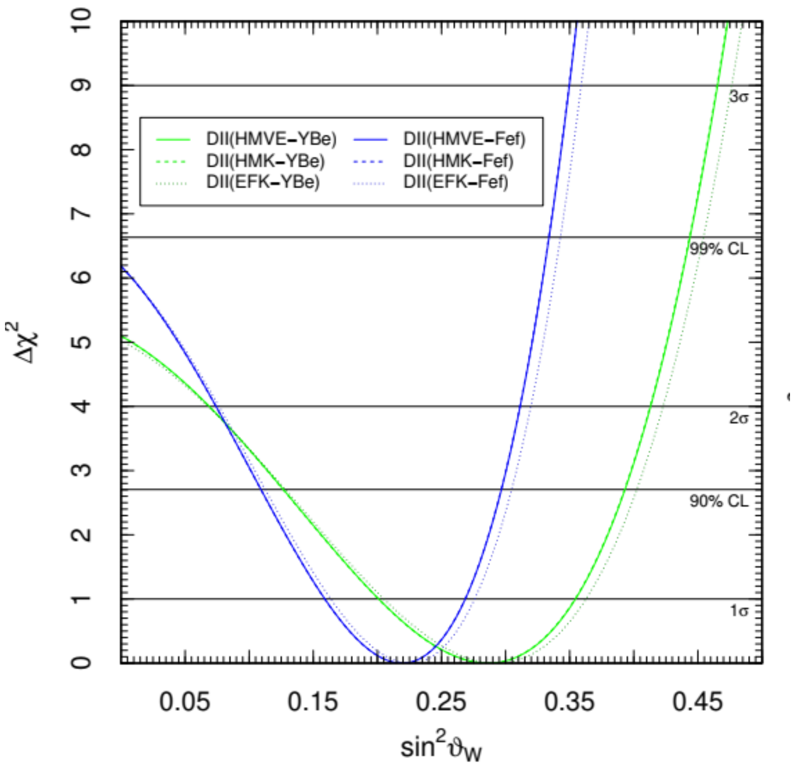

See also D. Papoulias's talk

- Very sensitive to the Ge quenching factor parametrization

Needs to be measured accurately at low energies

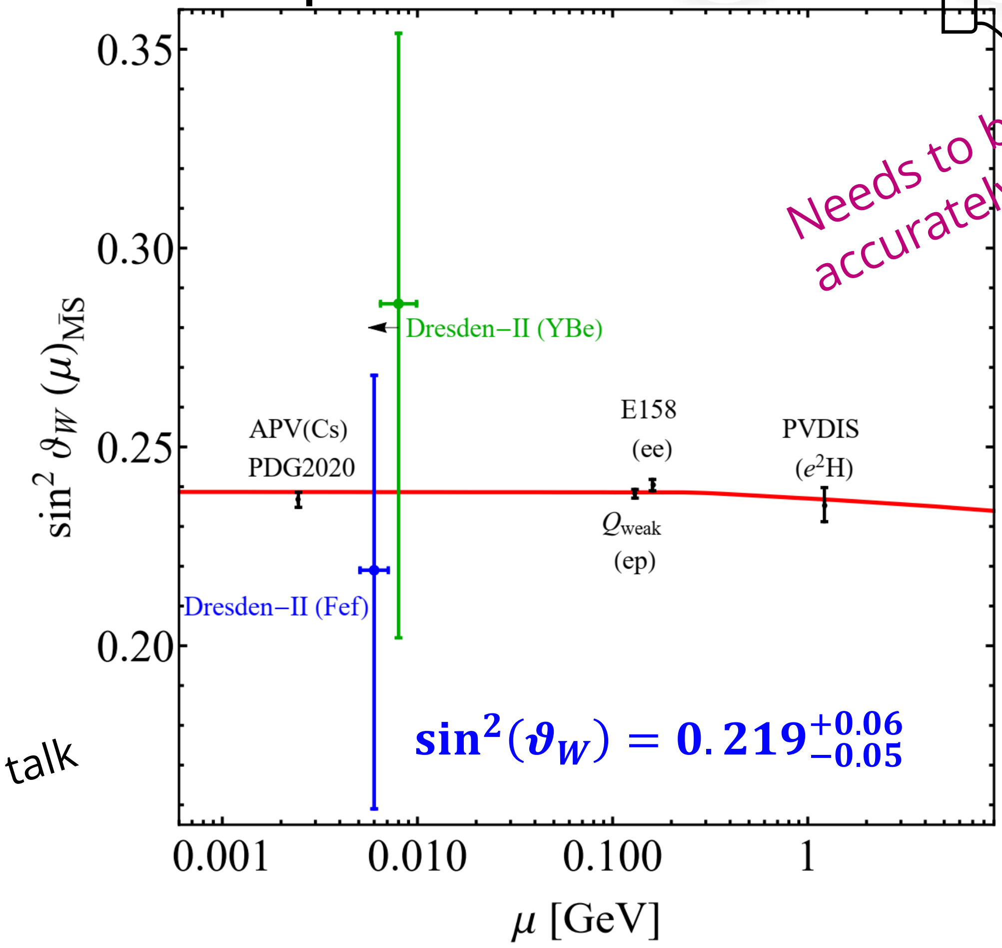

$$\sin^2(\vartheta_W) = 0.219^{+0.06}_{-0.05}$$

Neutron nuclear radius in argon

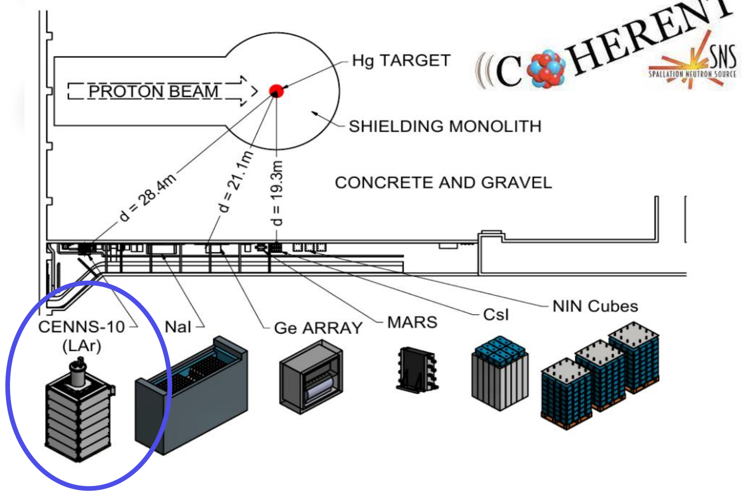

Combined fit in (time, energy, PSP) space suggest >3σ CEvNS detection significance

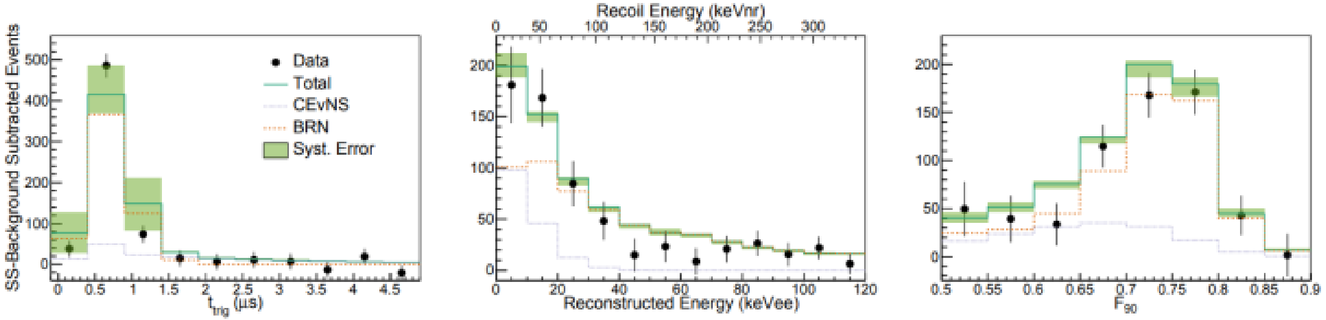

Dominant backgrounds:

1. ^{39}Ar beta decay
2. Beam related neutrons

Akimov et al, COHERENT Coll. PRL 126, 01002 (2021)

Cadeddu et al., PRD 102, 015030 (2020)

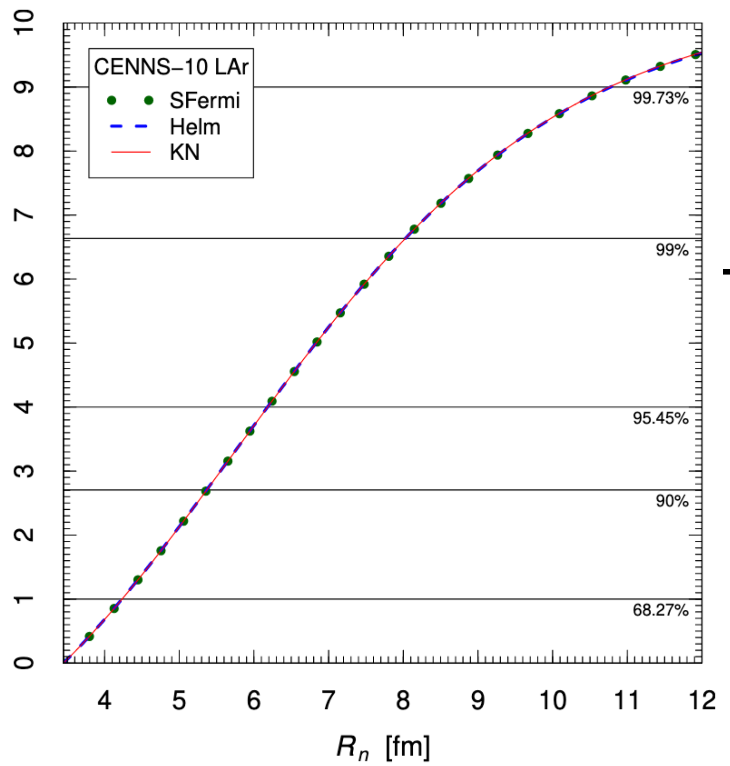

COHERENT Argon

$$R_n(^{40}\mathrm{Ar}) < 4.2\ \mathrm{fm}$$

More statistics needed.

Theoretical values

Interaction	R_p^{point}	R_n^{point}
Sky3D		
SkI3 [37]	3.33	3.43
SkI4 [37]	3.31	3.41
Sly4 [38]	3.38	3.46
Sly5 [38]	3.37	3.45
Sly6 [38]	3.36	3.44
Sly4d [39]	3.35	3.44
SV-bas [40]	3.33	3.42
UNEDF0 [41]	3.37	3.47
UNEDF1 [42]	3.33	3.43
SkM* [43]	3.37	3.45
SkP [44]	3.40	3.48

See also:
Payne et al.,
PRC 100, 061304 (2019)

See also:
Miranda et al.,
JHEP 05 (2020) 130

COHERENT future argon: "COH-Ar-750"
LAr based detector for precision CEνNS

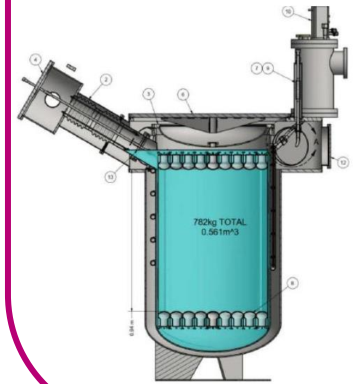

- Single phase, scintillation only, 750 kg total (610 kg fiducial)
- 3000 CEνNS/year

Conclusions

- The weak-mixing angle-neutron radius degeneracy is always present in weak processes on nuclei
- To break this degeneracy one can combine different EW measurements: Complementarity is the key!
- In this game CEνNS is a powerful tool for measuring the neutron form factor and in turn the rms neutron radius, even if not explicitly designed for this purpose.
- The current precision is not competitive with PVES, but these detectors are scalable and many new results are expected in coming years.

BACKUP

+COHERENT data analysis details

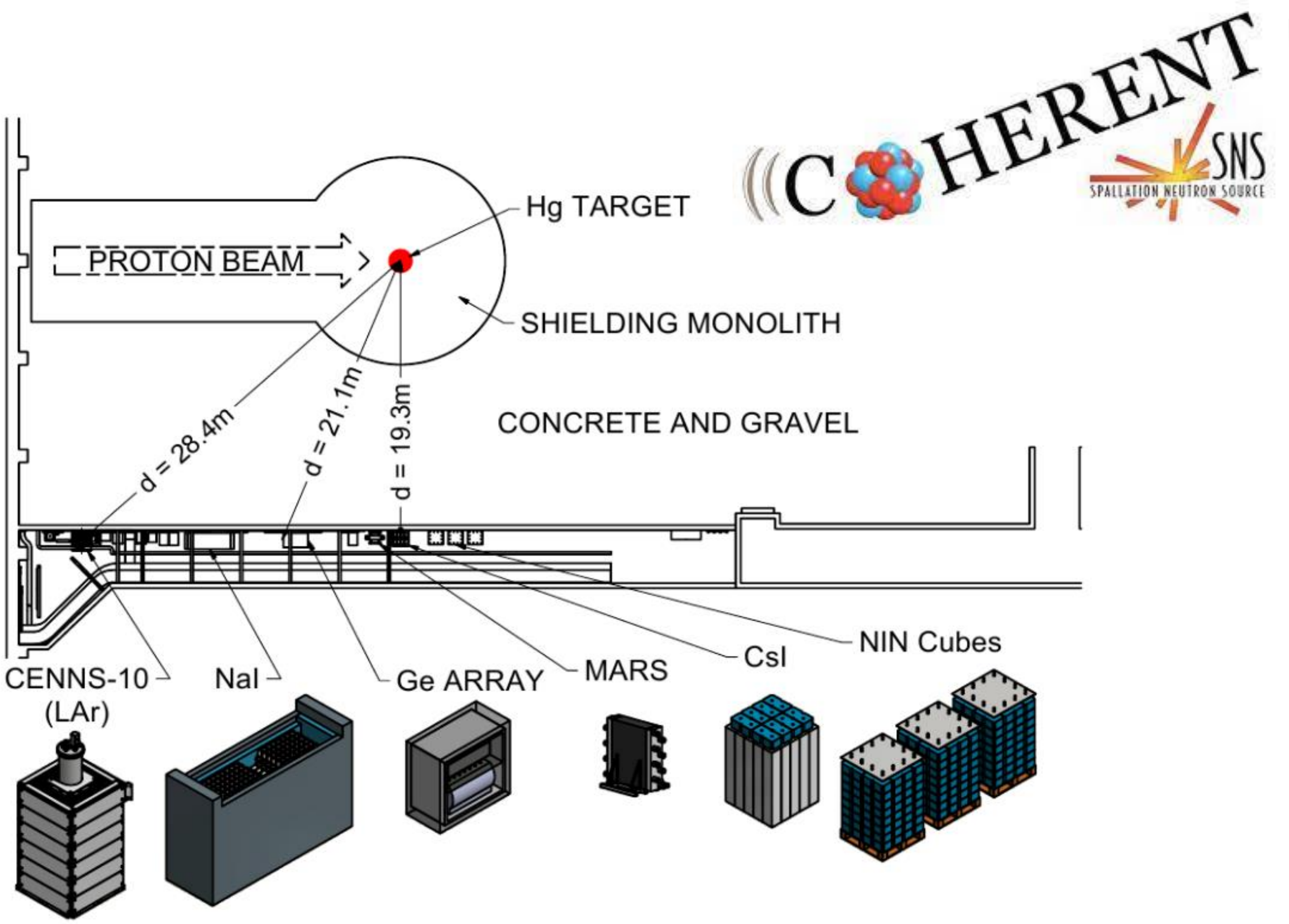

Neutron form factor fitted from COHERENT CsI data in binned

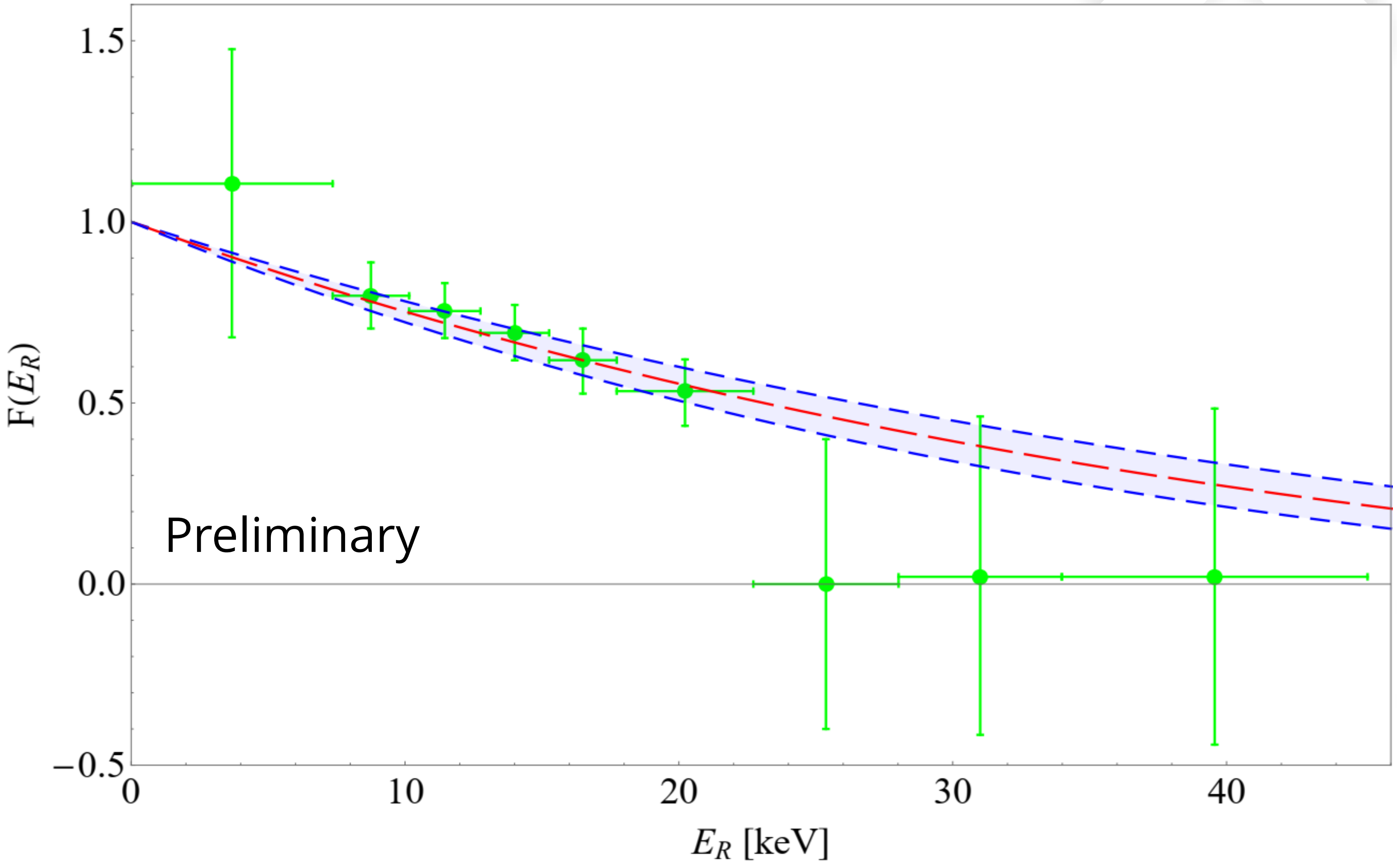

CENNS-10 LAr detector

Built by J. Yoo et al. in Fermilab, moved to SNS late 2016

After light collection upgrade of 2017 single phase LAr detector with fiducial mass of 24 kg provides the light yield of 4.5 PE/keV_{ee} and a ~20 keV_{nr} threshold

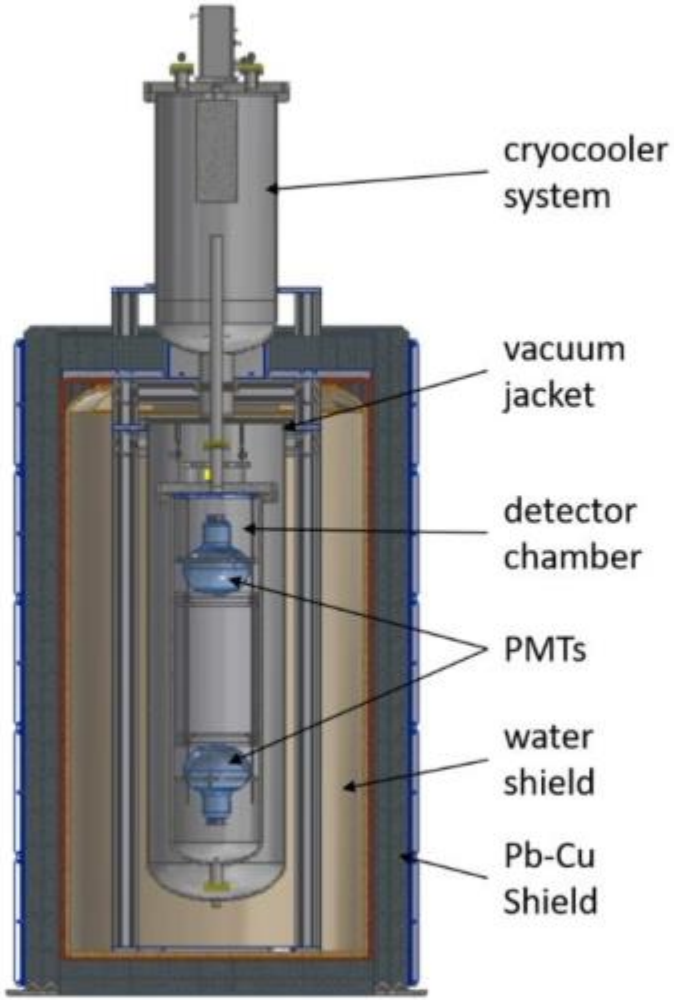

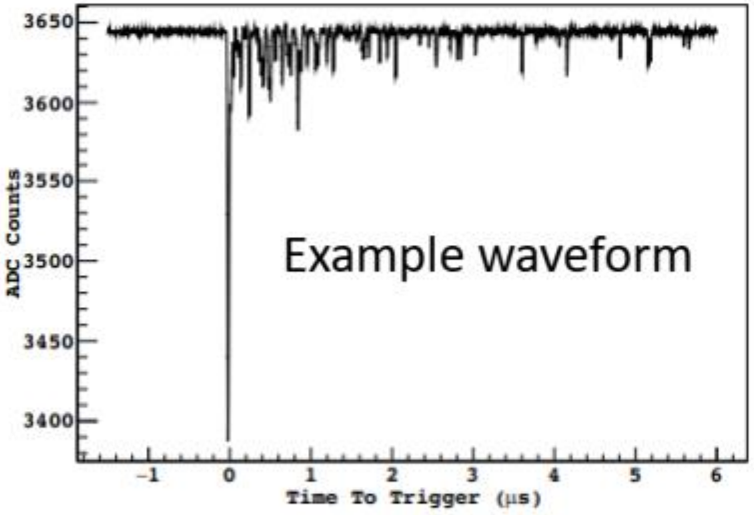

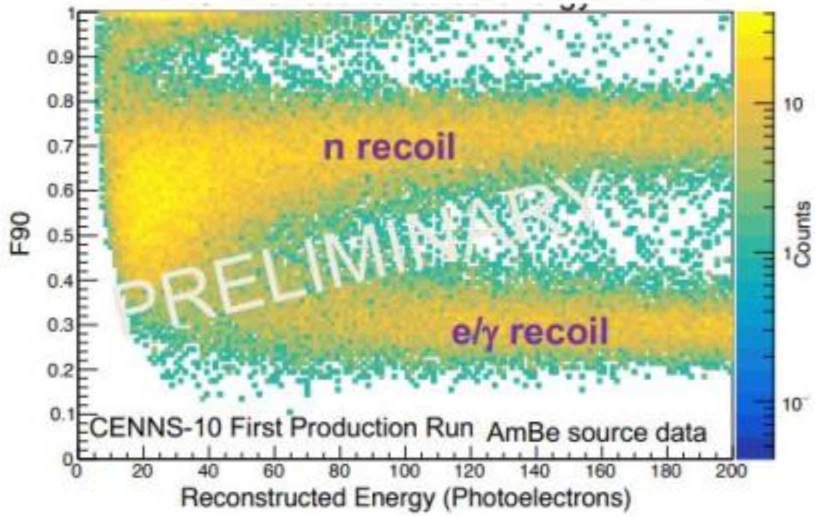

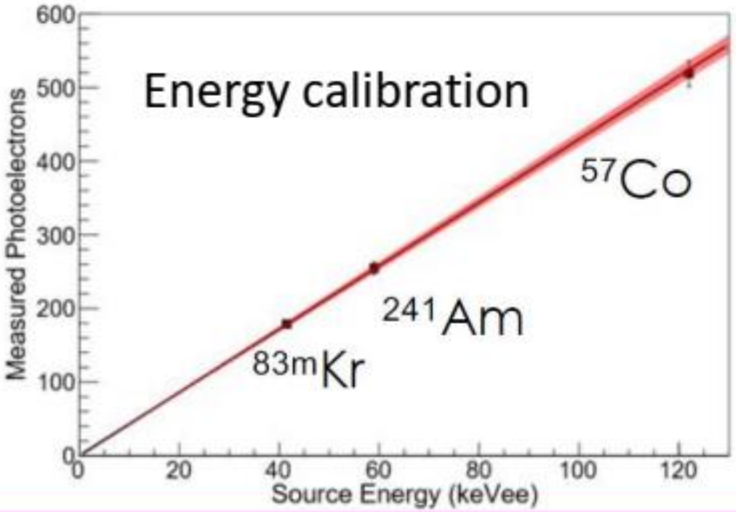

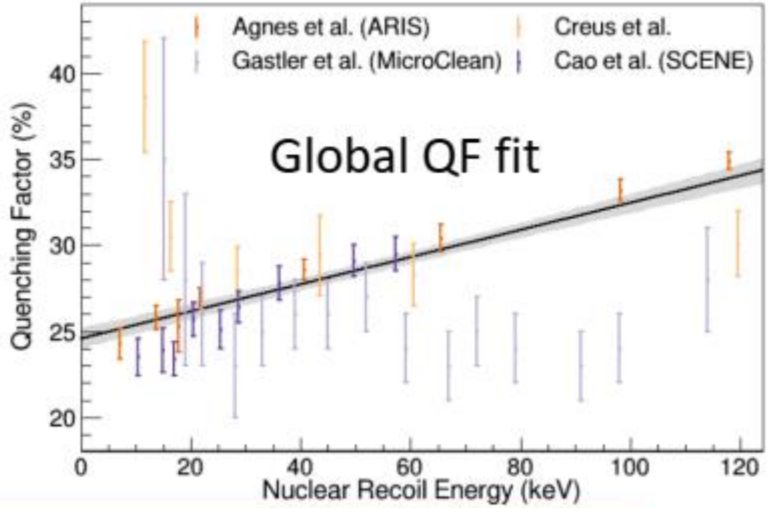

Matthew Heath (IU) thesis (2019), D. Akimov et al., PRD 100, 115020, J. Zettlemoyer (IU) thesis (2020)

First CEvNS detection on LAr

Combined fit in (time, energy, PSP) space suggest >3σ CEvNS detection significance

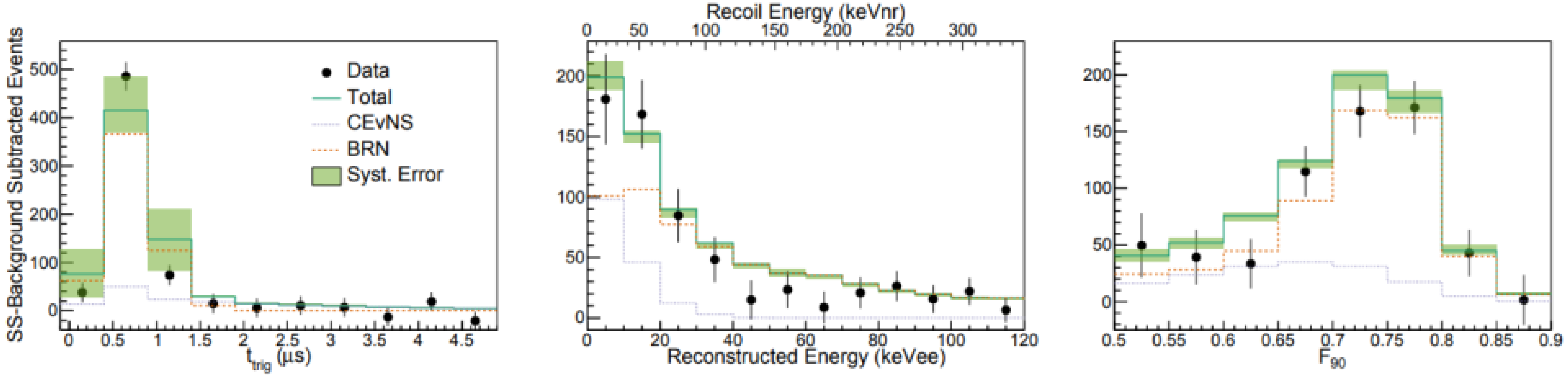

Dominant backgrounds:

1. ^{39}Ar beta decay
2. Beam related neutrons

Two independent blind analyses results agree with the SM CEvNS rate prediction

PRL 126, 012002 (2021)

arXiv:2006.12659 – LAr data release

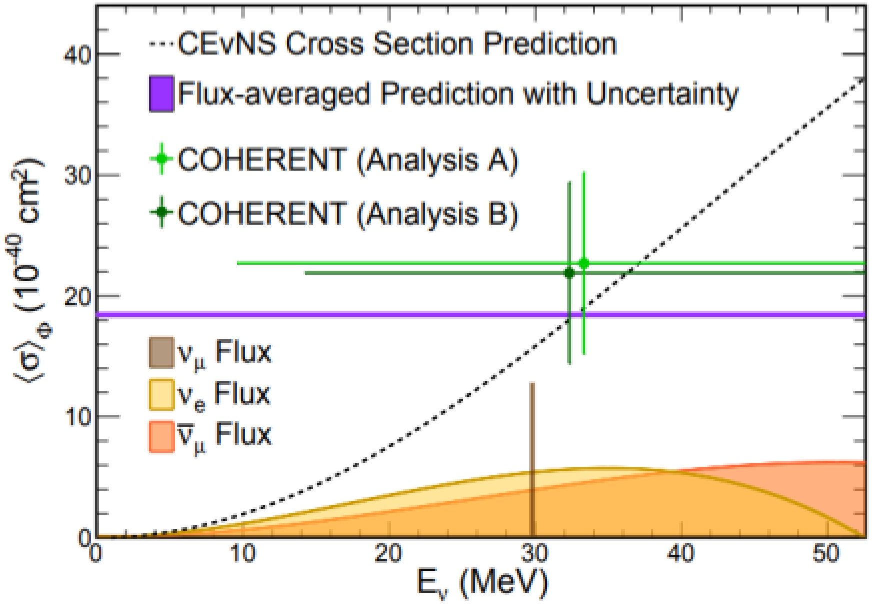

	Analysis A	Analysis B
SM-predicted ($\times10^{-39}$ cm^2)	1.8	
fit CEvNS events	159 ± 43	121 ± 36
cross section systematic errors:		
detector efficiency	3.6%	1.6%
energy calibration	0.8%	4.6%
F_{90} calibration	7.8%	3.3%
quenching factor	1.0%	1.0%
nuclear form factor	2.0%	2.0%
neutrino flux	10%	10%
total cross section sys. error	13%	12%
measured ($\times10^{-39}$ cm^2)	2.3 ± 0.7	2.2 ± 0.8

The result accuracy is dominated by statistical uncertainty at this point

CENNS-10 continues data taking and 5σ significance is expected by the end of the year 2020

$$\chi_S^2 = \sum_{i=1}^{12} \left(\frac{N_i^{\text{exp}} - \eta_{\text{CE}\nu\text{NS}} N_i^{\text{CE}\nu\text{NS}} - \eta_{\text{PBRN}} B_i^{\text{PBRN}} - \eta_{\text{LBRN}} B_i^{\text{LBRN}}}{\sigma_i} \right)^2 + \left(\frac{\eta_{\text{CE}\nu\text{NS}} - 1}{\sigma_{\text{CE}\nu\text{NS}}} \right)^2 + \left(\frac{\eta_{\text{PBRN}} - 1}{\sigma_{\text{PBRN}}} \right)^2 + \left(\frac{\eta_{\text{LBRN}} - 1}{\sigma_{\text{LBRN}}} \right)^2,$$

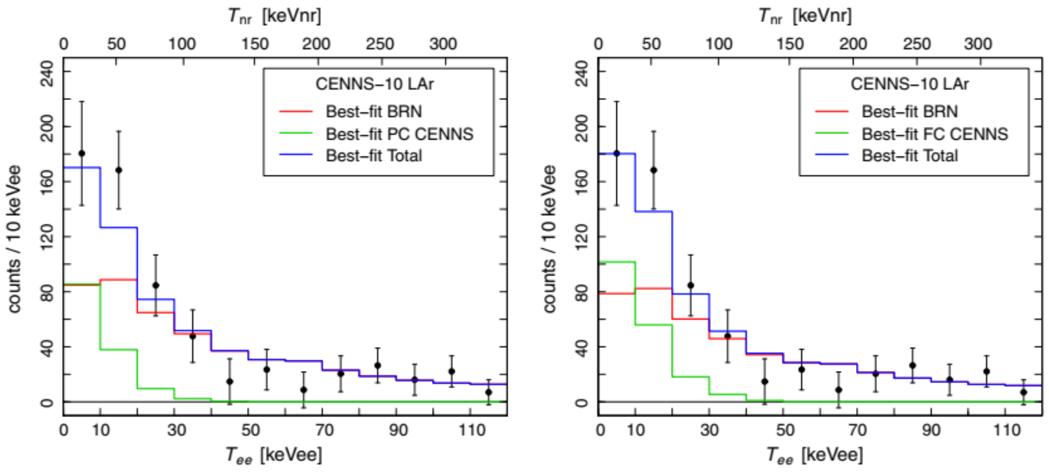

(a) (b)

Physics results from the first COHERENT observation of coherent elastic neutrino-nucleus scattering in argon and their combination with cesium-iodide data

M. Cadeddu,[1,*] F. Dordei,[1,†] C. Giunti,[2,‡] Y. F. Li,[3,4,§] E. Picciau,[5,6,‖] and Y. Y. Zhang[3,4,¶]

[1] *Istituto Nazionale di Fisica Nucleare (INFN), Sezione di Cagliari, Complesso Universitario di Monserrato—S.P. per Sestu Km 0.700, 09042 Monserrato (Cagliari), Italy*
[2] *Istituto Nazionale di Fisica Nucleare (INFN), Sezione di Torino, Via P. Giuria 1, I-10125 Torino, Italy*
[3] *Institute of High Energy Physics, Chinese Academy of Sciences, Beijing 100049, China*
[4] *School of Physical Sciences, University of Chinese Academy of Sciences, Beijing 100049, China*
[5] *Dipartimento di Fisica, Università degli Studi di Cagliari, and INFN, Sezione di Cagliari, Complesso Universitario di Monserrato—S.P. per Sestu Km 0.700, 09042 Monserrato (Cagliari), Italy*
[6] *University of Massachusetts, Amherst, Massachusetts 01003, USA*

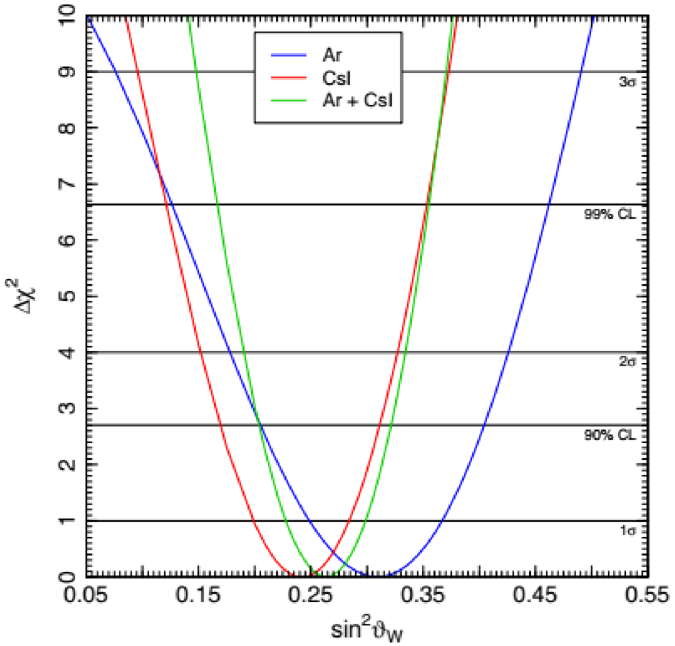

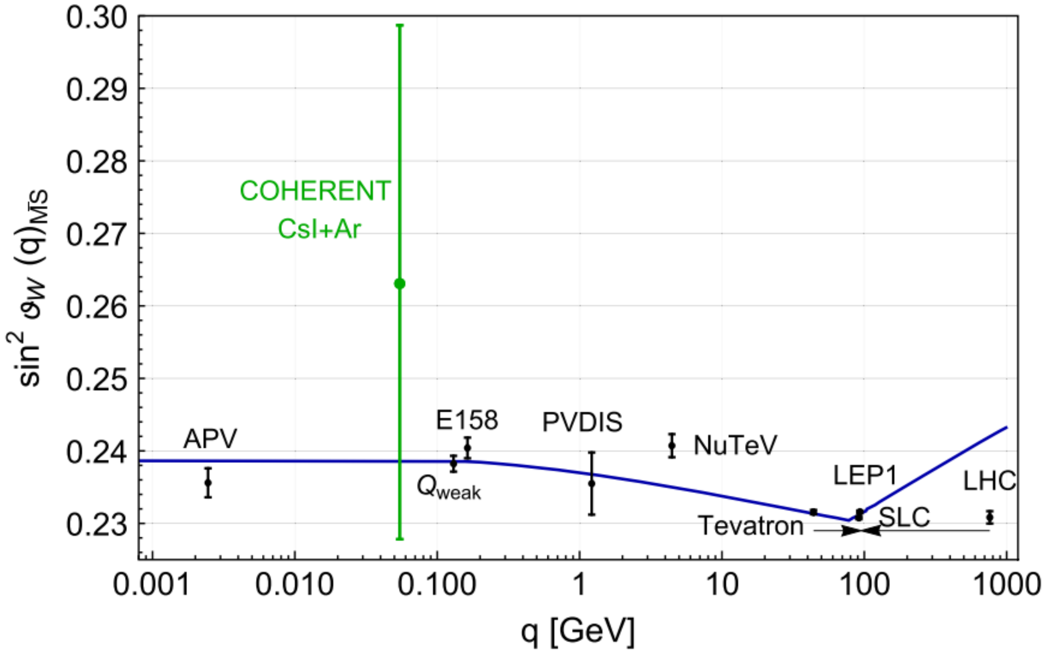

COHERENT CsI χ^2

+ Poissonian least-square function:

+ Since in some energy-time bins the number of events is zero, we used the Poissonian least-squares function

$$\chi^2_{\mathrm{CsI}} = 2\sum_{i=1}^{9}\sum_{j=1}^{11}\left[\sum_{z=1}^{4}(1+\eta_z)N_{ij}^{z} - N_{ij}^{\mathrm{exp}} + N_{ij}^{\mathrm{exp}}\ln\left(\frac{N_{ij}^{\mathrm{exp}}}{\sum_{z=1}^{4}(1+\eta_z)N_{ij}^{z}}\right)\right] + \sum_{z=1}^{4}\left(\frac{\eta_z}{\sigma_z}\right)^2$$

where the indices i and j denote, respectively, the energy and time bins, and the indices $z = 1, 2, 3, 4$ stand for CEνNS, beam-related neutron (BRN), neutrino-induced neutron (NIN), and steady-state (SS) backgrounds, respectively. In our notation, N_{ij}^{exp} is the experimental event number obtained from coincidence (C) data, $N_{ij}^{\mathrm{CE}\nu\mathrm{NS}}$ is the predicted number of CEνNS events that depends on the physics model under consideration, N_{ij}^{BRN} is the estimated BRN background, N_{ij}^{NIN} is the estimated NIN background, and N_{ij}^{SS} is the SS background obtained from the anti-coincidence (AC) data. We took into account the systematic uncertainties described in Ref. [23] with the nuisance parameters η_z and the corresponding uncertainties $\sigma_{\mathrm{CE}\nu\mathrm{NS}} = 0.12$ (which is the systematic uncertainty of the signal rate considering the effects of the 10%, 3.8%, 4.1%, and 3.4% uncertainties of the neutrino flux, quenching factor, CEνNS efficiency, and neutron form factors, respectively), $\sigma_{\mathrm{BRN}} = 0.25$, $\sigma_{\mathrm{NIN}} = 0.35$, and $\sigma_{\mathrm{SS}} = 0.021$.

COHERENT CsI 2D

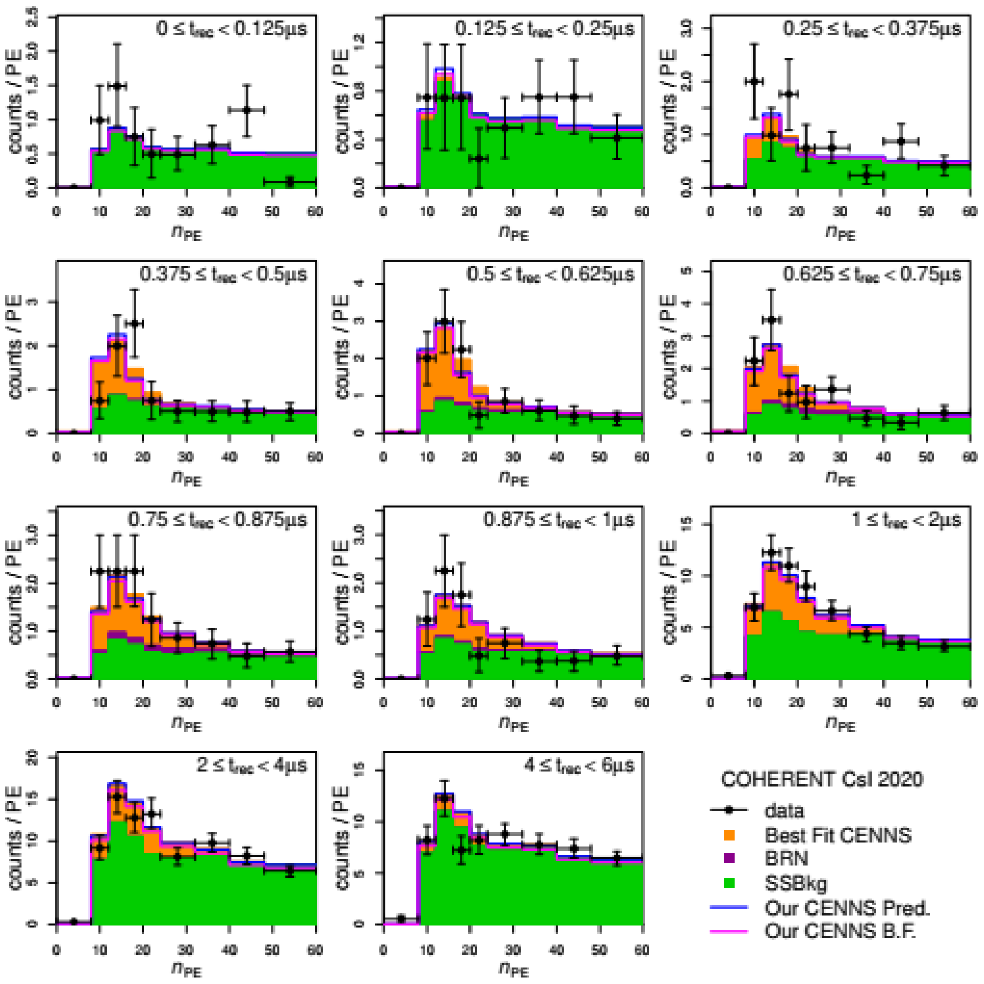

Figure 1: 2020 COHERENT CsI CEνNS calculation without energy resolution. Best fit: $\chi^2_{\mathrm{CsI}}/\mathrm{NDF}_{\mathrm{CsI}} = 100.8/88$, GoF = 17%. The total number of predicted and best-fit CEνNS events are, respectively, 300.4 and 287.2.

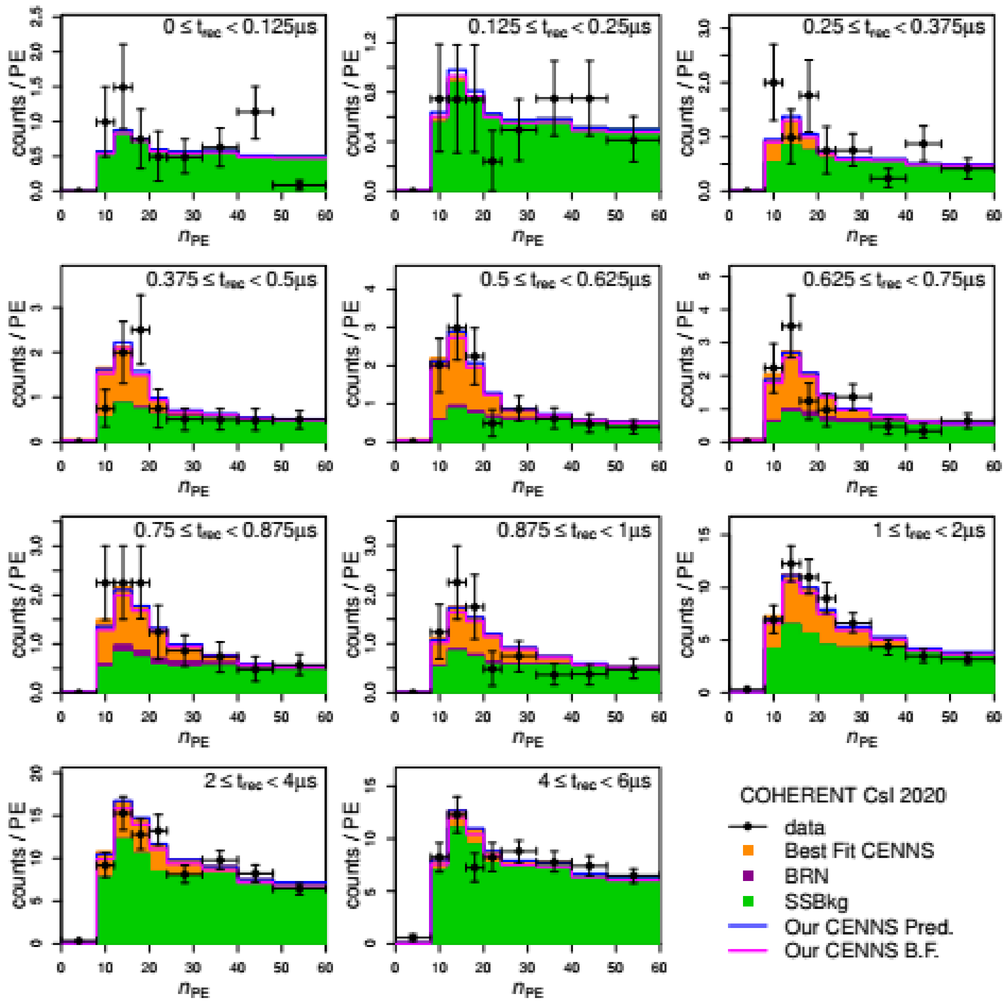

Figure 2: 2020 COHERENT CsI CEνNS calculation with energy resolution. Best fit: $\chi^2_{\mathrm{CsI}}/\mathrm{NDF}_{\mathrm{CsI}} = 103.1/88$, GoF = 13%. The total number of predicted and best-fit CEνNS events are, respectively, 311.8 and 292.2.

COHERENT (CsI) @fixed skin

+ CEνNS is sensitive to the neutron skin
+ But less sensitive to the weak mixing angle

$\sin^2\theta_W = 0.233^{+0.027}_{-0.024}$

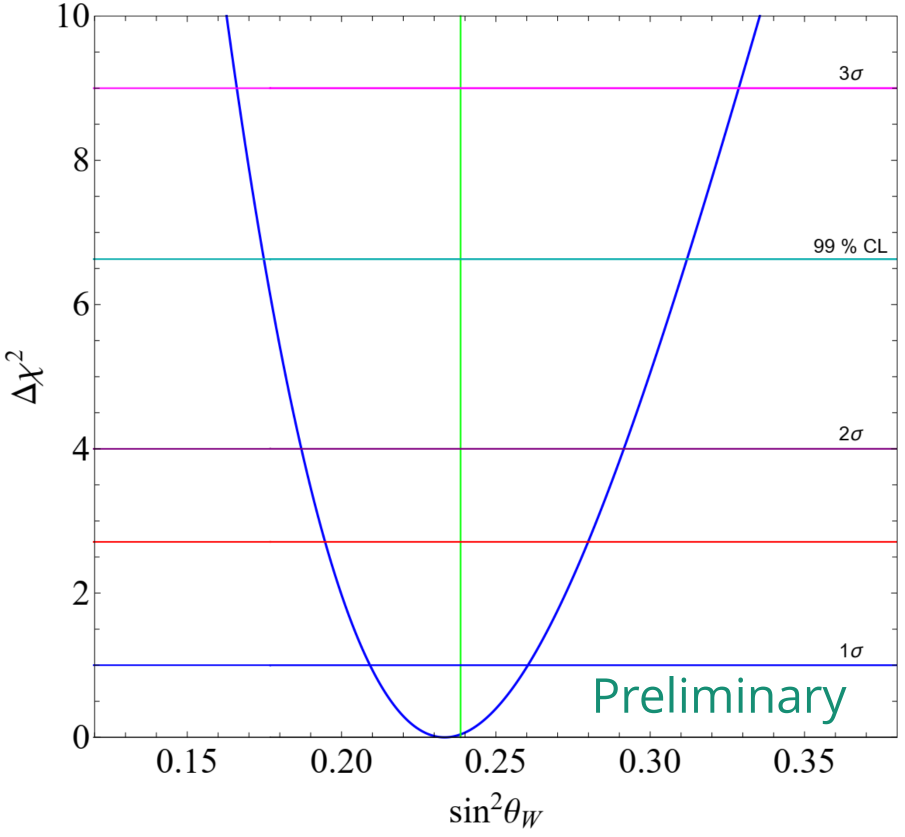

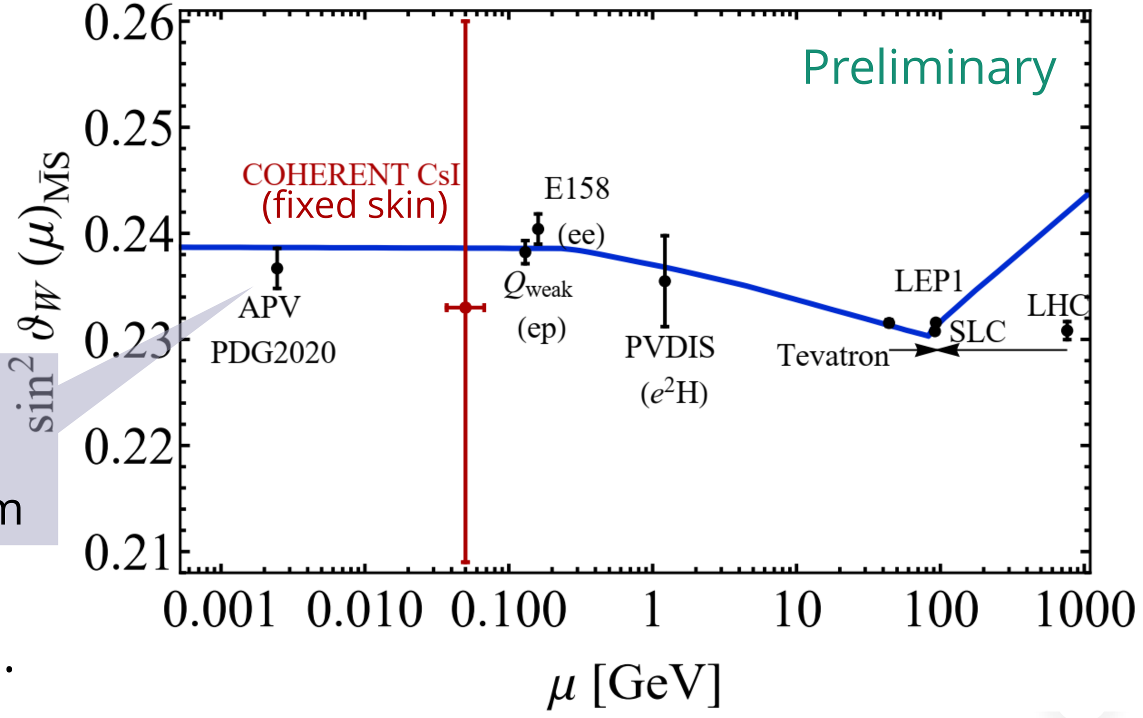

APV(Cs) PDG2020 corresponds to $\Delta R_{np}^{Cs}(\mathrm{Extr.}) = 0.13$ fm

Extrapolated from antiprotonic atoms…

New CsI CEvNS result: refinements in the analysis

Refinements:

1. New CsI[Na] QF measurements and global fit
2. Better model of the steady state background
3. Better understanding of detector resolution

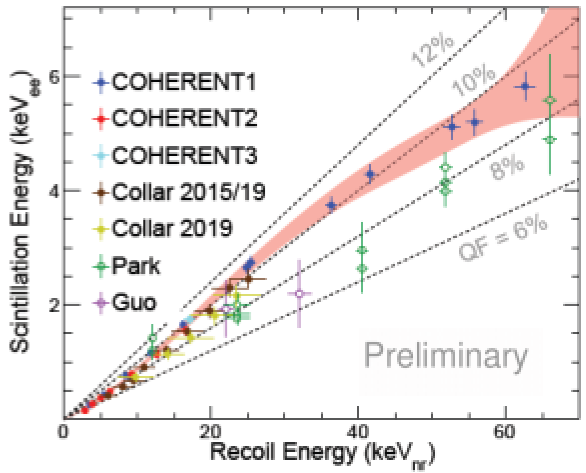

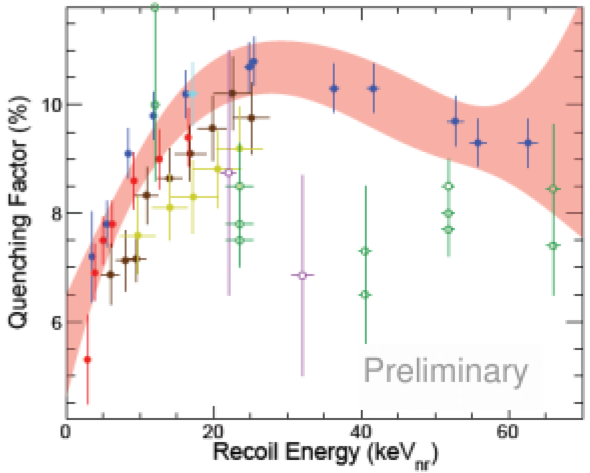

More details on QF in the backup

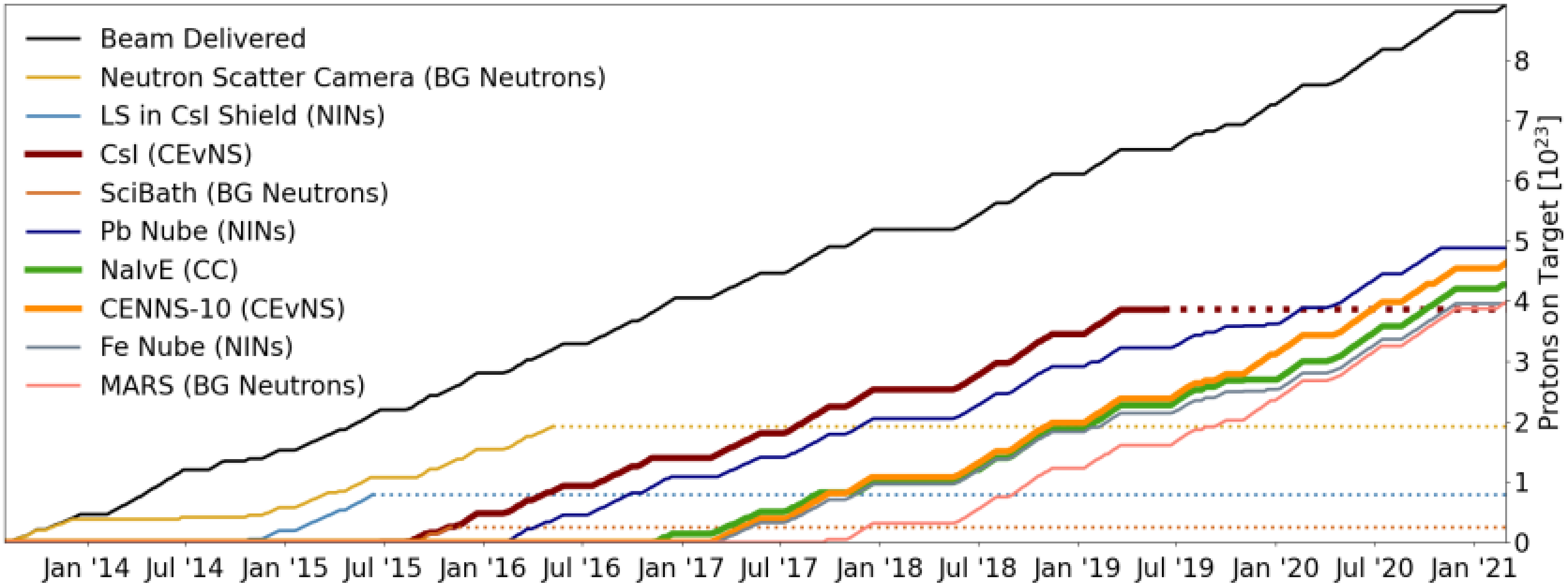

Full dataset has more than 2x statistics

CsI quenching factor

Akimov et al. (COHERENT Collaboration), arXiv:2111.02477

Measurement of scintillation response of CsI[Na] to low-energy nuclear recoils by COHERENT

D. Akimov,[a] P. An,[b,c] C. Awe,[b,c] P.S. Barbeau,[b,c] B. Becker,[d] V. Belov,[e,a] I. Bernardi,[d]
M.A. Blackston,[f] C. Bock,[g] A. Bolozdynya,[a] J. Browning,[h] B. Cabrera-Palmer,[i]
D. Chernyak,[g,1] E. Conley,[b] J. Daughhetee,[f] J. Detwiler,[j] K. Ding,[g] M.R. Durand,[j]
Y. Efremenko,[d,f] S.R. Elliott,[k] L. Fabris,[f] M. Febbraro,[f] A. Gallo Rosso,[l]
ith,[f] S. Hedges,[b,c] D. Hoang,[m]
ovalov,[a,e] E. Kozlova,[a,e] A. Kumpan,[a]
ff,[p,c] J. Mastroberti,[n] Y.A. Melikyan,[q]
la,[f] D. Pershey,[b] R. Rapp,[m] H. Ray,[r]
h,[c] J. Ross,[p,c] D. Rudik,[a] J. Runge,[b,c]
A. Shakirov,[a] G. Simakov,[a,e] G. Sinev,[b,2]
[n] K. Tellez-Giron-Flores,[o] I. Tolstukhin,[n,3]
tue,[l] G. Visser,[s] T. Wongjirad,[t] Y.-R. Yen,[m]
ENT Collaboration)

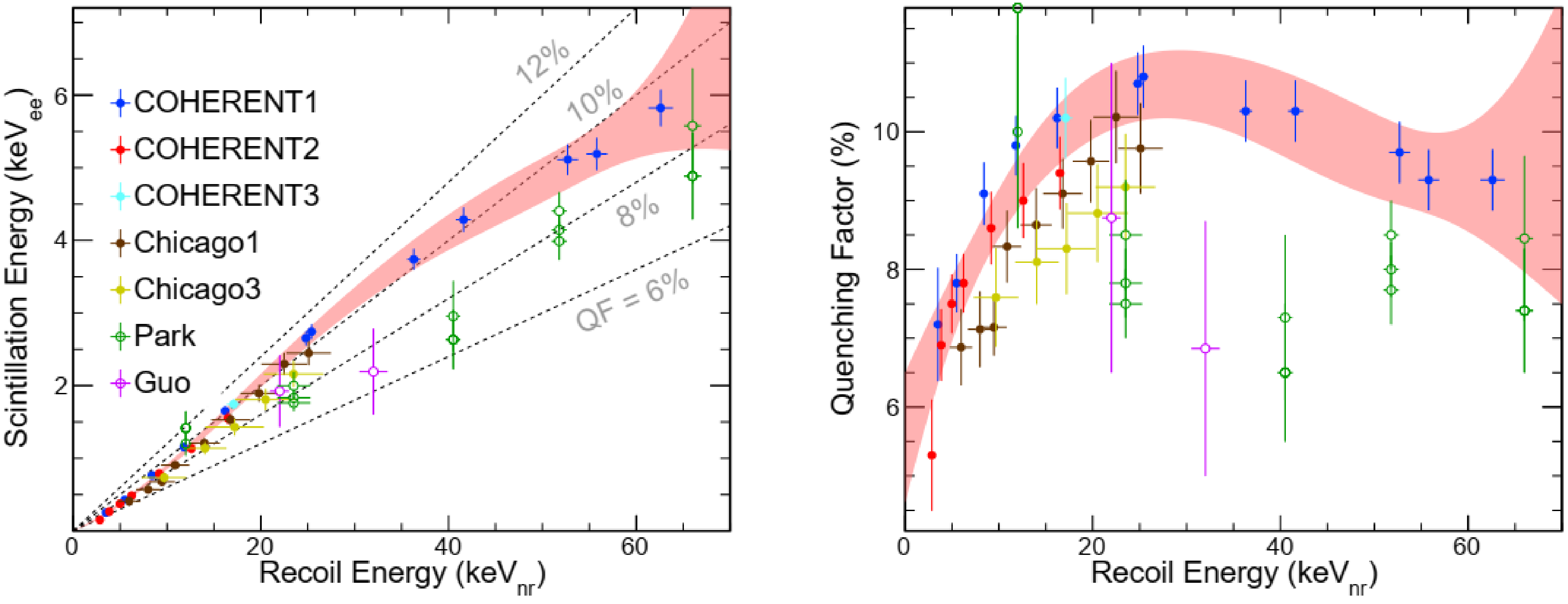

See also J.I. Collar et al. arXiv:1907.04828

Figure 14. Quenching data in CsI[Na] along with our best fit and error band. We fit the scintillation response curve (left) and also plot the QF (right). When plotting the quenching factor, the relative error in the recoil energy is propagated into the QF error. Data with empty circular points are not included in the fit.

$$E_{vis}(E_{nr}) = 0.05546 \times E_{nr} + 4.307 \times E_{nr}^2 - 111.7 \times E_{nr}^3 + 840.4 \times E_{nr}^4$$

Rn(Cs) and Rn(I) and surface thickness

Green lines Plausible theoretical values can be obtained using the recent nuclear shell model (NSM) estimate of the corresponding neutron skins, the differences between the neutron and the proton rms radii, 0.27 fm and 0.26 fm [57], leading to

$$R_n^{\rm NSM}(^{133}{\rm Cs}) \simeq 5.09 \text{ fm}, \quad R_n^{\rm NSM}(^{127}{\rm I}) \simeq 5.03 \text{ fm}. \qquad (4)$$

These values are slightly larger than those in Table I, that we obtained using nonrelativistic Skyrme-Hartree-Fock (SHF) and relativistic mean-field (RMF) nuclear models.

[57] M. Hoferichter, J. Menéndez, and A. Schwenk, Phys. Rev. D **102**, 074018 (2020).

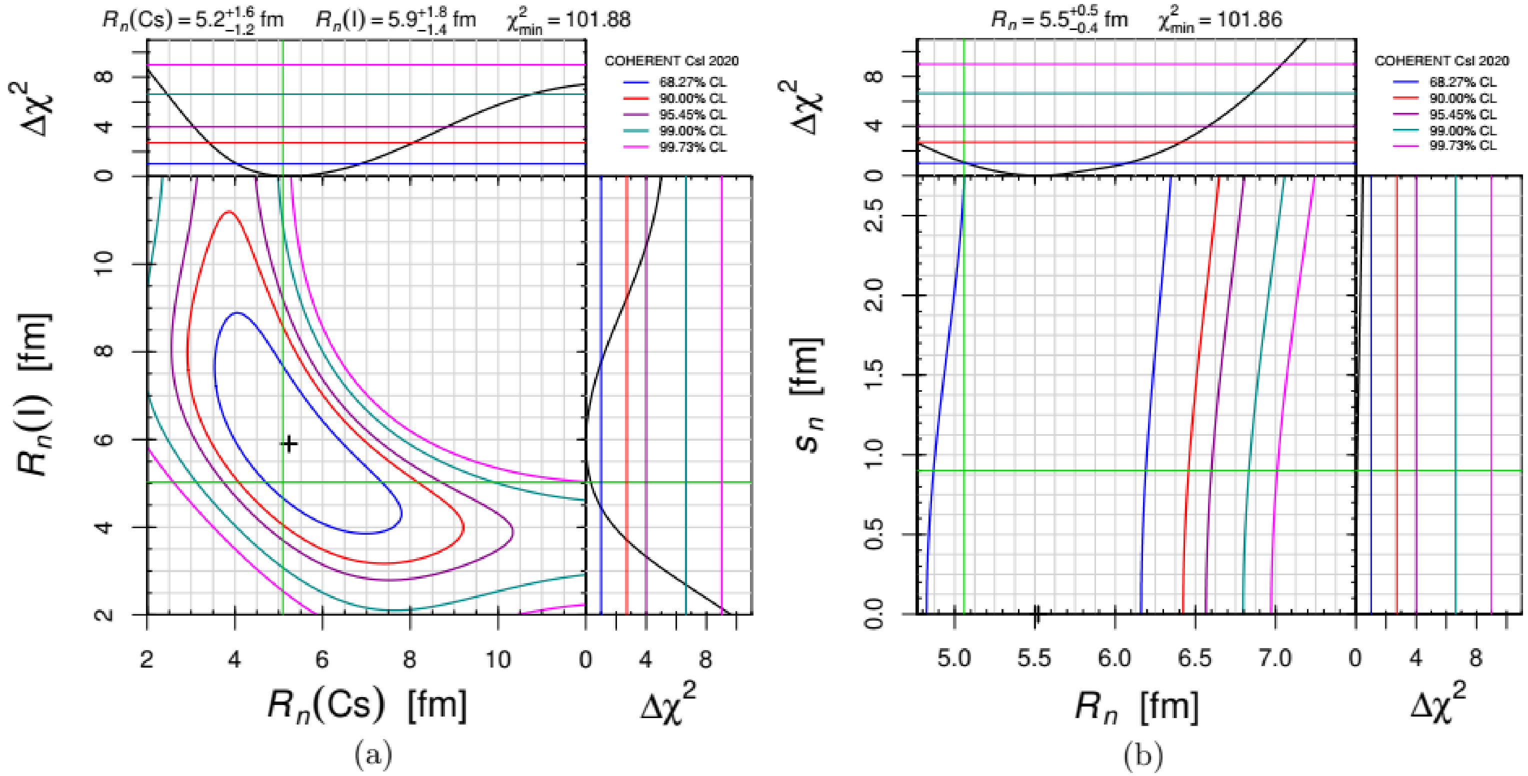

Figure 6: 2020 COHERENT CsI CEνNS fit with (a) free $R_n(\mathrm{Cs})$ and $R_n(\mathrm{I})$, and (b) free $R_n = R_n(\mathrm{Cs}) = R_n(\mathrm{I})$ and surface thickness $s_n = s_n(\mathrm{Cs}) = s_n(\mathrm{I})$ in the Helm parameterization. Both with energy resolution. The green lines indicate the theoretical values (a) $R_n^{\rm the}(\mathrm{Cs}) = 5.09\,\mathrm{fm}$ and $R_n^{\rm the}(\mathrm{I}) = 5.03\,\mathrm{fm}$, and (b) $R_n^{\rm the} = 5.06\,\mathrm{fm}$ and $s_n^{\rm the} = 0.9\,\mathrm{fm}$.

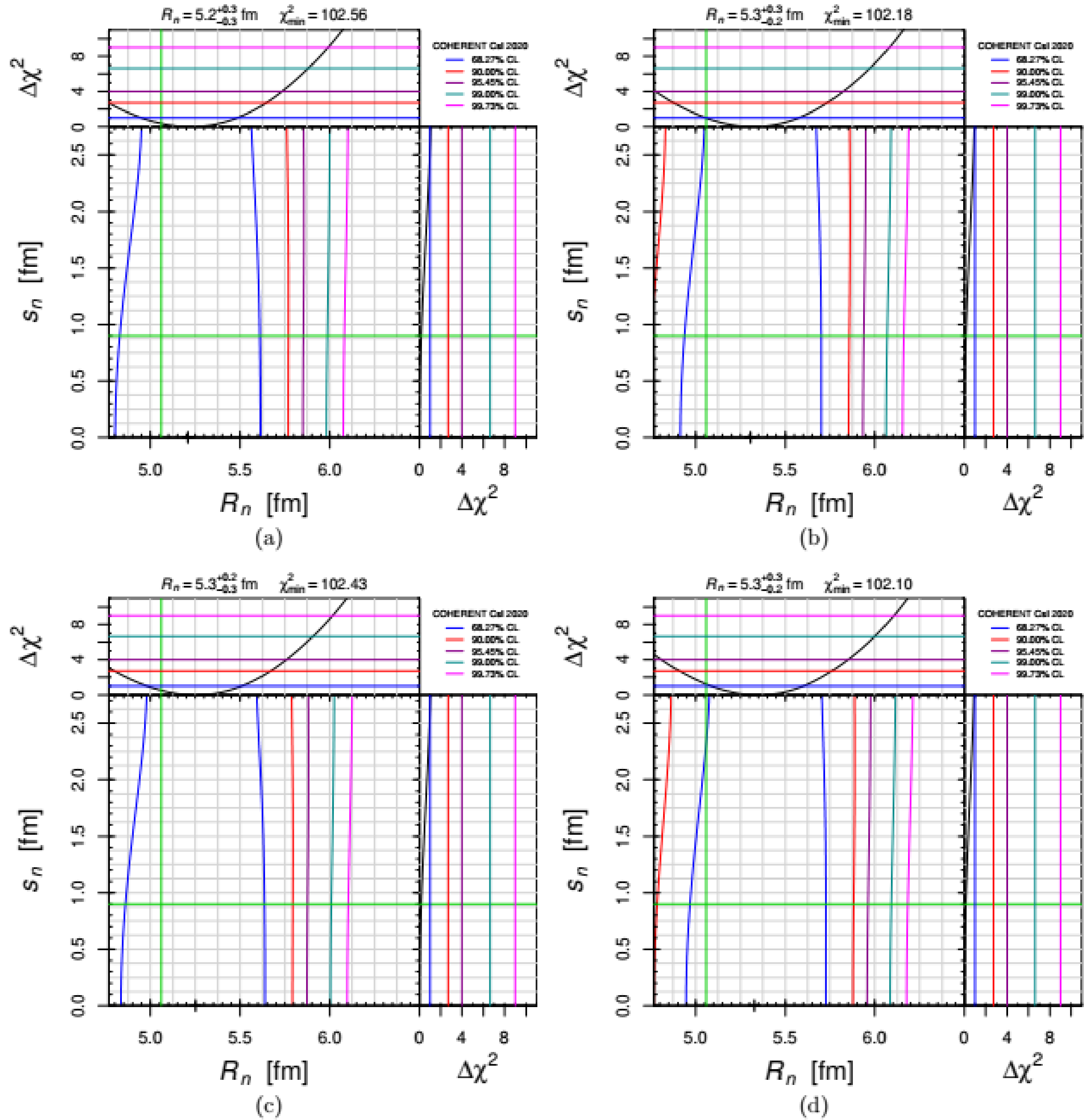

Figure 13: 2020 COHERENT CsI CEνNS + APV(Cs) fits.

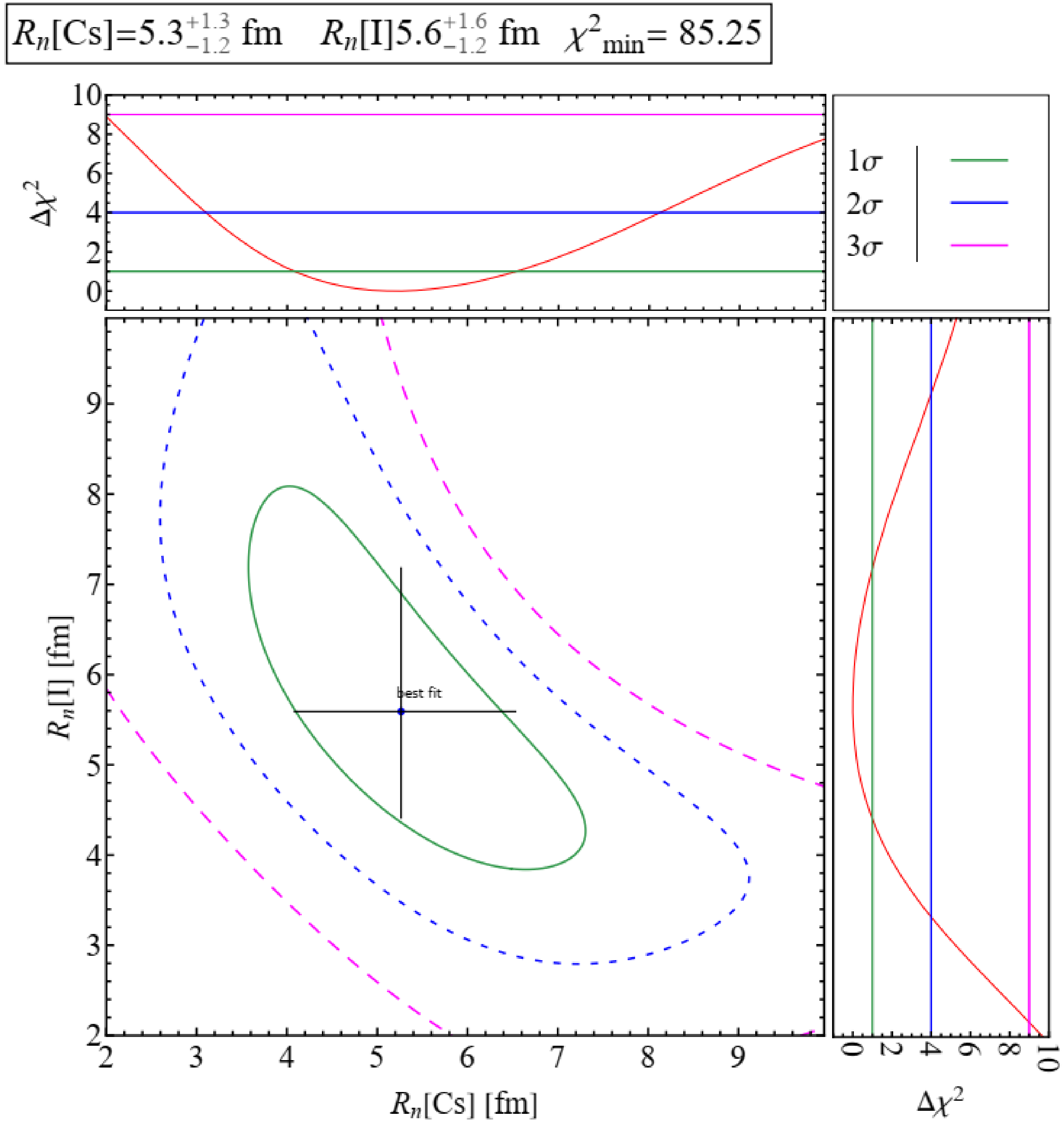

$R_n[\mathrm{Cs}]=5.3^{+1.3}_{-1.2}$ fm $R_n[\mathrm{I}]5.6^{+1.6}_{-1.2}$ fm $\chi^2_{\mathrm{min}}= 85.25$
$\Delta\chi^2$
1σ
2σ
3σ
best fit
$R_n[\mathrm{I}]$ [fm]
$R_n[\mathrm{Cs}]$ [fm]
$\Delta\chi^2$

Response of CsI[Na] to Nuclear Recoils:
Impact on Coherent Elastic Neutrino-Nucleus Scattering (CEνNS)

J.I. Collar,* A.R.L. Kavner, and C.M. Lewis
Enrico Fermi Institute, Kavli Institute for Cosmological Physics, and Department of Physics
University of Chicago, Chicago, Illinois 60637, USA
(Dated: July 16, 2019)

A new measurement of the quenching factor for low-energy nuclear recoils in CsI[Na] is presented. Past measurements are revisited, identifying and correcting several systematic effects. The resulting global data are well-described by a physics-based model for the generation of scintillation by ions in this material, in agreement with phenomenological considerations. The uncertainty in the new model is reduced by a factor of four with respect to an energy-independent quenching factor initially adopted as a compromise by the COHERENT collaboration. A significantly improved agreement with Standard Model predictions for the first measurement of CEνNS is generated. We emphasize the critical impact of the quenching factor on the search for new physics via CEνNS experiments.

J.I. Collar et al. arXiv:1907.04828

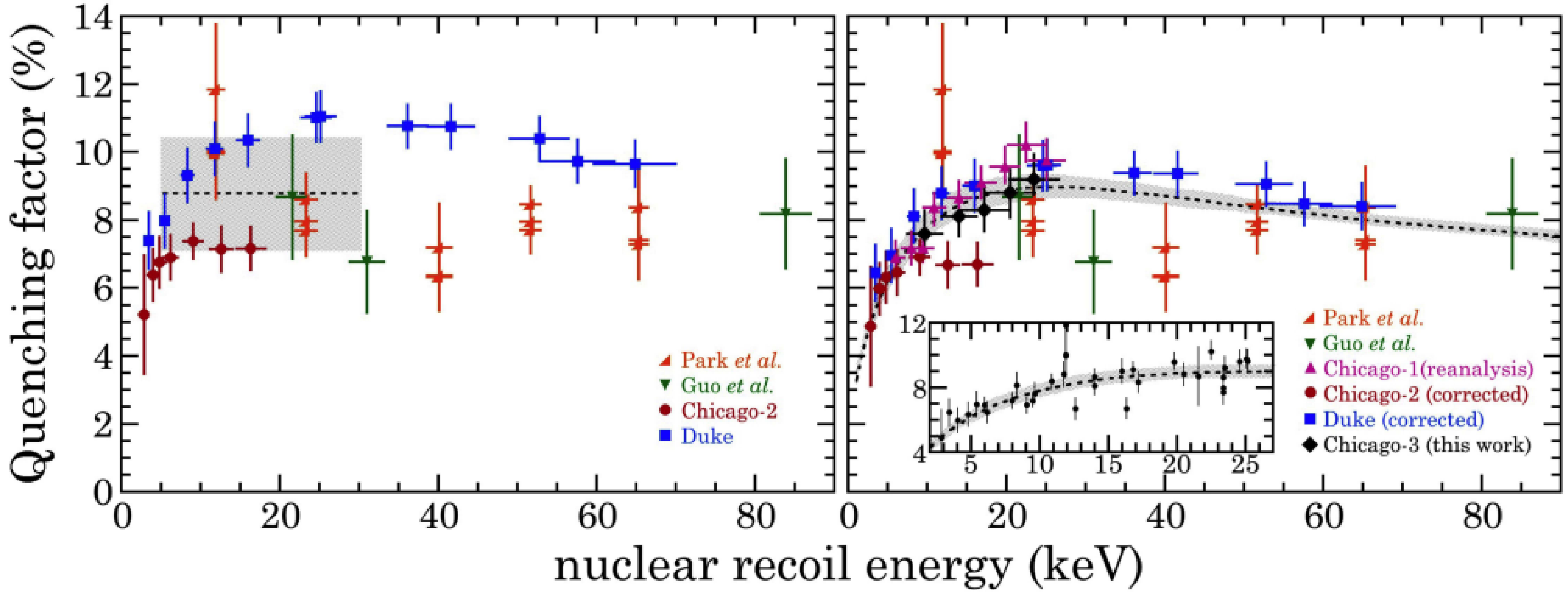

FIG. 1. *Left:* quenching factor suggested in [3] for CsI[Na]. An unphysical energy-independent behavior was adopted to accommodate the large dispersion in calibration data available at the time [5, 7, 14, 15], visible in the figure. The resulting 1-σ uncertainty is shown as a grayed band. *Right:* present global data and physics-based QF model developed in Sec. V (dotted line). The inset expands the CEνNS ROI for CsI[Na] at a spallation source. Horizontal error bars are removed for clarity.

New ingredients… Quenching Factor and β

[Akimov et al. **Science** 357 (2017) 6356]

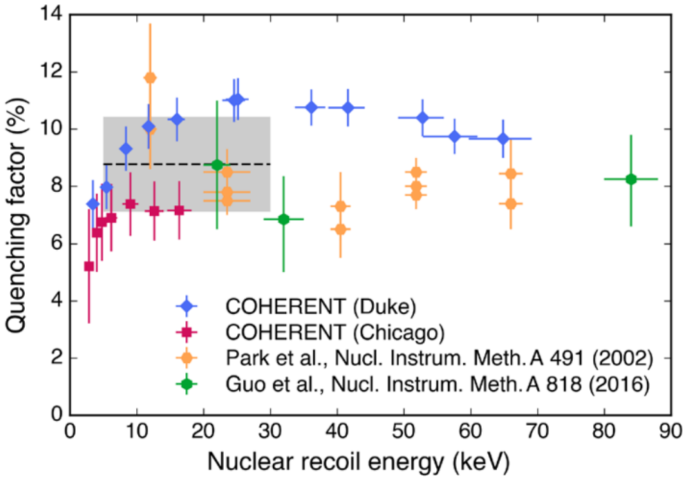

Quenching factor for CsI

[Collar et al. PRD 100, 033003 (2019)]

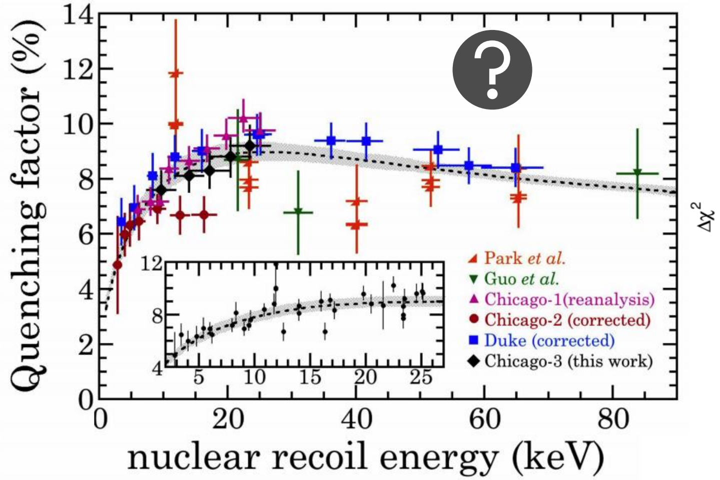

Determination of the Scalar and Vector Polarizabilities of the Cesium $6s\,^2S_{1/2} \rightarrow 7s\,^2S_{1/2}$ Transition and Implications for Atomic Parity Nonconservation

George Toh, Amy Damitz, Carol E. Tanner, W. R. Johnson, and D. S. Elliott

Phys. Rev. Lett. **123**, 073002 – Published 16 August 2019

ABSTRACT

Using recent high-precision measurements of electric dipole matrix elements of atomic cesium, we make an improved determination of the scalar (α) and vector (β) polarizabilities of the cesium $6s\,^2S_{1/2} \rightarrow 7s\,^2S_{1/2}$ transition calculated through a sum-over-states method. We report values of $\alpha = -268.82(30)a_0^3$ and $\beta = 27.139(42)a_0^3$ with the highest precision to date. We find a discrepancy between our value of β and the past preferred value, resulting in a significant shift in the value of the weak charge Q_w of the cesium nucleus. Future work to resolve the differences in the polarizability will be critical for interpretation of parity nonconservation measurements in cesium, which have implications for physics beyond the standard model.

New β

Old β

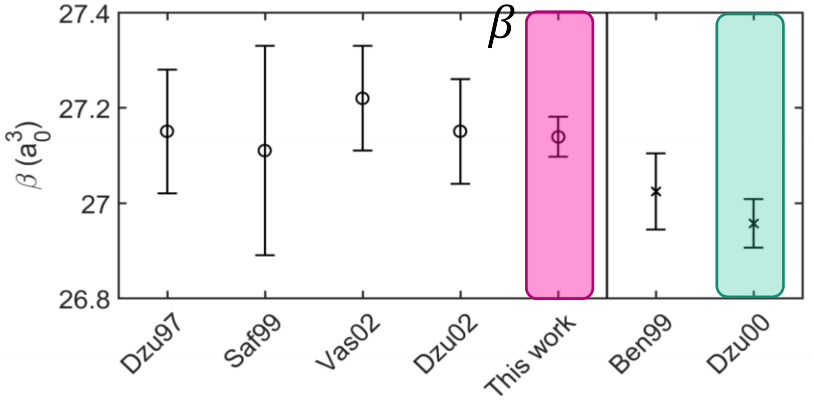

Year	Authors	Remarks	β (a_0^3)
2019	**This work**	**Sum over states (α)**	**27.139 (42)**
2002	Dzu02 [27]	Sum over states (α)	27.15 (11)
2002	Vas02 [34]	Sum over states (α)	27.22 (11)
2000	**Dzu00** [31]	**$M1_{hf}$ calculation**	**26.957 (51)**
1999	Ben99 [32]	$M1_{hf}/\beta$ expt	27.024 (80)
1999	Saf99 [33]	Sum over states (α)	27.11 (22)
1999	Saf99 [33]	Sum over states (β)	27.16
1997	Dzu97 [56]	Sum over states (α)	27.15 (13)
1992	Blu92 [22]	Sum over states (β)	27.0 (2)

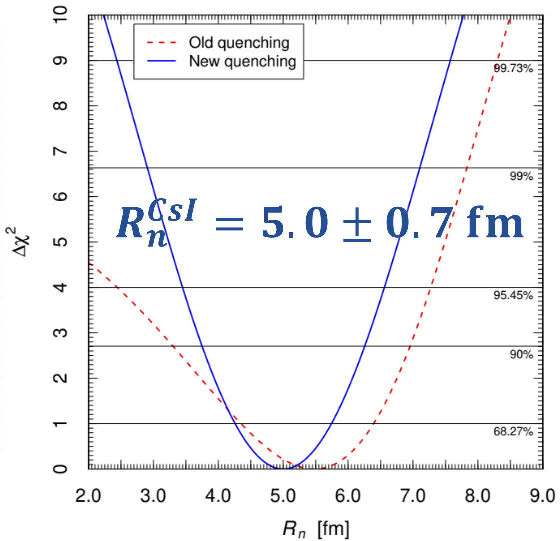

$$R_n^{CsI} = 5.0 \pm 0.7\ \mathrm{fm}$$

CsI neutron density distribution measurements

Neutrino, Electroweak and Nuclear Physics from COHERENT Elastic Neutrino-Nucleus Scattering with a New Quenching Factor

M. Cadeddu,[1,*] F. Dordei,[2,†] C. Giunti,[3,‡] Y.F. Li,[4,5,§] and Y.Y. Zhang[4,5,¶]

[arXiv:1908.06045v3]

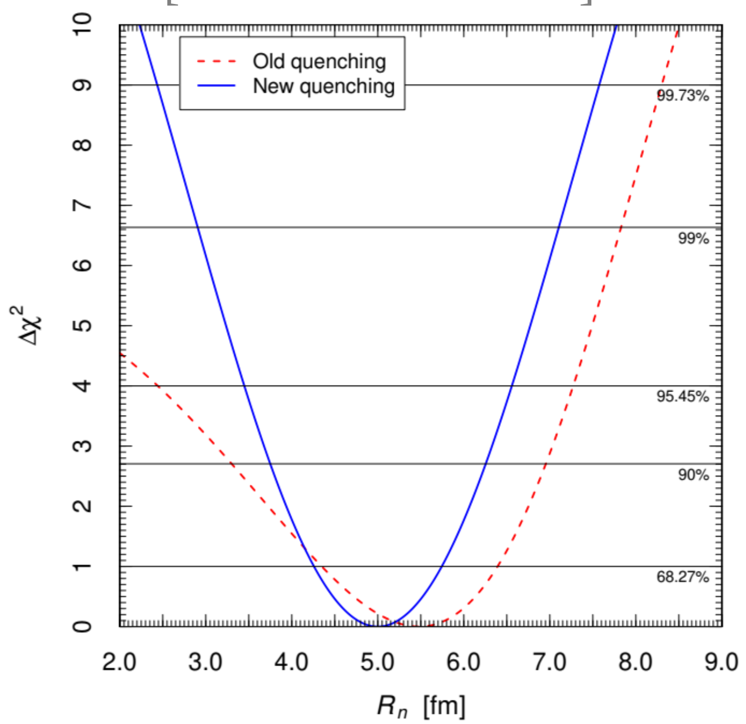

$$R_n = 5.0^{+0.7}_{-0.7}(1\sigma)^{+1.5}_{-1.5}(2\sigma)^{+2.5}_{-2.6}(3\sigma)\ \mathrm{fm}$$

$$\Delta R_{np} = 0.2^{+0.7}_{-0.7}(1\sigma)^{+1.5}_{-1.5}(2\sigma)^{+2.5}_{-2.6}(3\sigma)\ \mathrm{fm}$$

$$R_n = 5.5^{+0.9}_{-1.1}\ \mathrm{fm}$$ Official quenching factor

Theoretical values in [fm] with Skyrme-Hartree-Fock (SHF) and relativistic mean field (RMF) nuclear models.

Model	CsI R_p	CsI R_n	CsI $R_n - R_p$
SHF SkM* [26]	4.73	4.86	0.13
SHF SkP [27]	4.75	4.87	0.12
SHF SkI4 [28]	4.70	4.83	0.14
SHF Sly4 [29]	4.73	4.87	0.13
SHF UNEDF1 [30]	4.71	4.87	0.15
RMF NL-SH [31]	4.71	4.89	0.18
RMF NL3 [32]	4.72	4.92	0.20
RMF NL-Z2 [33]	4.76	4.97	0.21

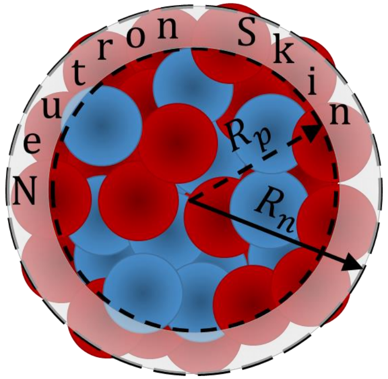

COHERENT constraints after the Chicago-3 quenching factor measurement

D.K. Papoulias*

[arXiv:1907.11644v1]

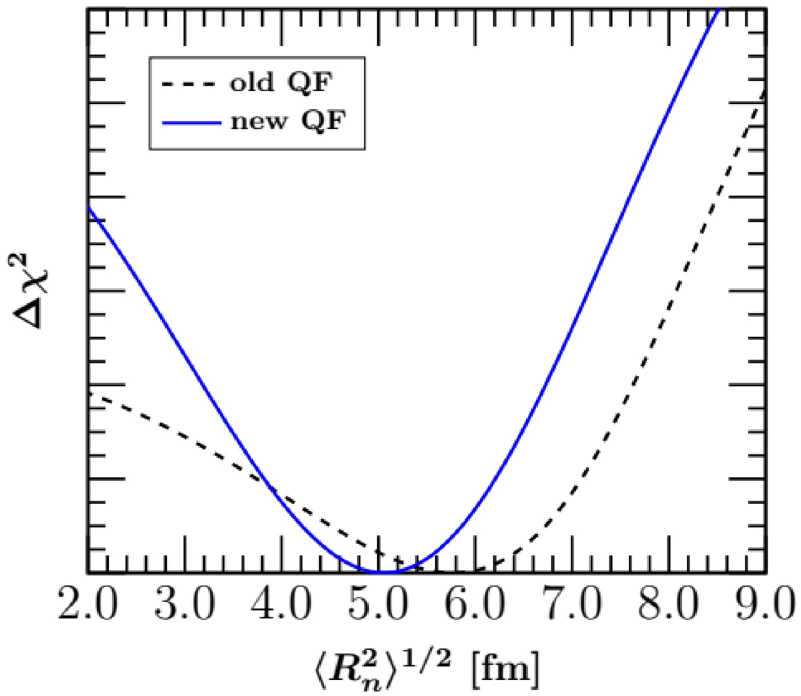

$$\langle R_n^2\rangle^{1/2} = 5.1^{+1.3}_{-1.5}\ \mathrm{fm} \quad (\text{new QF}).$$

$$\langle R_n^2\rangle^{1/2} = 5.8^{+1.5}_{-2.6}\ \mathrm{fm} \quad (\text{old QF}),$$

CsI neutron density distribution measurement (2)

[Khan et al. arXiv:1907.12444v2]

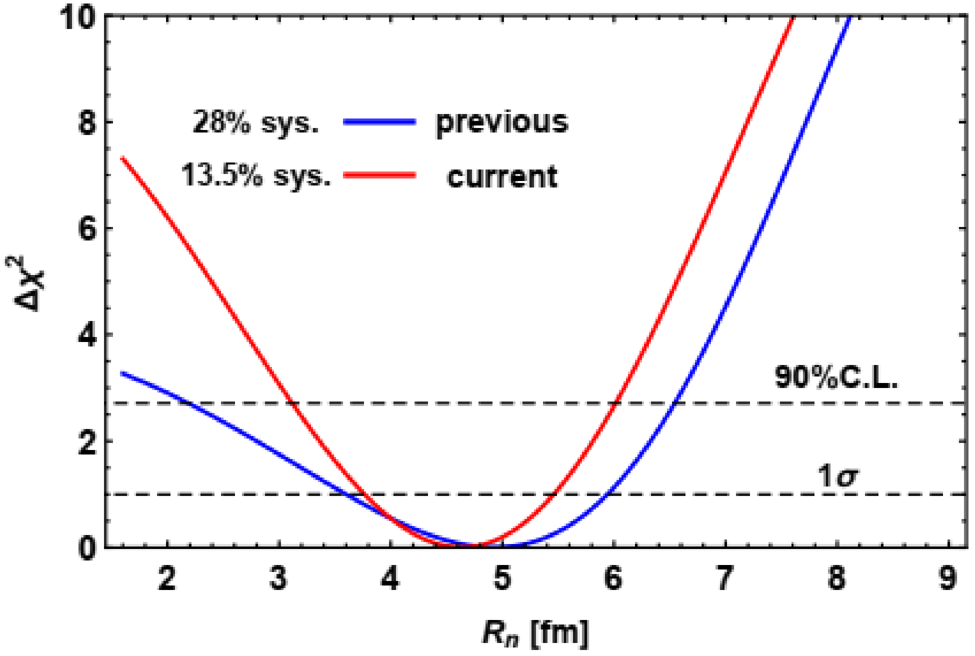

$$R_n = 4.6^{+0.9}_{-0.8}\ \mathrm{fm}\ (1\sigma)\quad \text{(current)},$$
$$R_n = 4.9^{+1.1}_{-1.3}\ \mathrm{fm}\ (1\sigma)\quad \text{(previous)}.$$

$$\Delta R_{np} = R_n - R_p \simeq -0.18^{+0.9}_{-0.8}\ \mathrm{fm}$$

Caveat: Klein-Nystrand form factor and quenching factor was assumed to be constant with a small uncertainty.

[Coloma et al. arXiv:2006.08624v2]

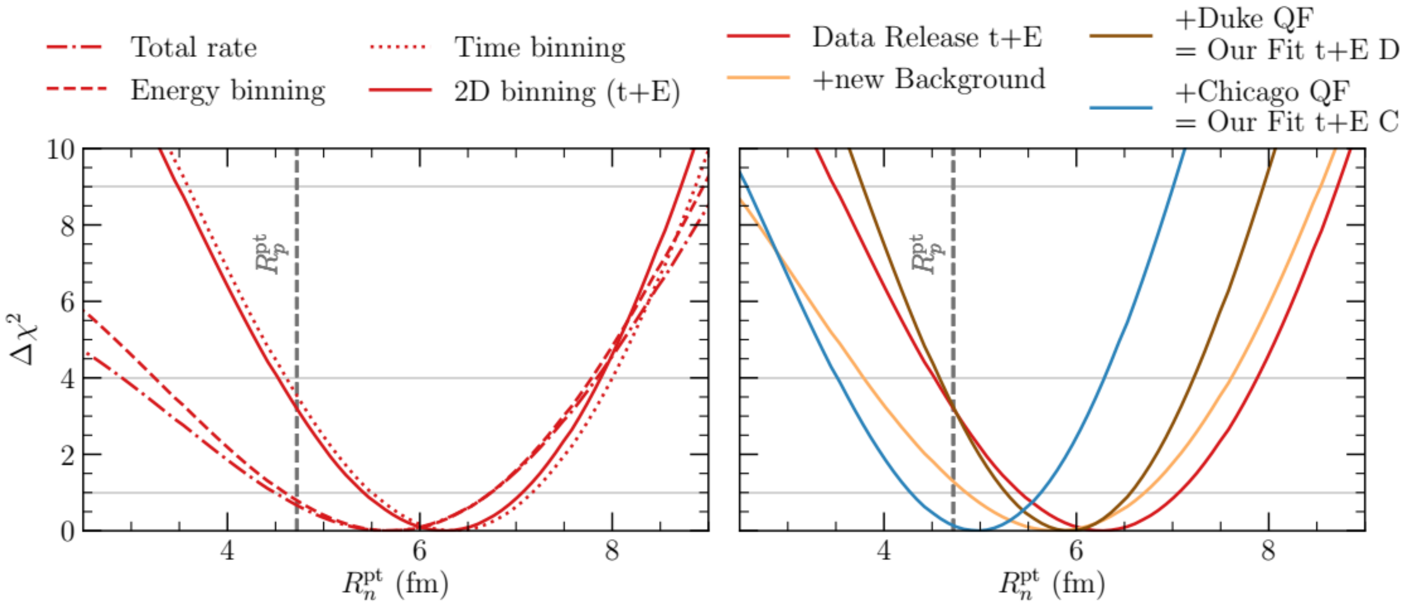

$R_n^{\rm pt} = 6.28^{+0.77}_{-0.85}$ fm For Data Release t + E

$R_n^{\rm pt} = 5.80^{+0.89}_{-0.93}$ fm For Data Release t + E + new Background

$R_n^{\rm pt} = 5.96^{+0.57}_{-0.59}$ fm For Our Fit t + E D

$R_n^{\rm pt} = 4.99^{+0.65}_{-0.73}$ fm For Our Fit t + E C +Chicago QF = Our Fit t+E C

Compatible with what found in arXiv:1908.06045v3 and arXiv:1907.11644v1.

First advantage of the combination

✓ Assuming to know the value of the weak mixing angle at low energy $\sin^2\hat{\theta}_W(0) = 0.23857(5)$

COHERENT χ^2 APV χ^2

$$\chi^2 = \chi^2_{\rm C} + \left(\frac{Q_W^{\rm Cs\,ns}(R_n) - Q_W^{\rm th}(\sin^2\vartheta_W)}{\sigma_{\rm APV}(R_n, \sin^2\vartheta_W)} \right)^2$$

$$\Delta R_{np}(^{127}\mathrm{I}) = R_n - R_p = 1.1^{+1.0}_{-0.9}\ \mathrm{fm}$$

$$\Delta R_{np}(^{133}\mathrm{Cs}) = R_n - R_p = 0.45^{+0.33}_{-0.33}\ \mathrm{fm}$$

Contribution of Cs and I disentangled!!

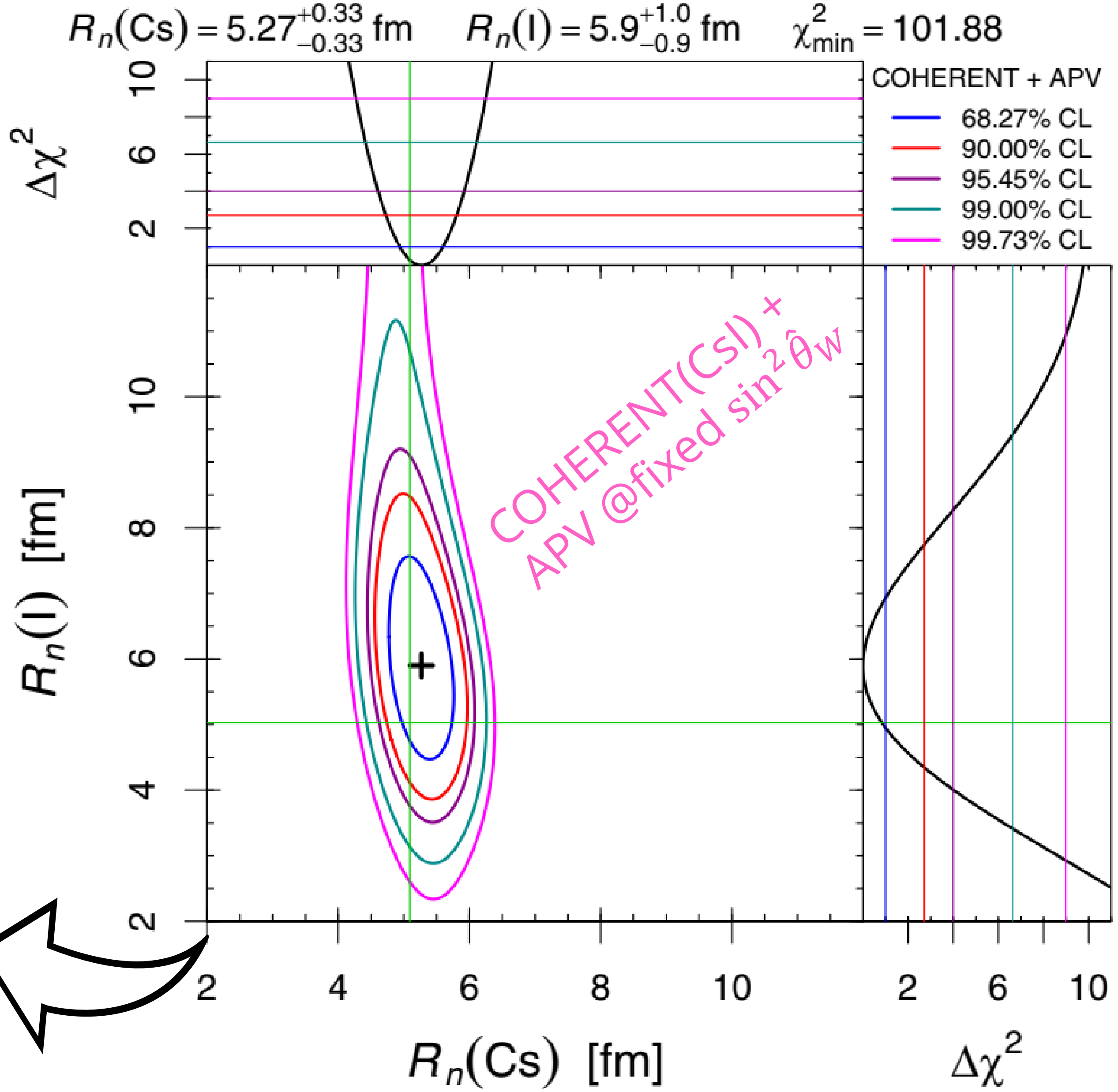

Cadeddu et al., PRC 104, 065502
arXiv:2102.06153

First argon constraints on neutron radius

Using COHERENT CENNS-10 [arXiv:2003.10630]

[O. G. Miranda et al. arXiv:2003.12050v3]

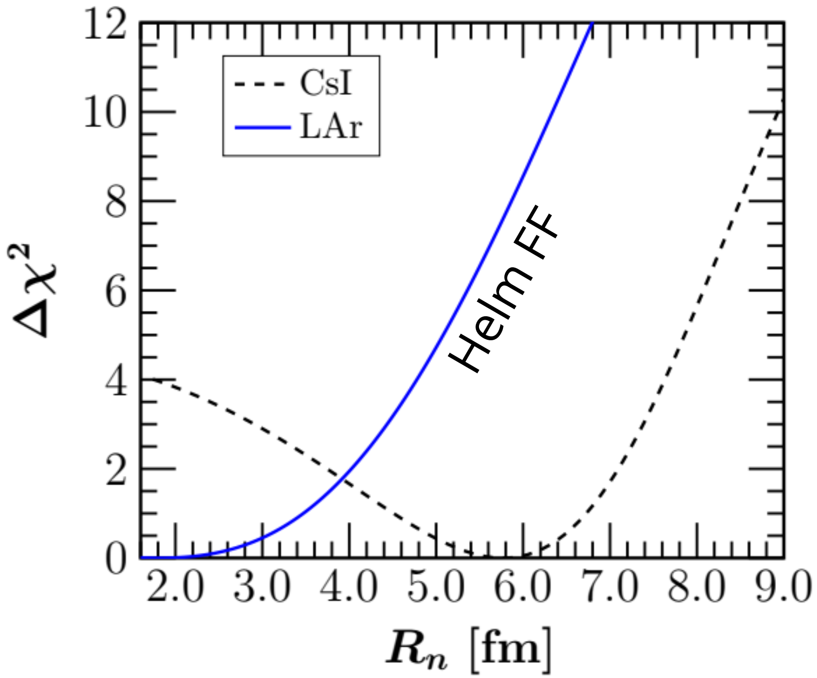

$$\chi^2(X) = \min_{\alpha}\left[\frac{(N_{\rm meas} - N_{\rm theor}(X)[1+\alpha])^2}{\sigma^2_{\rm stat}} + \left(\frac{\alpha}{\sigma_\alpha}\right)^2\right]$$

$\boxed{R_n < 4.33 \text{ fm}}$ @90 % CL

Single energy bin analysis for LAr

[M. C. et al. arXiv:2005.01645v2]

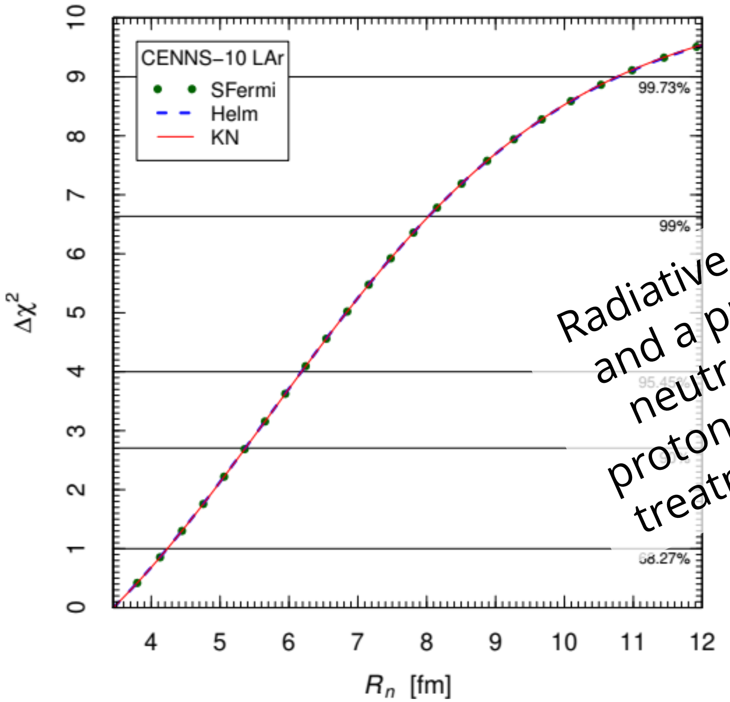

Radiative corrections and a proper point-neutron vs folded proton/neutron radius treatment included in the analysis!

$$R_p = 3.448 \pm 0.003 \text{ fm}$$

$$R_n(^{40}\text{Ar}) < 4.2\,(1\sigma),\ 6.2\,(2\sigma),\ 10.8\,(3\sigma) \text{ fm}$$

These bounds are in agreement with the nuclear model predictions, but unfortunately they are too weak to allow us a selection of the models.

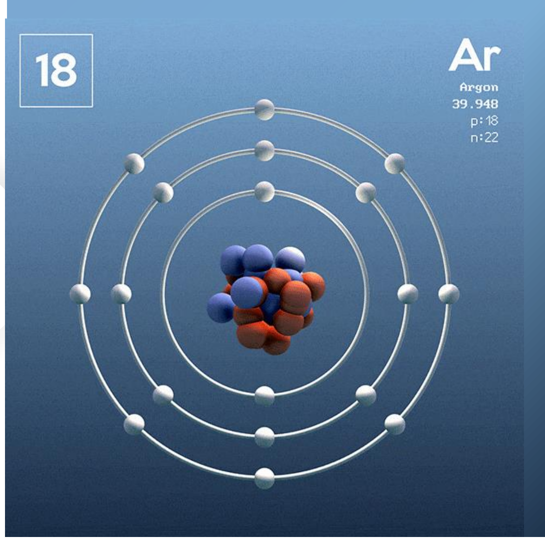

Theoretical values for Ar in [fm] with Skyrme-Hartree-Fock (SHF) and relativistic mean field (RMF) nuclear models.

Interaction		$R_p^{\rm point}$	$R_n^{\rm point}$
Sky3D			
SkI3	[37]	3.33	3.43
SkI4	[37]	3.31	3.41
Sly4	[38]	3.38	3.46
Sly5	[38]	3.37	3.45
Sly6	[38]	3.36	3.44
Sly4d	[39]	3.35	3.44
SV-bas	[40]	3.33	3.42
UNEDF0	[41]	3.37	3.47
UNEDF1	[42]	3.33	3.43
SkM*	[43]	3.37	3.45
SkP	[44]	3.40	3.48
DIRHB			
DD-ME2	[45]	3.30	3.39
DD-PC1	[46]	3.30	3.39

[arXiv:2005.01645v2]

Nuclear Structure Physics in Coherent Elastic Neutrino-Nucleus Scattering

N. Van Dessel,[1] V. Pandey,[2,*] H. Ray,[2] and N. Jachowicz[1,†]
[1] *Department of Physics and Astronomy, Ghent University, Proeftuinstraat 86, B-9000 Gent, Belgium*
[2] *Department of Physics, University of Florida, Gainesville, FL 32611, USA*

They perform **microscopic many-body nuclear structure physics calculations** of charge and weak nuclear form factors and CEνNS cross sections on different nuclei, including Ar.

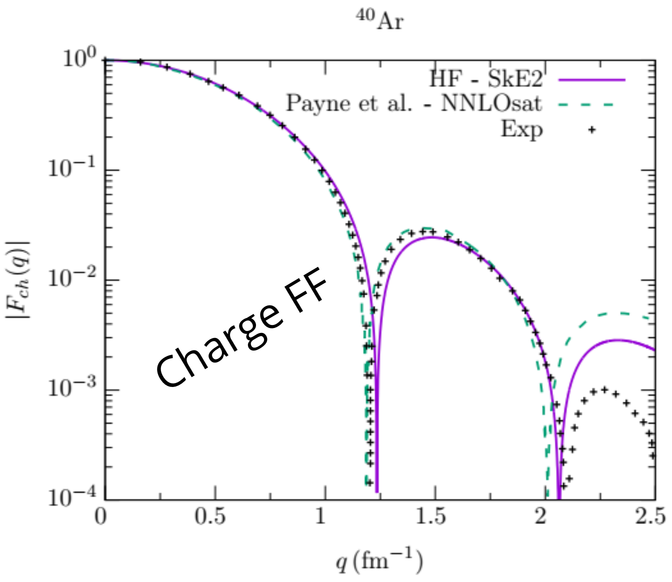

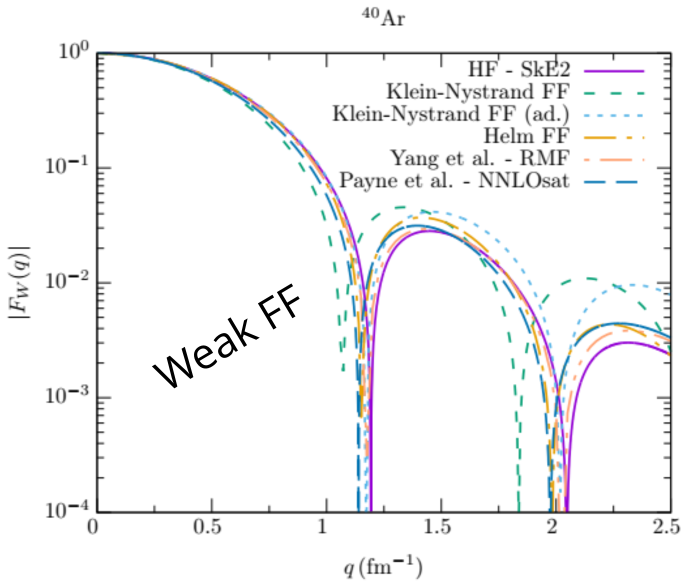

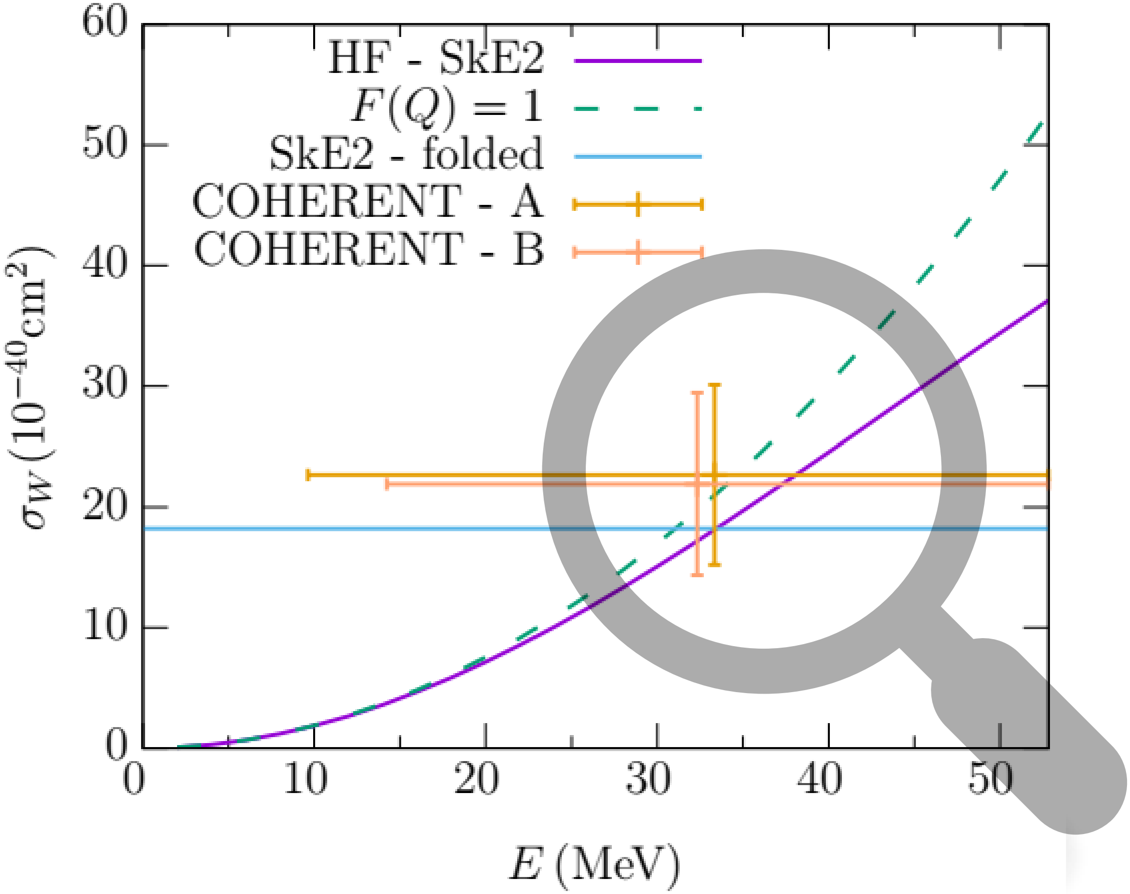

- ✓ After validating Ar charge form factor calculation, they make predictions for the Ar weak form factor.
- ➢ They calculate differential cross section and compare it with widely used phenomenological form factor predictions and recent measurements of the COHERENT collaboration. Future precise measurements of CEνNS will aid in constraining neutron densities.

See also C. G. Payne, et al Phys. Rev. C **100**, 061304 (2019)

Coherent elastic neutrino–nucleus scattering: EFT analysis and nuclear responses

Martin Hoferichter,[1, 2, *] Javier Menéndez,[3, 4, †] and Achim Schwenk[5, 6, 7, ‡]

They provide weak form factor calculated using the large-scale nuclear shell model for a wide range of nuclei including Cs, I and Ar.

Rate = BSM couplings ⊗ hadronic matrix elements ⊗ $\boxed{\text{nuclear structure}}$ ⊗ neutrino flux

- **Nuclear matrix element** of the single-nucleon and few-nucleon amplitudes
- Ideally: based on nuclear interactions from chiral EFT
  ↪ "ab-initio" calculation Coupled-cluster calculation for ^{40}Ar, Payne et al. 2019
- Not yet available for heavier nuclei
- Therefore: here us **nuclear shell model** with phenomenological interactions
- Main uncertainty from **neutron skin**
  ↪ no direct experimental validation of neutron distribution

Weak form factor of ^{40}Ar

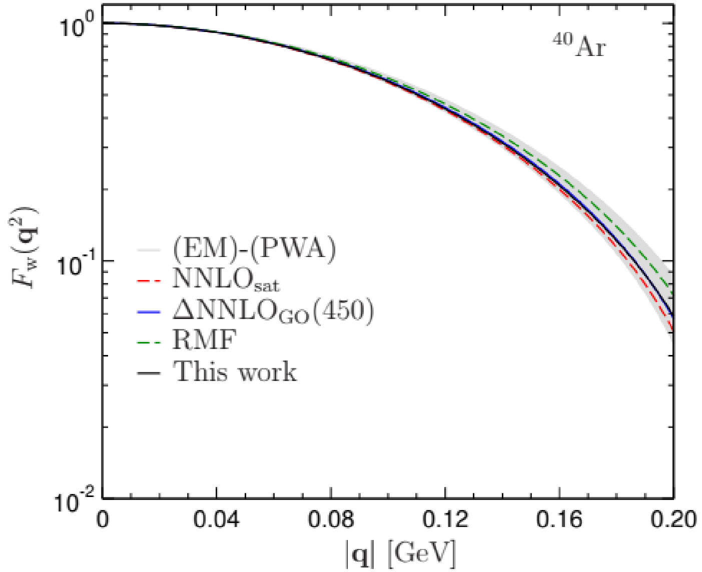

EFT motivation: CEvNS spans very large range of energy scales

Λ_{BSM}
1. **BSM scale** Λ_{BSM}: $\mathcal{L}_{BSM}$
2. **Effective Operators**:

Λ_{EW}
3. Integrate out **EW physics** (start here if only SM)

$\Lambda_{hadrons}$
4. **Hadronic scale**: nucleons and pions
   ↪ effective interaction Hamiltonian H_I

Λ_{nuclei}
5. **Nuclear scale**: $\langle \mathcal{N}|H_I|\mathcal{N}\rangle$
   ↪ nuclear wave function

BSM: impact on weak FF

$$\frac{d\sigma_A}{dT} = \frac{m_A}{2\pi}\left(1 - \frac{m_A T}{2E_\nu^2} - \frac{T}{E_\nu}\right)\tilde{Q}_w^2|\tilde{F}_w(\mathbf{q}^2)|^2$$

Both the weak charge AND the form factor are affected by BSM effects!

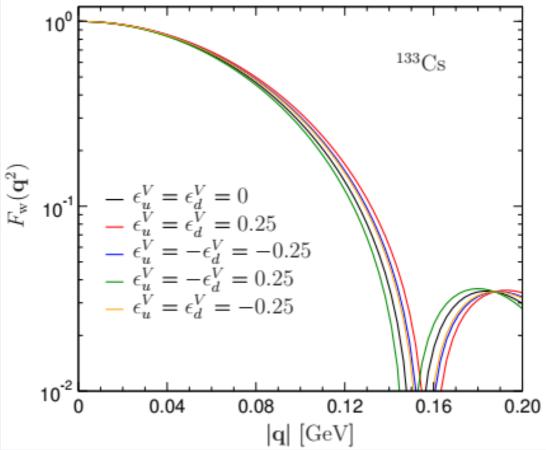

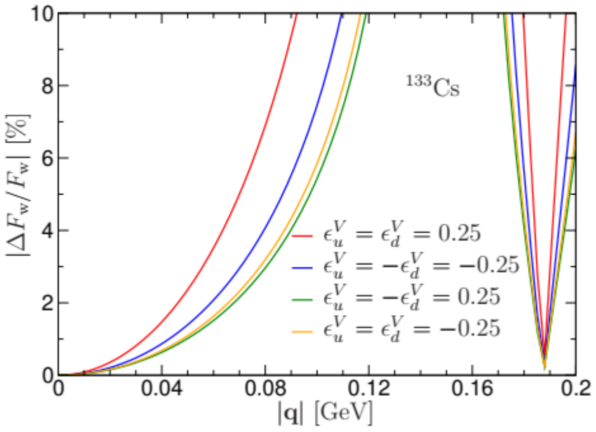

THE NUCLEAR FORM FACTOR

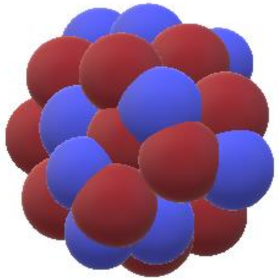

- The nuclear form factor, F(q), is taken to be the **Fourier transform** of a spherically symmetric ground state **mass distribution (both proton and neutrons)** normalized so that **F(0) = 1**:

For a weak interaction like for CEvNS you deal with the **weak form factor**: the Fourier transform of the weak charge distribution (neutron + proton distribution weighted by the weak mixing angle)

$$\frac{d\sigma}{dE_r} \cong \frac{G_F^2\, m_N}{4\pi}\left(1-\frac{m_N E_r}{2E_\nu^2}\right) Q_w^2 \times |F_{weak}(E_r)|^2$$

Weak charge × weak form factor

$$\left[g_V^p Z F_Z(E_r, R_p) + g_V^n N F_N(E_r, R_n)\right]^2$$

Proton + Neutron from factor

Extensively studied
Huge bibliography

Poorly known…

Helm R. Phys. Rev. **104**, 1466 (1956)

It is convenient to have an analytic expression like the **Helm form factor**

$$\boxed{F_N^{\text{Helm}}(q^2) = 3\,\frac{j_1(qR_0)}{qR_0}\,e^{-q^2 s^2/2}}$$

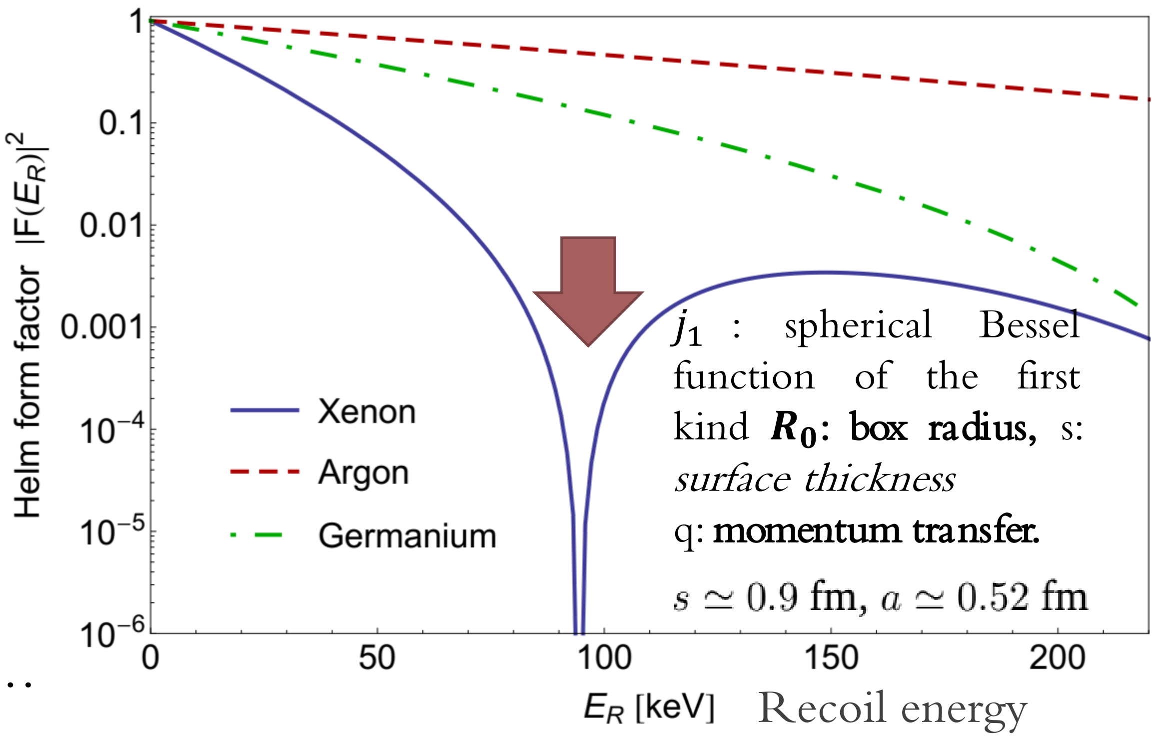

Recoil energy

FITTING THE COHERENT CsI DATA FOR THE NEUTRON RADIUS

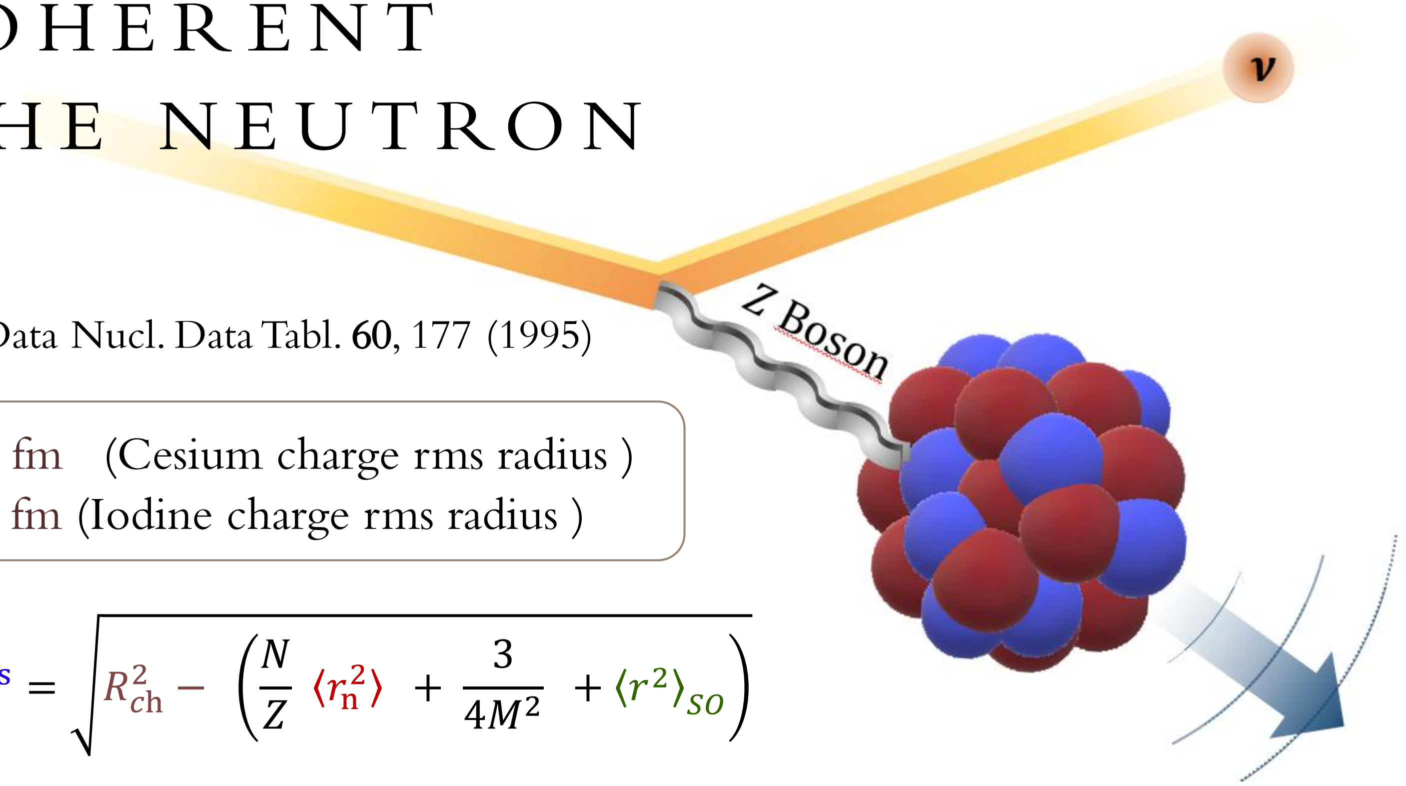

G. Fricke et al., Atom. Data Nucl. Data Tabl. **60**, 177 (1995)

✓ From muonic X-rays data we have

(For fixed $t = 2.3$ fm)

$R_{ch}^{Cs} = 4.804$ fm (Cesium charge rms radius)

$R_{ch}^{I} = 4.749$ fm (Iodine charge rms radius)

$$R_p^{\mathrm{rms}} = \sqrt{R_{\mathrm{ch}}^2 - \left(\frac{N}{Z}\langle r_{\mathrm{n}}^2\rangle + \frac{3}{4M^2} + \langle r^2\rangle_{SO}\right)}$$

$$\underbrace{\begin{array}{l} R_p^{Cs} = 4.821 \pm 0.005 \text{ fm (Cesium rms proton radius)} \\ R_p^{I} = 4.766 \pm 0.008 \text{ fm (Iodine rms-proton radius)} \end{array}}$$

$$\frac{d\sigma}{dE_r} \cong \frac{G_F^2\, m_N}{4\pi}\left(1 - \frac{m_N E_r}{2E_\nu^2}\right)\left[g_V^p Z F_Z\left(E_r, R_p^{Cs/I}\right) + g_V^n N F_N\left(E_r, R_n^{CsI}\right)\right]^2$$

R_n^{Cs} & R_n^{I} very well known so we fitted COHERENT CsI data looking for R_n^{CsI} ...

FROM THE CHARGE TO THE PROTON RADIUS

One need to take into account finite size of both protons and neutrons plus other corrections

$$R_{ch}^2 = R_{\text{point}}^2 + \langle r_{\text{p}}^2 \rangle + \frac{N}{Z}\langle r_{\text{n}}^2 \rangle + \frac{3}{4M^2} + \langle r^2 \rangle_{SO}$$

Charge radius

Point-proton radius

Mean squared charge radius of a single proton

$\langle r_{\text{p}}^2 \rangle = 0.7071\ \text{fm}^2$

Mean squared charge radius of a single neutron

$\langle r_{\text{n}}^2 \rangle = -0.1161\ \text{fm}^2$

Relativistic Darwin-Foldy correction

$\sim 0.033\ \text{fm}^2$

Spin-orbit correction

$\sim 0.09\ \text{fm}^2$ for ^{48}Ca

$\sim 0.028\ \text{fm}^2$ for ^{208}Pb

G. Hagen et al. *Nature Physics* **12**, 186–190 (2016), Arxiv: 1509.07169

M. Cadeddu et al. PRD 102, 015030 (2020), Arxiv: 2005.01645

$$R_p^{\text{rms}} = \sqrt{R_{\text{point}}^2 + \langle r_{\text{p}}^2 \rangle} =$$

$$= \sqrt{R_{ch}^2 - \left(\frac{N}{Z}\langle r_{\text{n}}^2 \rangle + \frac{3}{4M^2} + \langle r^2 \rangle_{SO}\right)}$$

RMS proton distribution radius

+COHERENT+APV

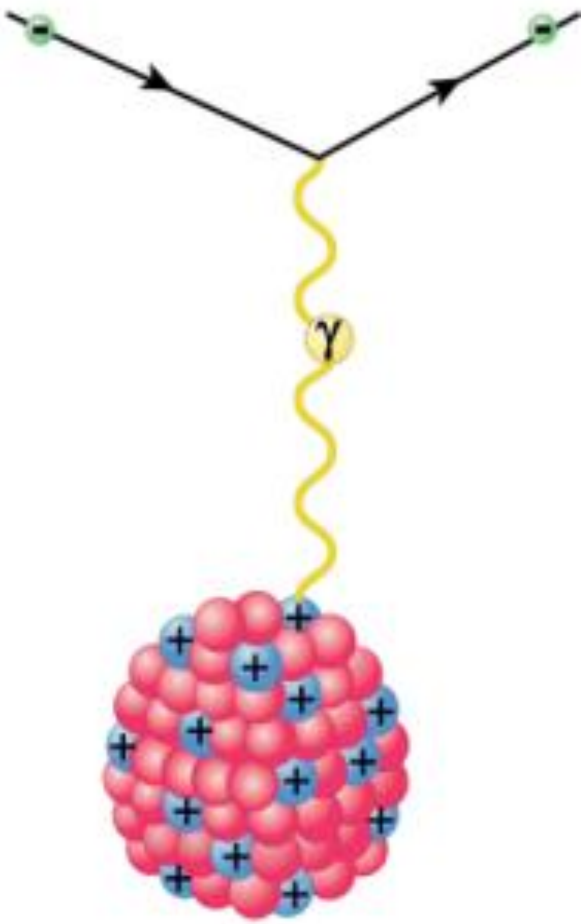

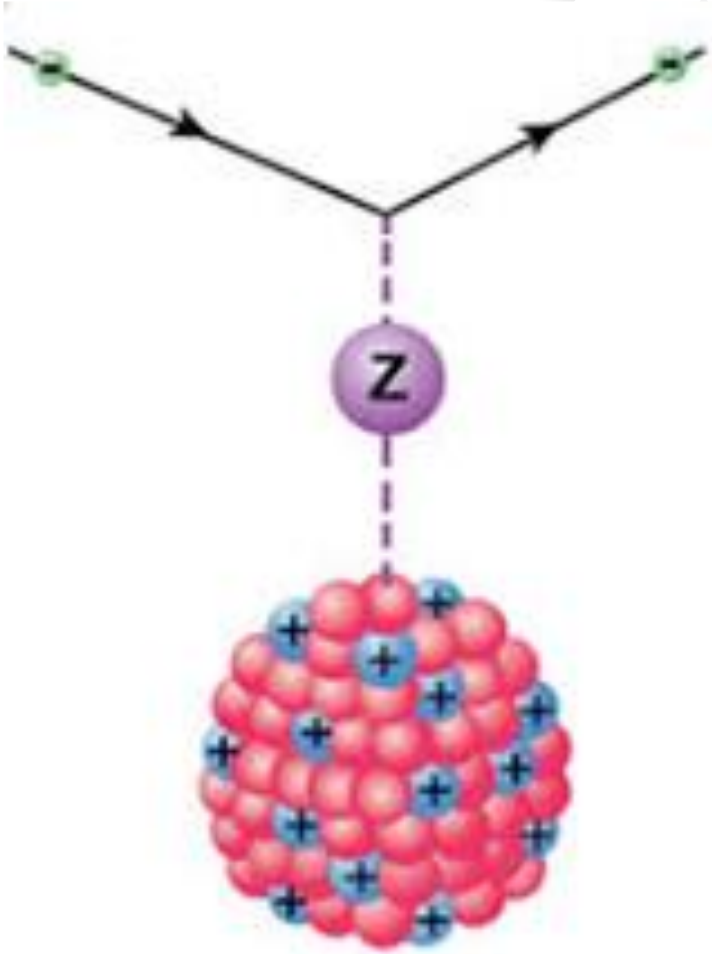

S. J. Novario et al. arXiv:2111.12775

See G. Hagen's talk

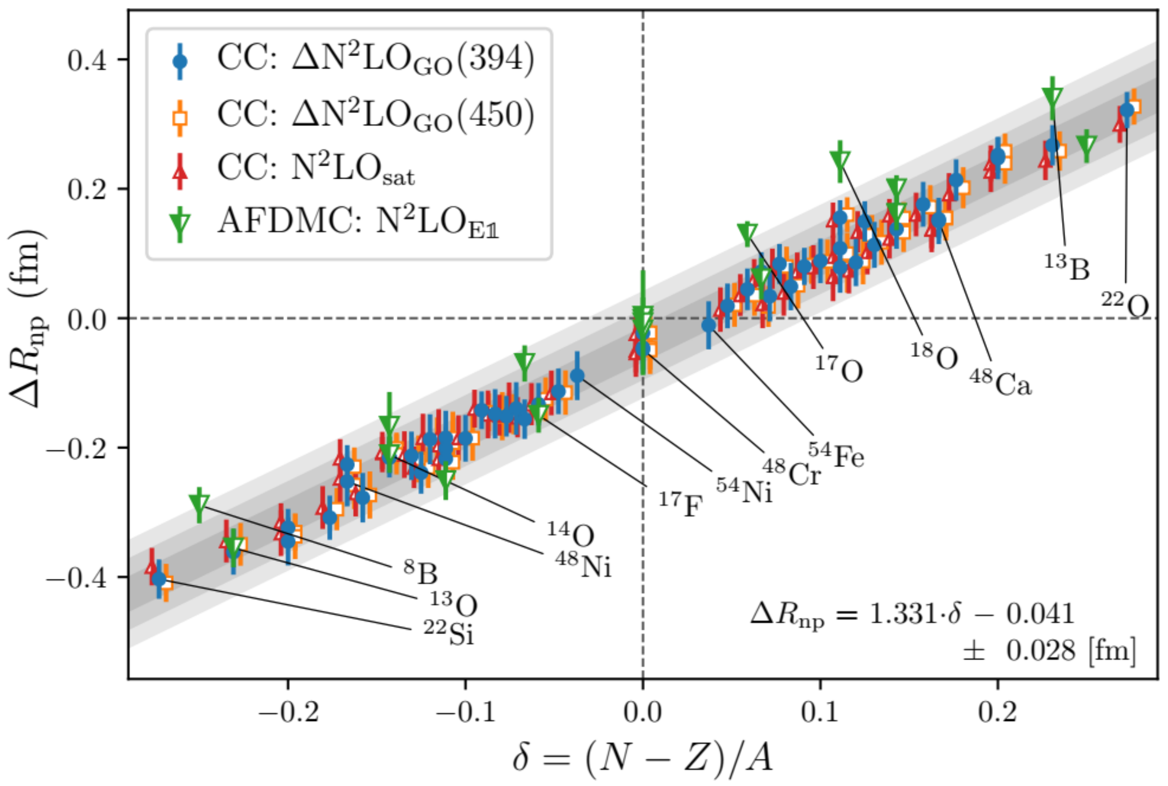

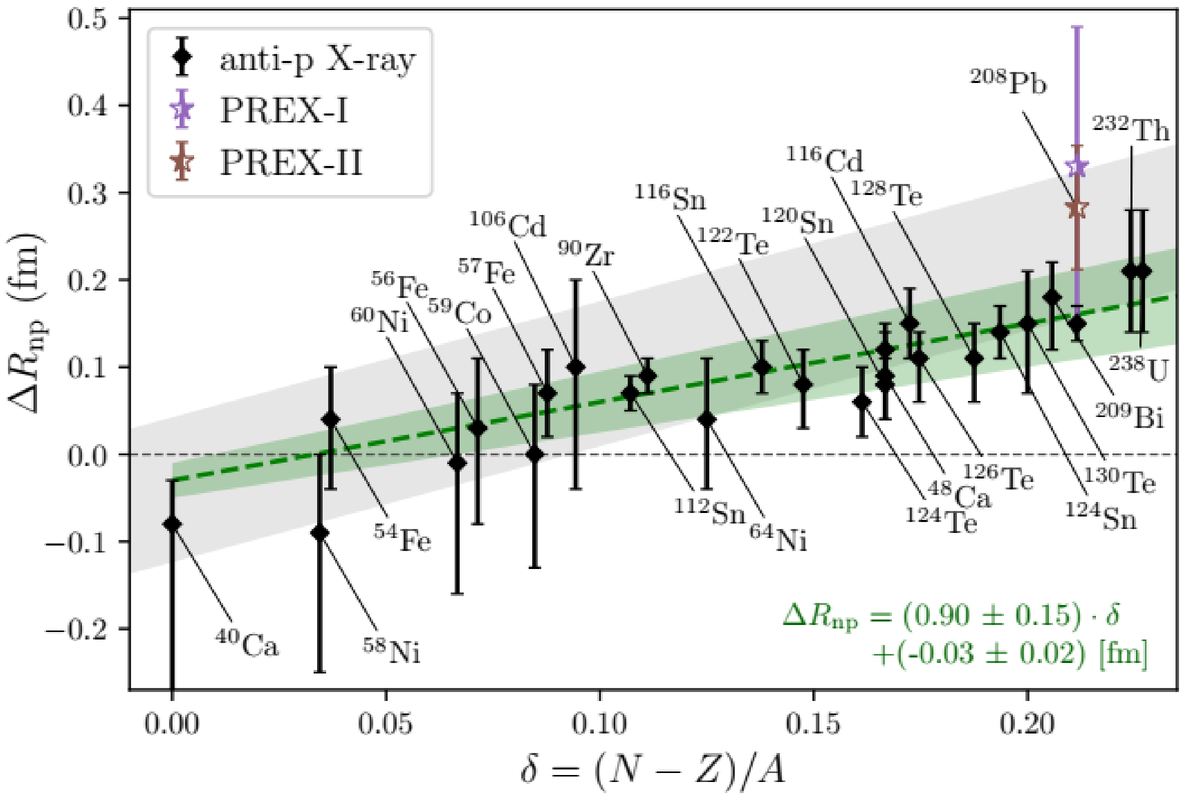

$$\Delta R_{np}[\mathrm{fm}] = 1.331\frac{N-Z}{A} - 0.041 \pm 0.028\ \mathrm{fm}$$

$$\Delta R_{np}(^{133}\mathrm{Cs}) = 0.189 \pm 0.028\ \mathrm{fm}$$

Atomic parity violation* on Cs

*also known as PNC (Parity nonconservation)

- In the absence of electric fields and weak neutral currents, **an electric dipole** (E1) transition between two atomic states with same parity (6*S* and 7*S* in Cs) is forbidden by the parity selection rule.
- However an electric dipole transition amplitude can be induced by a Z boson exchange between atomic electrons and nucleons → Atomic Parity Violation (APV)

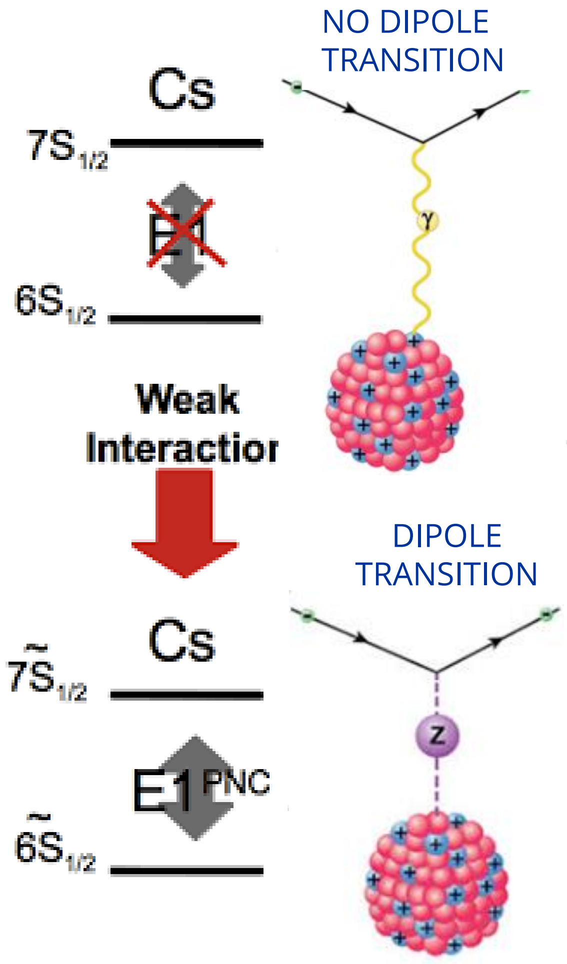

> ➢ The weak NC interaction violates parity and mixes a small amount of the *P* state into the 6*S* and 7*S* states ($\sim 10^{-11}$), characterized by the quantity $\mathbf{Im}(\boldsymbol{E1_{PNC}})$, giving rise to a 7S → 6S transition.

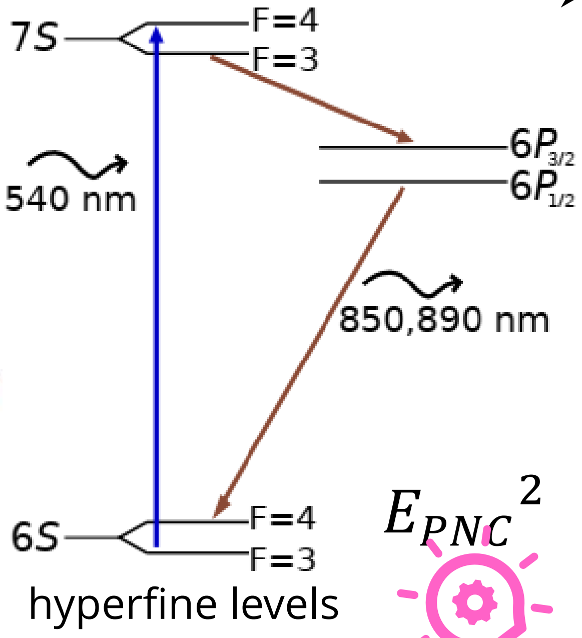

> ➢ To obtain an observable that is at first order in this amplitude, an electric field **E** (that also mixes S & P) is applied. **E** gives rise to a "**Stark induced**" E1 transition amplitude, $\mathbf{A_E}$ that is typically 10^5 times larger than $\mathbf{A_{PNC}}$ and can **interfere** with it.

$$R_{7S\to 6S} = |A_E \pm A_{PNC}|^2 = \\ = \boldsymbol{E1_\beta}^2 \pm 2\boldsymbol{E1_\beta E1_{PNC}} + E_{PNC}{}^2$$

Because the interference term is linear in $\boldsymbol{E1_{PNC}}$ it can be large enough to be measured, but it must be distinguished from the large background contribution ($E1_\beta{}^2$).

The experimental technique

For there to be a nonzero interference term, **the experiment must have a "handedness",** and if the handedness is reversed, the interference term will change sign, and can thereby be distinguished as a modulation in the transition rate

$$R_{7S\to 6S} = |A_E \pm A_{PNC}|^2 \simeq E1_\beta{}^2 \pm 2\boldsymbol{E1_\beta E1_{PNC}}$$

- **Stark-interference technique**: cesium atoms pass through a region of perpendicular electric, magnetic, and laser fields. The "handedness" of the experiment is changed by reversing the direction of all fields.

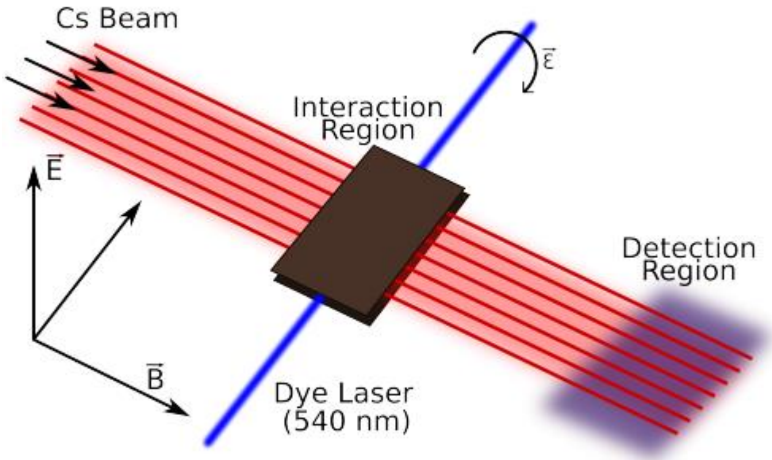

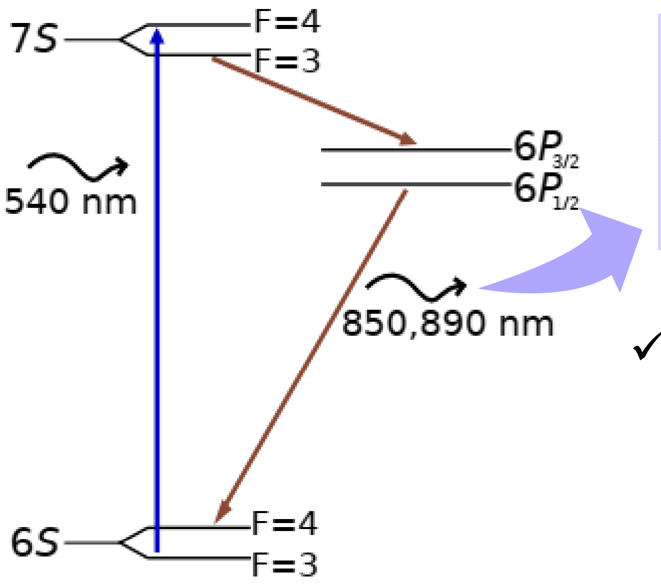

The transition rate is obtained by measuring the amount of 850- and 890-nm light emitted in the 6P-6S step of the 7S-6S decay sequence.

- ✓ The measurements culminated in 1997 when the Boulder group performed a measurement of A_{PNC}/A_E with an uncertainty of just 0.35%.

$$\mathrm{Im}\left(\frac{E_{PNC}}{\beta}\right) = -1.5935(56)\ \frac{\mathrm{mV}}{\mathrm{cm}}$$

[C. S. Wood et al., Science **275**, 1759 (1997)]

The PV amplitude is in units of the equivalent electric field required to give the same mixing of S and Pstates as the PV interaction

[Roberts et al., Annu. Rev. Nucl. Part. Sci. 65, 63 (2015)]

State of the art of E_{PNC} and weak charge

[Dzuba V.A. et al. PRL 109, 203003 (2012)]

TABLE IV. All significant contributions to the E_{PNC} [in $10^{-11} i(-Q_W/N)$ a.u.] for Cs.

Contribution	Value	Source
Core ($n < 6$)	0.0018 (8)	This work
Main ($n = 6$–9)	0.8823 (17)	Ref. [10]
Tail ($n > 9$)	0.0238 (35)	This work
Subtotal	0.9079 (40)	This work
Breit	−0.0055 (1)	Refs. [5,6]
QED	−0.0029 (3)	Ref. [7]
Neutron skin	−0.0018 (5)	Ref. [5]
Total	0.8977 (40)	This work

$$E_{\text{PNC}} = 0.8977(40) \times 10^{-11} i(-Q_W/N)$$

$$Q_W^{\text{exp.}}({}^{133}_{55}Cs) = -72.58(29)_{\text{expt}}(32)_{\text{theory}}$$

$$\mathbf{\sin^2 \theta_W^{APV} = 0.2356(20)}$$

✓ Weak charge in the SM including radiative corrections

$$Q_W^{SM+\text{r.c.}} \equiv -2\left[Z\left(g_{AV}^{ep} + 0.00005\right) + N\left(g_{AV}^{en} + 0.00006\right)\right]\left(1 - \frac{\alpha}{2\pi}\right)$$

$$\approx Z\left(1 - 4\sin^2\theta_W^{SM}\right) - N \quad \Rightarrow \quad Q_W^{SM+r.c.}({}^{133}_{55}Cs) = -73.23(1)$$

SM prediction: $\sin^2\hat{\theta}_W(0) = 0.23857(5)$

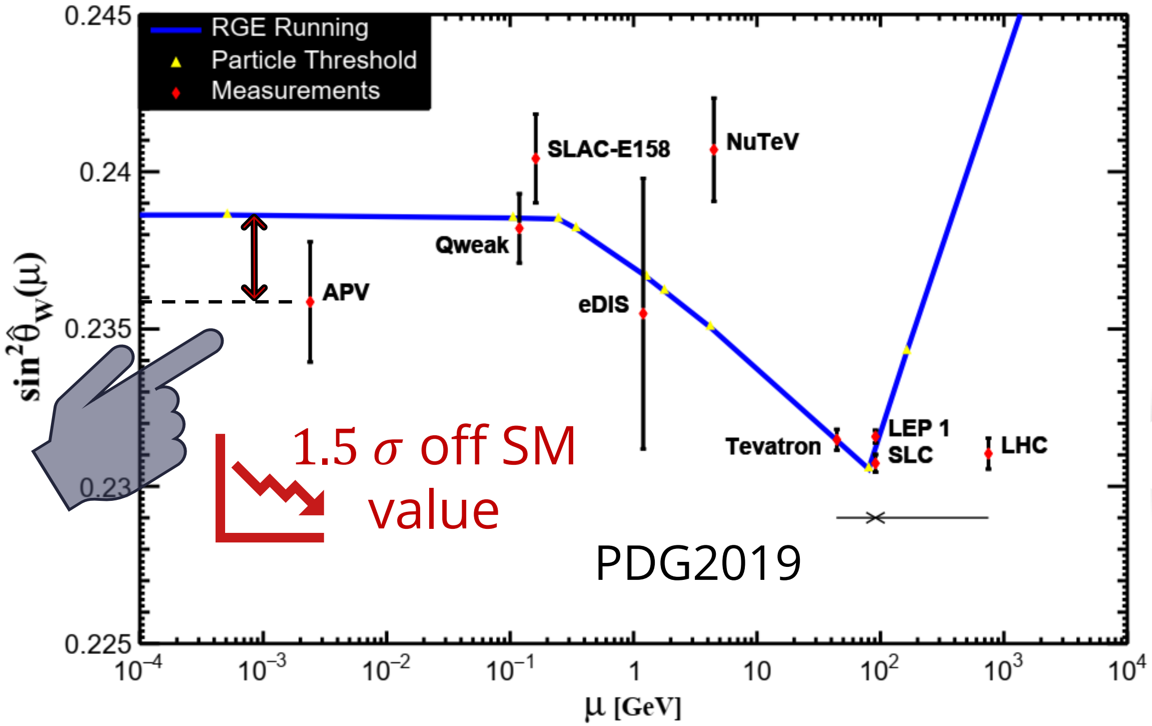

COHERENT+APV compared to PREX

$\Delta R_{np}(^{133}\mathrm{Cs}) = 0.45^{+0.33}_{-0.33}$ fm

@fixed $\sin^2\hat{\theta}_W$

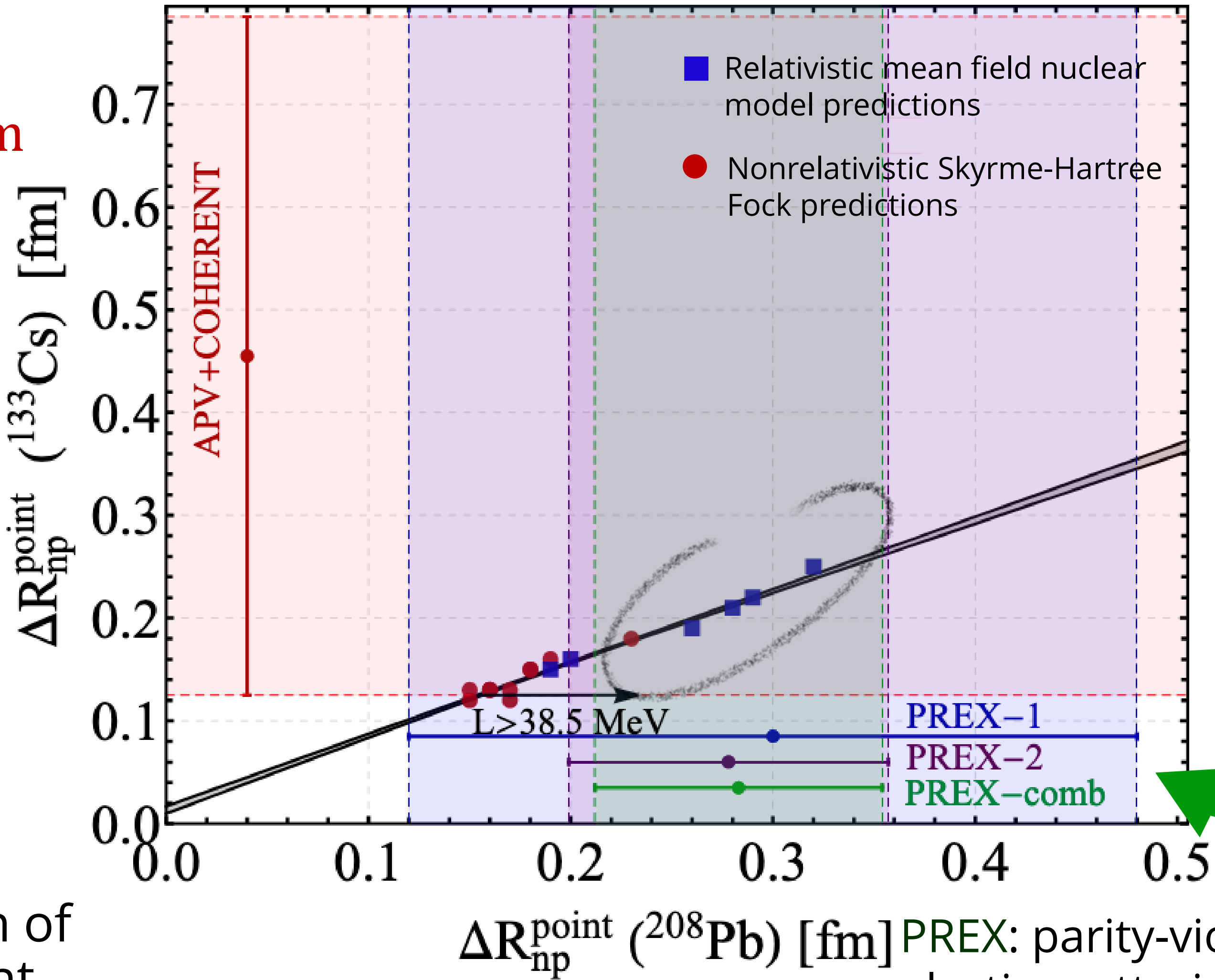

Cadeddu et al., PRC 104, 065502
arXiv:2102.06153

@fixed $\sin^2\hat{\theta}_W$

+ Strong linear correlation between the neutron skin of Cs and Pb among different nuclear model predictions

PREX: parity-violating asymmetry in the elastic scattering of longitudinally polarized electrons on ^{208}Pb

$$A_{\mathrm{PV}} = \frac{\sigma_R - \sigma_L}{\sigma_R + \sigma_L} \approx \frac{G_F Q^2 |Q_W|}{4\sqrt{2}\pi\alpha Z} \frac{F_{\mathrm{W}}(Q^2)}{F_{\mathrm{ch}}(Q^2)}$$

PREX, PRL 126, 172502 (2021)

Neutron skin correction APV

A. V. Viatkina, D. Antypas, M. G. Kozlov, D. Budker, and V. V. Flambaum, Phys. Rev. C **100**, 034318 (2019).
S. J. Pollock, E. N. Fortson, and L. Wilets, Phys. Rev. C **46**, 2587 (1992).

Assuming to know the SM prediction at low energy $\sin^2\hat{\theta}_W(0) = 0.23857(5)$

The weak charge for APV with the neutron skin contribution reads

$$\widetilde{Q}_W \equiv Z q_p (1 - 4\sin^2\vartheta_W) - N q_n$$

This coupling depends on the integrals

$$q_{p,n} = 4\pi \int_0^\infty \rho_{p,n}(r) f(r) r^2 \mathrm{d}r$$

where **ρ(r) are the proton and neutron densities** in the nucleus and **f(r)** is the matrix element of the electron axial current between the atomic $s_{1/2}$ and $p_{1/2}$ wave functions inside the nucleus normalized to f(0) = 1.

$$f(r) = 1 - 2\int_0^r \frac{V(r')}{r'^2} \int_0^{r'} V(r'') r''^2 \mathrm{d}r'' \mathrm{d}r' + \left(\frac{1}{r}\int_0^r V(r') r'^2 \mathrm{d}r'\right)^2,$$

where **V(r)** represents the **radial electric potential** determined uniquely by the **charge distribution** $\rho_c(r)$ of the nucleus.

$$V(r) = 4\pi Z\alpha \left[\frac{1}{r}\int_0^r \rho_c(r') r'^2 \mathrm{d}r' + \int_r^\infty \rho_c(r') r' \mathrm{d}r'\right]$$

We performed the calculations considering charge, proton and neutron distribution densities that correspond to the form factors in the CEνNS cross section using both Helm and 2pF parametrization.

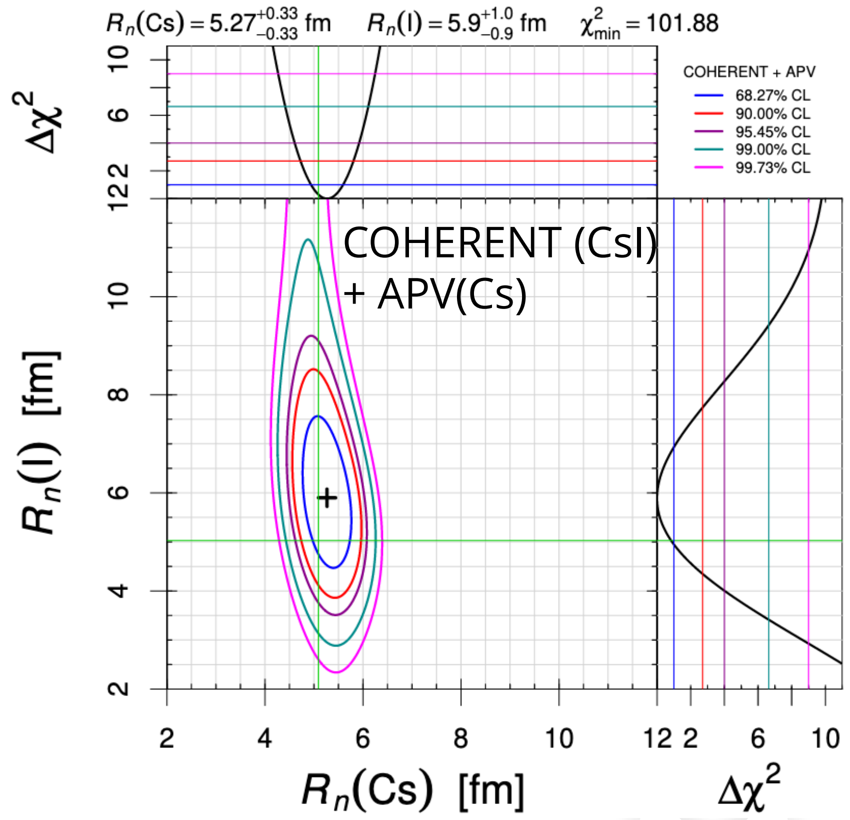

$$\Delta R_{np}(^{127}\mathrm{I}) = R_n - R_p = 1.1^{+1.0}_{-0.9}\ \mathrm{fm}$$

$$\boldsymbol{\Delta R_{np}(^{133}\mathrm{Cs}) = R_n - R_p = 0.45^{+0.33}_{-0.33}\ \mathrm{fm}}$$

Contribution of Cs and I disentangled!!

State of the art of E_{pnC} and weak charge

Early atomic calculations of k_{PV} for ^{133}Cs at the level of 0.4% uncertainty [21–24] gave a value of Q_W that is 2.5σ away from the SM prediction. Later developments resulted in the inclusion of sub-1% contributions from Breit and QED corrections and culminated in the most detailed coupled-cluster single double and valence triple calculation (CCSDvT) with an uncertainty of 0.27% and a value for Q_W in perfect agreement with the SM [25]. A more recent reevaluation yielded a Q_W which is 1.5σ away from the SM value whilst raising the uncertainty back to 0.5% [26]. The latest calculation [27] gives a result agreeing with Ref. [25] with an uncertainty of 0.3%, although objections have been raised with regards to its error estimates [28]. A new parity-mixed coupled-cluster approach to calculating k_{PV} is under development [29], with a goal of reducing the uncertainty to 0.2%.

[21] V. A. Dzuba, V. V. Flambaum, P. G. Silvestrov, and O. P. Sushkov, J. Phys. B **18**, 597 (1985).

[22] V. Dzuba, V. Flambaum, and O. Sushkov, Phys. Lett. A **141**, 147 (1989).

[23] S. A. Blundell, W. R. Johnson, and J. Sapirstein, Phys. Rev. Lett. **65**, 1411 (1990).

[24] S. A. Blundell, J. Sapirstein, and W. R. Johnson, Phys. Rev. D **45**, 1602 (1992).

[25] S. G. Porsev, K. Beloy, and A. Derevianko, Phys. Rev. D **82**, 036008 (2010).

[26] V. A. Dzuba, J. C. Berengut, V. V. Flambaum, and B. Roberts, Phys. Rev. Lett. **109**, 203003 (2012).

[27] B. K. Sahoo, B. P. Das, and H. Spiesberger, Phys. Rev. D **103**, L111303 (2021).

[28] B. M. Roberts and J. S. M. Ginges, Comment on "new physics constraints from atomic parity violation in ^{133}Cs" (2022).

[29] H. B. Tran Tan, D. Xiao, and A. Derevianko, Phys. Rev. A **105**, 022803 (2022).

COHERENT CsI+ APV using E_{PNC} B. K. Sahoo et al. PRD 103, L111303 (2021)

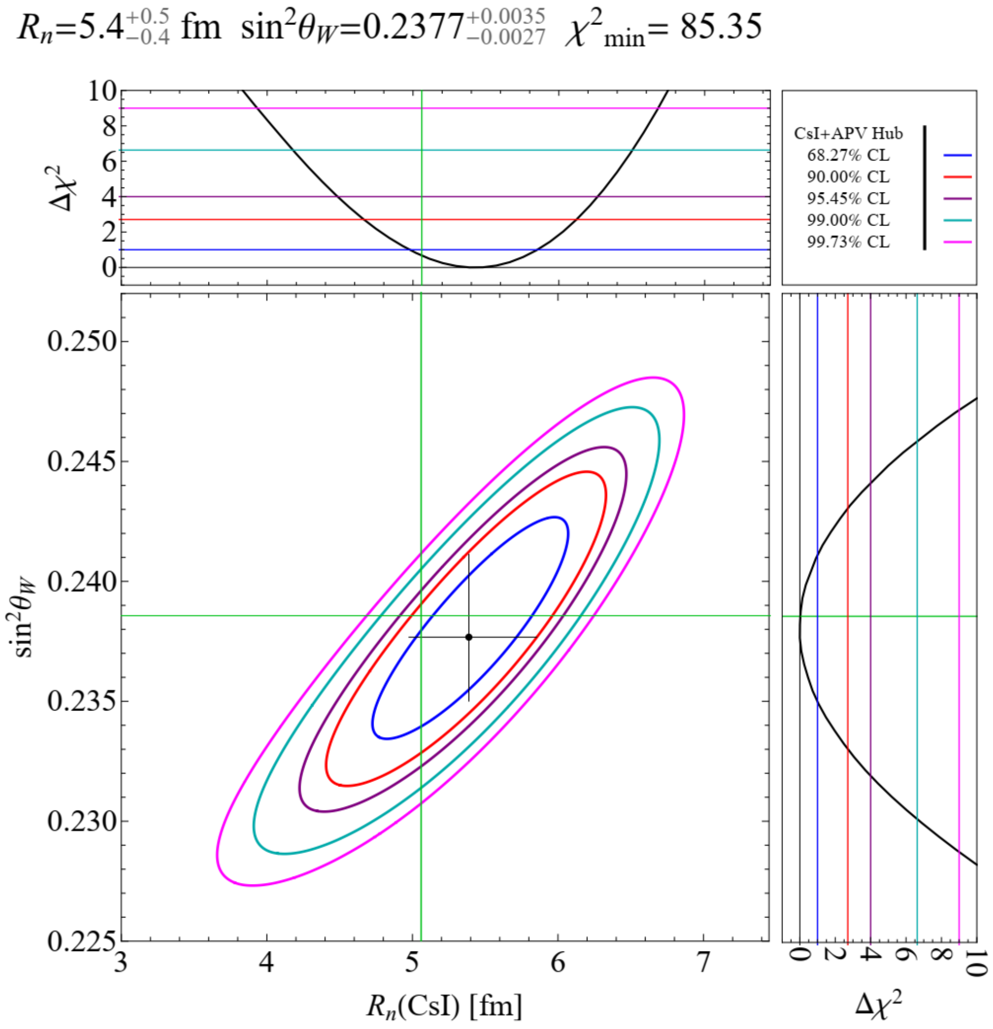

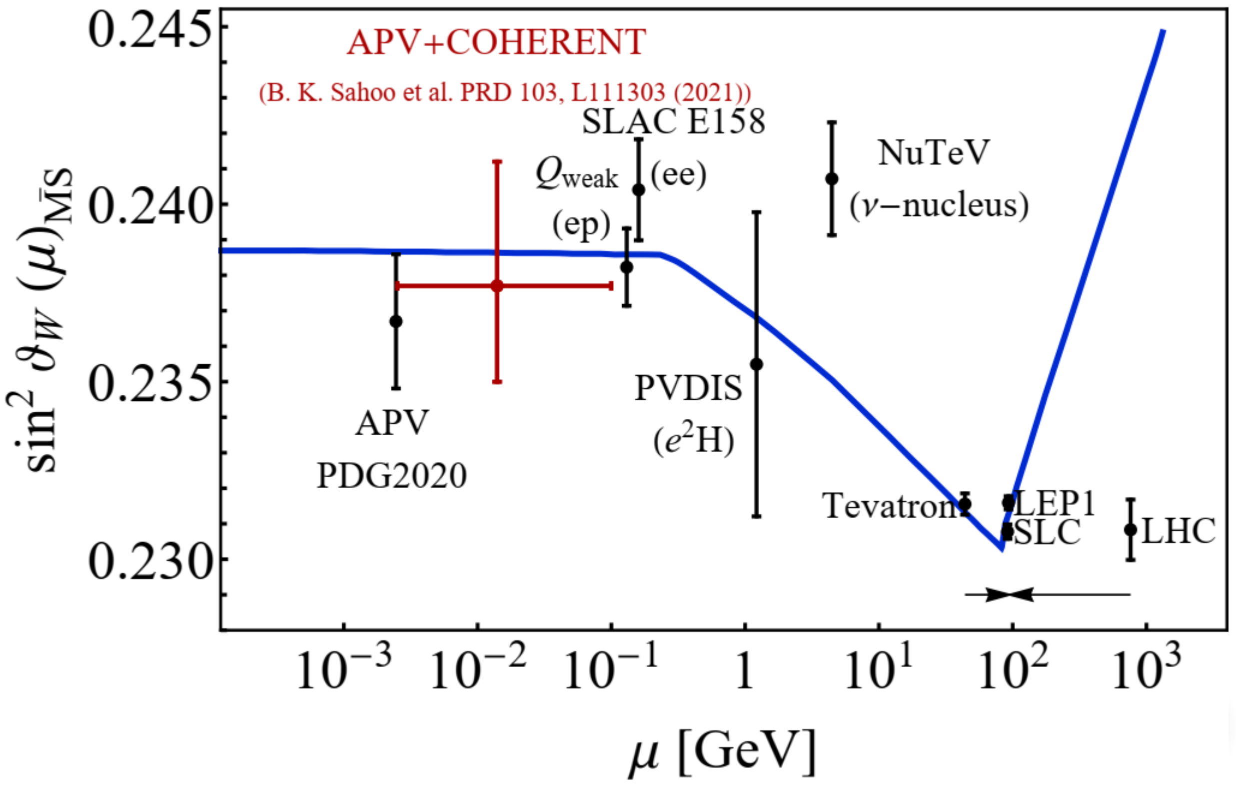

+ Dresden-II quenching

Photo-neutron Ionization Yield in Context

- Multiple yield measurements in Ge are inconsistent with each other
- Variations in operating temperature, electric field and experiment specific parameters suggest a more nuanced yield response at low recoil energies
- Git repository being assembled to collect literature values of yield and operating conditions

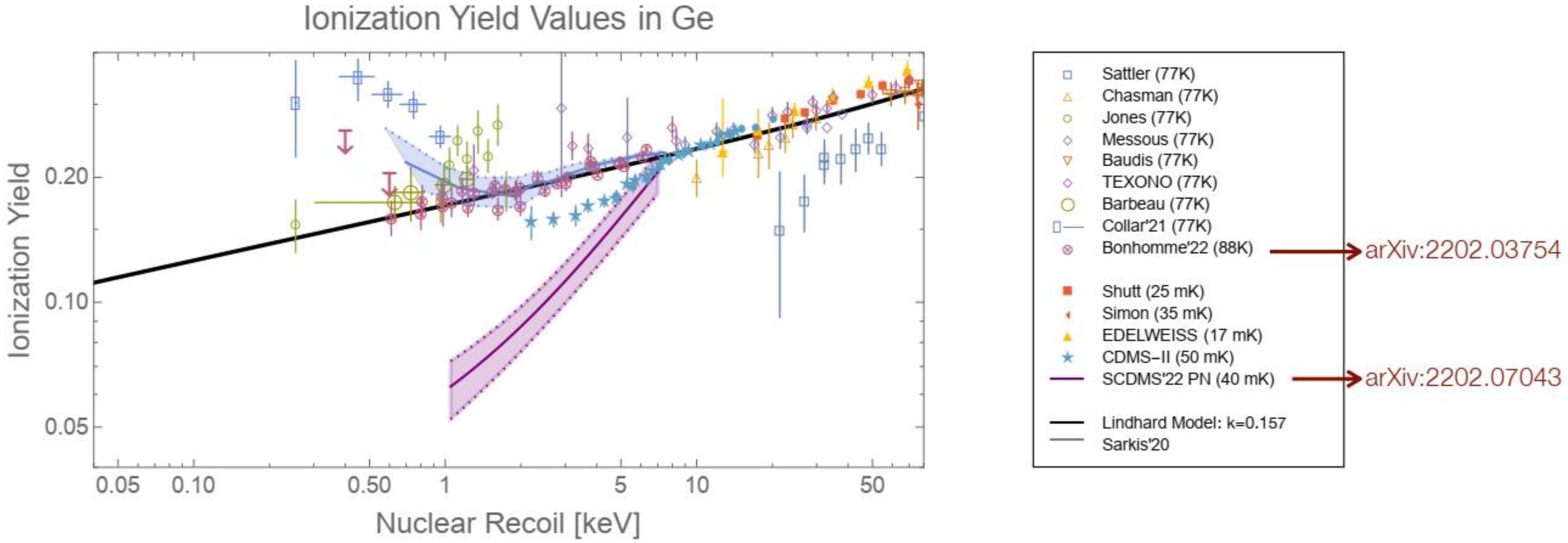

Credits to T. Saab @ EXCESS Workhosp

Germanium quenching factor and EM limits

Process	Collaboration	Limit [10^{-32} cm^2]	C.L.	Ref.
Reactor $\bar{\nu}_e$-e	Krasnoyarsk	$\lvert\langle r^2_{\nu_e}\rangle\rvert < 7.3$	90%	[84]
	TEXONO	$-4.2 < \langle r^2_{\nu_e}\rangle < 6.6$	90%	[85][a]
Accelerator ν_e-e	LAMPF	$-7.12 < \langle r^2_{\nu_e}\rangle < 10.88$	90%	[86][a]
	LSND	$-5.94 < \langle r^2_{\nu_e}\rangle < 8.28$	90%	[87][a]
Accelerator ν_μ-e and $\bar{\nu}_\mu$-e	BNL-E734	$-5.7 < \langle r^2_{\nu_\mu}\rangle < 1.1$	90%	[88][a,b]
	CHARM-II	$\lvert\langle r^2_{\nu_\mu}\rangle\rvert < 1.2$	90%	[89][a]
COHERENT + Dresden-II	w/o transition CR	$-7.1 < \langle r^2_{\nu_e}\rangle < 5$	90%	This work
	w transition CR	$-56 < \langle r^2_{\nu_e}\rangle < 5$	90%	This work
COHERENT + Dresden-II	w/o transition CR	$-5.9 < \langle r^2_{\nu_\mu}\rangle\rvert < 4.3$	90%	This work
	w transition CR	$-58.2 < \langle r^2_{\nu_\mu}\rangle < 4.0$	90%	This work

[a] Corrected by a factor of two due to a different convention, see Ref. [21].
[b] Corrected in Ref. [83].

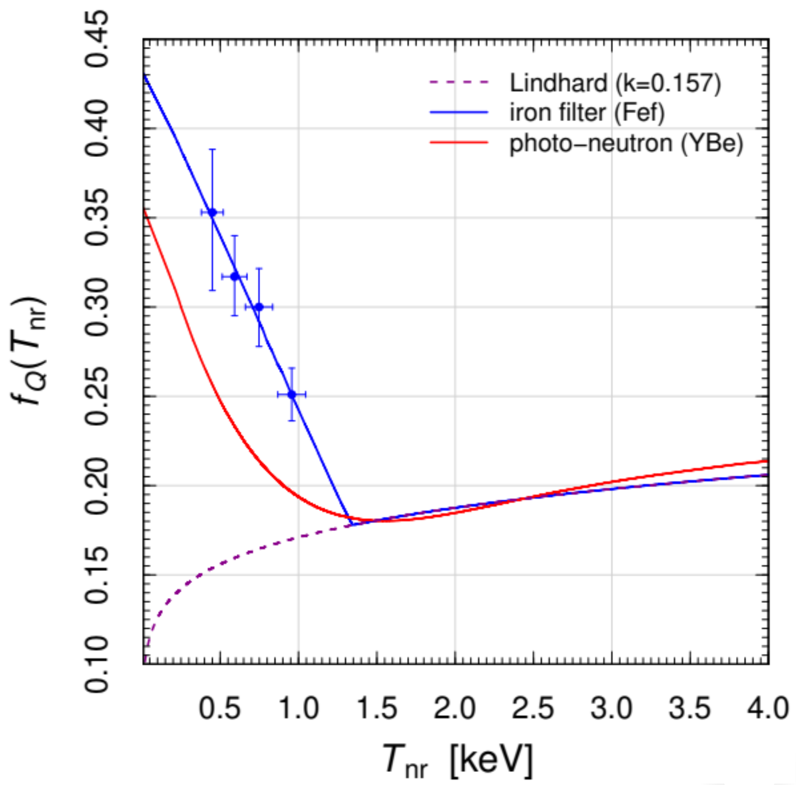

The proton form factor

$$\frac{d\sigma_{\nu-CsI}}{dT} = \frac{G_F^2 M}{4\pi}\left(1 - \frac{MT}{2E_\nu^2}\right)\left[N\, \boldsymbol{F_N(T, R_n)} - \varepsilon Z\, \boldsymbol{F_Z(T, R_p)}\right]^2$$

The proton structures of $^{133}_{55}Cs$ $(N = 78)$ and $^{127}_{53}I$ $(N = 74)$ have been studied with muonic spectroscopy and the data were fitted with **two-parameter Fermi density distributions** of the form

$$\boxed{\rho_F(r) = \frac{\rho_0}{1 + e^{(r-c)/a}}}$$

Where, the **half-density radius c** is related to the **rms radius** and the a parameter quantifies the **surface thickness** $t = 4\, a\, \ln 3$ (in the analysis fixed to 2.30 fm).

- Fitting the data they obtained

$R_p^{Cs} = 4.804$ fm (Caesium proton rms radius)

$R_p^{I} = 4.749$ fm (Iodine proton rms radius)

[G. Fricke et al., Atom. Data Nucl. Data Tabl. **60**, 177 (1995)]

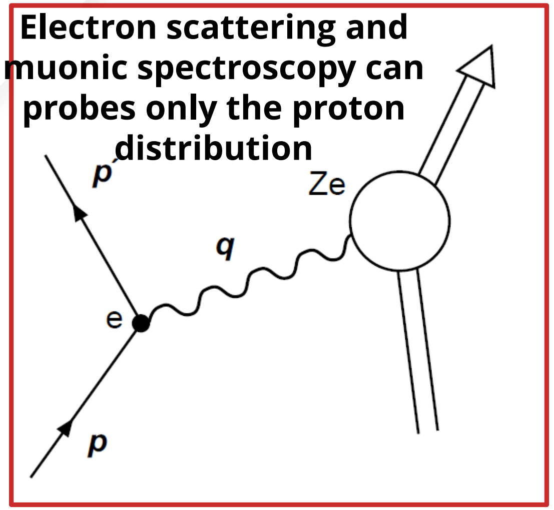

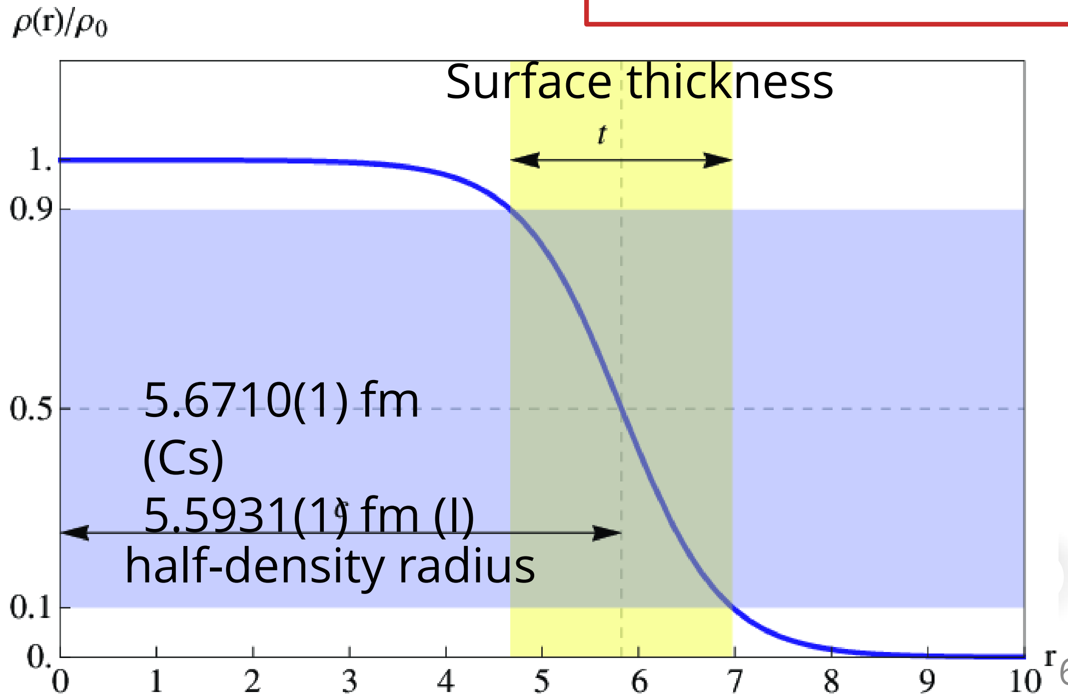

PREX-II

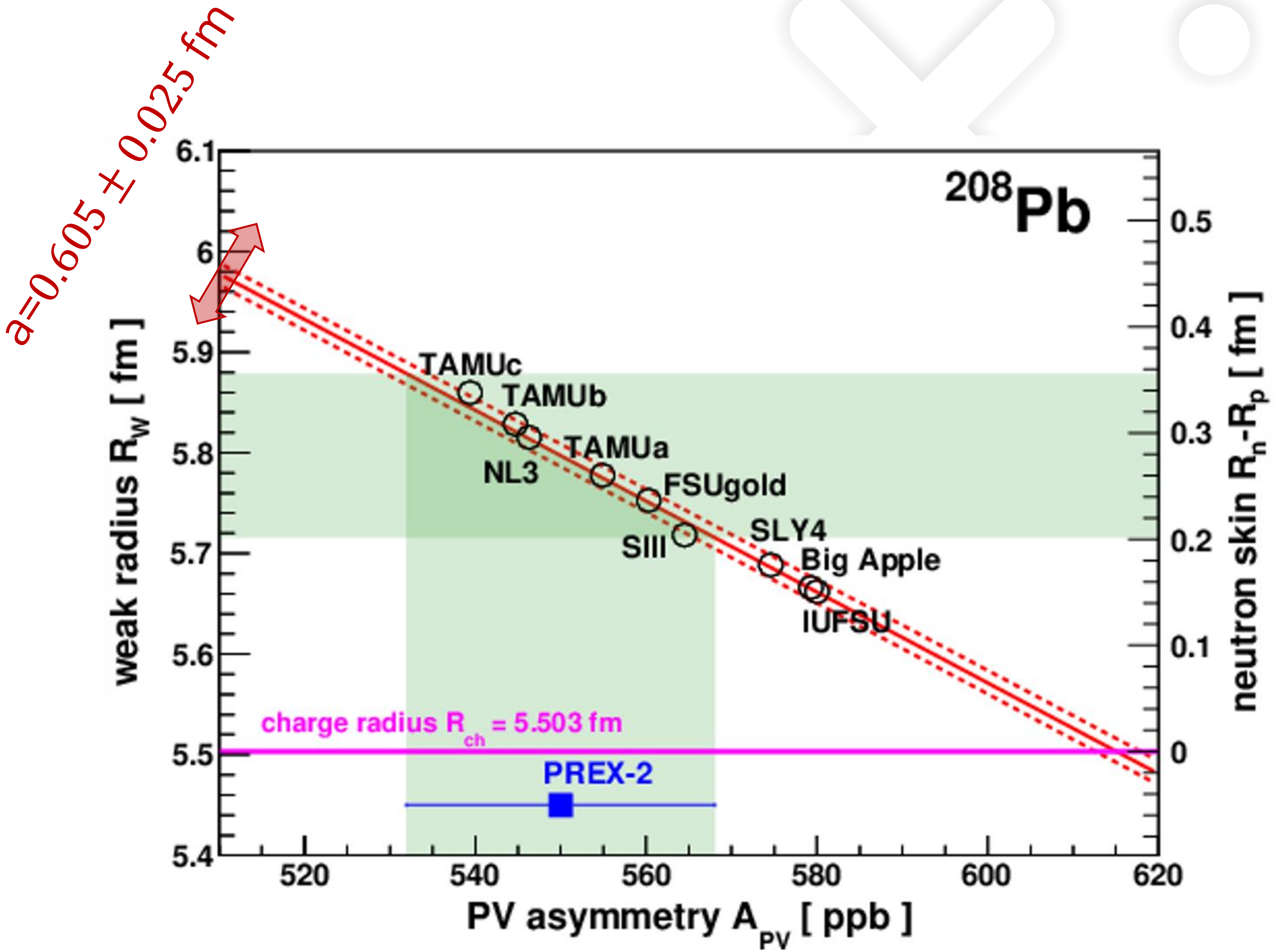

a=0.605 ± 0.025 fm
208Pb
weak radius R_W [fm]
neutron skin R_n-R_p [fm]
PV asymmetry A_PV [ppb]
TAMUc
TAMUb
TAMUa
NL3
FSUgold
SIII
SLY4
Big Apple
IUFSU
charge radius R_ch = 5.503 fm
PREX-2
6.1
6
5.9
5.8
5.7
5.6
5.5
5.4
520
540
560
580
600
620
0.5
0.4
0.3
0.2
0.1
0